

Effects of multivalent cations on the structure of soil organic matter (SOM)

von

Daniela Gildemeister
aus Berlin

Angenommene Dissertation zur Erlangung des akademischen Grades eines
Doktors der Naturwissenschaften
Fachbereich 7: Natur- und Umweltwissenschaften
Universität Koblenz – Landau

Berichterstatter:

Prof. Dr. Gabriele Schaumann, Universität Koblenz - Landau
Prof. Dr. Friederike Lang, Albert-Ludwigs Universität Freiburg

Tag der Disputation: 18. Februar 2015

Erklärung

Die vorliegende eingereichte Dissertation wurde selbständig von mir verfasst alle von mir benutzten Hilfsmittel und Quellen werden in der Arbeit angegeben. Die Anteile etwaig beteiligter Mitarbeiterinnen und Mitarbeiter sowie anderer Autorinnen und Autoren sind klar gekennzeichnet (s. „Anteile beteiligter Mitarbeiter und Mitarbeiterinnen“, S. 4). Ich habe nicht die entgeltliche Hilfe von Vermittlungs- und Beratungsdiensten (Promotionsberater oder anderen Personen) in Anspruch genommen. Ich habe diese Dissertation nicht in gleicher oder ähnlicher Form als Prüfungsarbeit für eine staatliche oder andere wissenschaftliche Prüfung im In- und Ausland eingereicht. Ich habe nicht die gleiche weder eine andere Abhandlung in einem anderen Fachbereich oder einer anderen wissenschaftlichen Hochschule als Dissertation eingereicht. Mir ist bewusst, dass ein Verstoß gegen einen der vorgenannten Punkte den Entzug des Dokortitels bedeutet und ggf. auch weitere rechtliche Konsequenzen haben kann.

Dessau, 07.08.2014

Ort, Datum

Unterschrift

Die folgenden Teile der vorliegenden Arbeit wurden bereits veröffentlicht bzw. sind zur Veröffentlichung bereits akzeptiert

Kap. 2: Alle Ergebnisse ausgenommen der Ergebnisse zu den Perkolationsversuchen

(Unterkapitel 2.3.3 sowie Teile des Kap. 2.4.1) wurden in die folgende Veröffentlichung integriert, auch Grafiken sind teilweise identisch:

Schaumann, G. E.; Gildemeister D.; Kunhi Mouvenchery, Y.; Spielvogel, S.; Diehl, D. 2013. Interactions between cations and water molecule bridges in soil organic matter.

Journal of soils and sediments.13 (9).1579-1588

Kap 3: Alle Ergebnisse und Grafiken wurden in angepasster Überarbeitung als folgende Veröffentlichung akzeptiert:

Gildemeister, D.; Metreveli, G.; Spielvogel, S.; Hens, S.; Lang, F.; Schaumann; G. E. 2014. Stabilisation of precipitates of pedogenic dissolved organic matter by multivalent cations. Journal of soils and sediments. DOI 10.1007/s11368-014-0946-9

Anteile beteiligter Mitarbeiter und Mitarbeiterinnen

Die vorgelegte Dissertation wurde im Rahmen eines DFG Forschungsprojektes angefertigt (SCHA 849/6-1; Einfluss der Quervernetzung der organischen Bodensubstanz durch mehrwertige Kationen auf die Reversibilität der Bleibindung in Humusaufgaben). Das genannte Projekt wurde von Gabriele E. Schaumann und Friederike Lang beantragt. Daher stammen die Idee zu diesem Thema und die grundsätzlichen Untersuchungskonzepte aus diesem Forschungsantrag. Gabi Schaumann und Fritzi Lang haben das Projekt und auch die Dissertation über die gesamte Laufzeit verfolgt und betreut, indem sie sich immer wieder in die Detailkonzeption und bei der Auswertung einbrachten. Dies gilt für alle hier vorgestellten Kapitel.

Kap 1 (Einleitungskapitel): Dieses Kapitel wurde vom mir zu 100% persönlich recherchiert und verfasst, es gab keine Zuarbeiten Dritter, Daten z. B. zu den Merkmalen der Ionen wurden der zitierten Literatur entnommen und sind entsprechend gekennzeichnet.

Kap 2 (Bodenproben): Versuchskonzeption, -durchführung, -auswertung und -interpretation wurden zu 80% von mir allein durchgeführt. Bei der Durchführung erfolgte Mithilfe durch das technische Personal der Universität Koblenz-Landau und der Uni Trier. Die Versuche zur Kontaktwinkelmessung inklusive der Auswertung wurden von Dr. Dörte Diehl durchgeführt, die Interpretation dieser Ergebnisse erfolgte gemeinsam.

Kap 3 (Präzipitate): Versuchskonzeption, -durchführung, -auswertung und -interpretation wurden zu 75% von mir allein durchgeführt. Bei der Durchführung erfolgte Mithilfe durch das technische Personal der Universität Koblenz-Landau und der Uni Trier. Ein Teil der Proben wurde während einer Bachelorarbeit von Sabina Hens hergestellt und gemessen, allerdings wurde die Auswertung der Ergebnisse und die Ergebnisinterpretation nicht dieser Arbeit entnommen, sondern von mir allein durchgeführt.

Kap 4 (Bleidesorption): Versuchskonzeption, -durchführung, -auswertung und -interpretation wurden zu 85 % von mir allein durchgeführt.

Kapitel 5 (finale Schlussfolgerungen & Ausblick): Dieses Kapitel wurde vom mir zu 100% persönlich verfasst.

Bei allen Konzeptionen und Interpretationen wurden Gedanken und Ideen der Betreuerinnen und der anderen Kolleginnen und Kollegen stets berücksichtigt.

Danksagung

Danksagungen sind ja immer etwas schwierig, da der Danksagende Gefahr läuft jemanden zu vergessen, der eigentlich hätte Erwähnung finden müssen, diese aber aus unbeabsichtigten Gründen nicht fand und nun enttäuscht womöglich gar wütend über den Undank ist. So bitte ich alle, die sich hier als erwähnenswert empfinden, aber im folgenden Abschnitt nicht schwarz auf weiß gefunden werden, sich dennoch meines Dankes versichert zu fühlen.

An allererster Stelle möchte ich, meinen Eltern danken, die mir meine langwährende Ausbildung ermöglicht haben und die mir in allen Lebenslagen geholfen haben und zu mir standen. Leider ist es mir nicht gelungen, den Erfolg ihrer Unterstützung, nämlich den Abschluss dieser Arbeit, meinem Vater noch zu seiner Zeit auf dieser Erde unter Beweis zu stellen. So hoffe ich, dass diese Nachricht auf anderen Kanälen seinen Weg zu ihm gefunden hat und dass es auch dort möglich ist ein wenig Stolz zu empfinden. Das Bewusstsein, eure Unterstützung zu haben, hat mich all die Jahre getragen.

Ich danke Kilian, Nikolai und Aljoscha, für ihre Geduld mit ihrer manchmal gestressten Mutter und für die Bereitschaft, ihre Lebenssituation meiner Karriereplanung anzupassen, auch wenn sie nie wirklich eine Wahl hatten. Ihr hättet es mir schwerer machen können, stattdessen war durch euch auch vieles einfacher, indem ihr mir ein abwechslungsreiches Leben neben meinem Beruf ermöglicht und durch euch oft klar wird, was am Ende wirklich zählt und wichtig ist.

Ich danke Fabian für seine Unterstützung (auch wenn diese quasi in den Sternen stand) und seine Kunst mich immer wieder aufzumuntern. Ohne mit dir lachen zu können, hätte ich das hier nicht mehr gepackt und so manches andere mehr, was für ein Glück dich geheiratet zu haben.

Ich danke, Dörte und Saida, für unsere gemeinsame Zeit in der Koblenzer Innenstadtwohnung, was uns den Anfang in der fremden Stadt sehr erleichterte und diesen Schritt eigentlich erst möglich machte. Ich danke, Gabi und Fritzi für ihr Vertrauen in meine Fähigkeiten zur Bearbeitung des Projektes und für ihre Unterstützung während des gesamten Zeitraumes. Insbesondere ist es Gabis intensiver Betreuung zu verdanken, dass diese Arbeit einen Abschluss fand. Ich danke der DFG für die Bereitstellung der Mittel für das Forschungsprojekt „Crosslink“, die mir die Dissertation finanziell ermöglichten.

Ich danke, den Kolleginnen und Kollegen der TU-Berlin dafür, mich wieder überhaupt erst einmal auf „Forschungsgeschmack“ gebracht zu haben, das war eine wirklich gute Zeit. Ich danke, der AG Chemie an der Universität Koblenz-Landau, Campus Koblenz, für ihre Unterstützung. Ich danke Sabina Hens, für ihre gute Arbeit im Labor und die Bereitschaft immer mitzudenken und ansprechbar zu sein. Ich danke, den Mitarbeiterinnen und Mitarbeitern der Kita „Eulenhorst“ für ihren Einsatz bei der Betreuung meiner Kinder bzw. den Einsatz diese Betreuung auch trotz aller bürokratischen Widerstände aufrecht zu erhalten. Ich danke, dem Umweltbundesamt für die Möglichkeit Sonderurlaub zur Fertigstellung der Dissertation nehmen zu können und ich danke, all meinen jetzigen Kolleginnen, die mich immer wieder darin bestärkten das Begonnene nun auch noch abzuschließen, was hiermit nun endgültig vollbracht ist.

Table of Contents

| | | |
|-------|---|----|
| 1 | General Introduction | 10 |
| 1.1 | T _g and T* in Soil Organic Matter (SOM) a short review | 10 |
| 1.2 | The role of multi-valent cations as cross-linking agents in SOM and NOM | 14 |
| 1.2.1 | Characteristics of cations | 14 |
| 1.2.2 | Bonding characteristics to humic substances | 15 |
| 1.3 | Effects of cations on soil and SOM properties | 16 |
| 1.4 | Objectives | 17 |
| 1.5 | Experimental Programme | 18 |
| 2 | Influence of multivalent cations on Soil Organic Matter: DSC experiments with solid samples (cation addition and depletion in samples)..... | 20 |
| 2.1 | Summary..... | 20 |
| 2.2 | Introduction | 21 |
| 2.3 | Material and Methods | 23 |
| 2.3.1 | General strategy..... | 23 |
| 2.3.2 | Soil Samples: Preparation, characteristics and storage | 24 |
| 2.3.3 | Preparative methodical study: developement of an optimized method to load SOM samples with cations | 25 |
| 2.3.4 | Demineralisation experiments..... | 29 |
| 2.3.5 | Chemical Analyses | 30 |
| 2.3.6 | DSC measurements | 30 |
| 2.3.7 | Contact angle measurements | 31 |
| 2.4 | Results and Discussion | 31 |
| 2.4.1 | Cation addition by percolation and by batch experiments | 31 |
| 2.4.2 | Wettability / repellency of the treated and untreated samples..... | 52 |
| 2.4.3 | Influence of demineralisation on matrix rigidity..... | 54 |
| 2.5 | Conclusion..... | 57 |
| 3 | Influence of several multivalent cations on structural characteristics of DOM based precepitates..... | 59 |
| 3.1 | Summary..... | 59 |

| | | |
|-------|---|-----|
| 3.2 | Introduction | 59 |
| 3.3 | Material and Methods | 61 |
| 3.3.1 | Sample properties and preparation | 61 |
| 3.3.2 | Preparation of the DOC solution | 61 |
| 3.3.3 | Formation of the precipitates in metal solutions | 62 |
| 3.3.4 | Chemical analyses of the filtrate solution | 63 |
| 3.3.5 | Preparation, storage and DSC measurements of the precipitates | 63 |
| 3.4 | Results and Discussion | 67 |
| 3.4.1 | Qualitative observations, analyses of the filtrate and water content of the samples 67 | |
| 3.4.2 | DSC results..... | 71 |
| 3.5 | Conclusion | 79 |
| 4 | Is there an influence on lead sorption / desorption by different cations inducing stable molecular networks in SOM? A search..... | 81 |
| 4.1 | Summary..... | 81 |
| 4.2 | Introduction | 81 |
| 4.3 | Material and Methods | 83 |
| 4.3.1 | Preparation and storage of the samples | 83 |
| 4.3.2 | Desorption experiments..... | 84 |
| 4.3.3 | Chemical analyses | 85 |
| 4.3.4 | DSC measurements | 86 |
| 4.4 | Results and Discussion | 86 |
| 4.5 | Conclusion | 93 |
| 5 | General conclusions & perspective: Forming a network | 94 |
| 6 | Literature | 98 |
| 7 | Curriculum Vitae..... | 110 |

Summary

The intention of this thesis was to characterise the effect of naturally occurring multivalent cations like Calcium and Aluminium on the structure of Soil Organic Matter (SOM) as well as on the sorption behaviour of SOM for heavy metals such as lead.

SOM is regarded as a polymer-like structure where macromolecules interact via organic functional groups and form a network. As is known from polymer science some polyvalent cations are able to form cross-links between the negatively charged functional groups. Therefore they substantially influence the degree of networking. Due to these cross-links side chain mobility of the organic molecules decreases and the matrix becomes more rigid. To characterise the resulting rigidity of such a matrix the glass transition temperature is determined with the Differential Scanning Calorimetric (DSC). It was shown that this method is also applicable for a wide range of soil samples to characterise the influence of water molecules on rigidity of SOM. Ca and Al are known as cross-linking agents and the aim of the conducted experiments was to change the rigidity of SOM by changing the cation composition. In literature it is described that flexible regions of SOM were responsible for fast and linear sorption and desorption whereas rigid areas of SOM were responsible for slow desorption, hysteresis effects, and sequestration of contaminants.

The first part of this thesis describes the results of experiments in which the Al and Ca cation content was changed for various samples originated from soils and peats of different regions in Germany. The second part focusses on SOM-metal cation precipitates to study rigidity in dependence of the cation content. In the third part the effects of various cation contents in SOM on the binding strength of Pb cations were characterised by using a cation exchange resin as desorption method.

It was found for soil and peat samples as well as precipitates that matrix rigidity was affected by both type and content of cation. The influence of Ca on rigidity was less pronounced than the influence of Al and of Pb used in the precipitation experiments. For each sample one cation content was identified where matrix rigidity was most pronounced. This specific cation content is below the cation saturation as expected by cation exchange capacity. These findings resulted in a model describing the relation between cation type, content and the degree of networking in SOM. Furthermore, it was found that the changes in matrix rigidity were well correlated to changes in hydrophobicity of the samples. That gives evidence for changes in the conformation of the organic molecule. For all treated soil and precipitate samples a step transition like glass transition was observed, determined by the step transition temperature T^* . It is known from literature that this type of step transition is due to bridges between water molecules and organic functional groups in SOM. In contrast to the glass transition temperature this thermal event is slowly reversing after days or weeks depending on the re-conformation of the water molecules. Therefore, changes of T^* with different cation compositions in the samples are explained by the formation of water-molecule-cation bridges between SOM-functional groups. An increase of T^* is correlated with storage time in former literature studies. These aging effects are also observed in this study especially for Ca treated samples that gives further evidence for the interaction of cations and water molecules in bridging. No influence on desorption kinetics of lead for different cation compositions in soil samples was observed. Therefore it can be assumed that the observed changes of matrix rigidity are highly reversible by changing the water status, pH or putting agitation energy by shaking in there.

Zusammenfassung

Ziel dieser Arbeit war die Beschreibung des Einflusses mehrwertiger Kationen auf die Struktur der organischen Bodensubstanz (OBS) und das daraus resultierende Vermögen andere Kationen wie beispielsweise Blei in der OBS zurückzuhalten.

OBS verfügt über polymerähnliche Strukturen. Dabei wird davon ausgegangen, dass Makromoleküle, die über ihre funktionellen Gruppen miteinander interagieren, ein Netzwerk bilden. Mehrwertige Kationen können die meist negativ geladenen funktionellen Gruppen miteinander verknüpfen und so Einfluss auf den Grad der Vernetzung innerhalb der OBS nehmen. Durch diese Brücken kann die Beweglichkeit der Molekülseitengruppen eingeschränkt werden und die Matrix wird insgesamt starrer. Diese Abnahme der Flexibilität ist über die Messung der Glasübergangstemperatur mit der Differential Scanning Kalorimetrie (DSC) möglich. Die Anwendung dieser Methode für Bodenproben ist hinreichend bekannt. Sie diente bisher dazu zu zeigen, wie Wassermoleküle die Starrheit der OBS beeinflussen. In der Literatur werden die weichen / flexiblen Regionen der OBS mit schneller und linearer Sorption und Desorption in Verbindung gebracht, während die starren Bereiche für langsame Prozesse mit Hystereseeffekte und Sequestrierung von Schadstoffen verantwortlich gemacht werden.

Im ersten Teil dieser Arbeit wird die Kationenzusammensetzung in unterschiedlichen Torfproben und einer organischen Auflage durch Variation der Aluminium- und Calciumgehalte verändert und die Proben werden wie oben beschrieben mit der DSC charakterisiert. Der zweite Teil beschäftigt sich spezifisch mit der Starrheit von Präzipitaten hergestellt aus gelöster OBS und verschiedenen Metallkationen. Im dritten Teil wurde versucht die zeitliche Abhängigkeit der Bleidesorption während eines Schüttelversuches mit einem sauren Kationenaustauscher Harz abzubilden. Eingesetzt wurden hierfür die bereits charakterisierten Bodenproben aus dem ersten Versuchsblock.

Eine Abhängigkeit der Starrheit in der organischen Auflage, den Torfproben und den Präzipitaten von Kationenart und -gehalt konnte nachgewiesen werden. Dabei war der Effekt von Calcium insgesamt weniger ausgeprägt als von Aluminium oder Blei. Für alle behandelten Proben konnte ein Maximum in der Starrheit identifiziert werden, wobei die mögliche Sättigung für das jeweilige Kation noch nicht erreicht war. Aus den Ergebnissen konnte ein Modell abgeleitet werden, das den Zusammenhang zwischen Kationengehalt und Vernetzung innerhalb der OBS beschreibt. Zudem wurde eine gute Korrelation zwischen der Starrheit in den Proben und ihrem wasserabweisenden Verhalten (Hydrophobizität) gefunden, was auf strukturelle Änderungen bei der Ausrichtung der Moleküle hindeutet. Ein echter Glasübergang konnte mit der DSC in keiner der untersuchten Proben ermittelt werden. Gemessen wurde nicht der klassische Glasübergang sondern ein Stufenübergang, der in Zusammenhang mit Wassermolekülbrücken innerhalb der OBS gebracht wird. Dieser Übergang ist nicht sofort sondern mit einer zeitlichen Verzögerung von Tagen oder Wochen in den Proben wiederkehrend. Das wird mit einer erneuten Ausrichtung und Bildung von Wassermolekülbrücken erklärt. Zusätzlich konnten bei den Proben Alterungsprozesse beobachtet werden, die bisher ebenfalls mit der Ausbildung von Wassermolekülbrücken erklärt wurden. Diese Ergebnisse legen den Schluss nahe, dass es ein enges Zusammenspiel zwischen Kationen, Wassermolekülen und funktionellen organischen Gruppen geben muss, das zur Ausbildung von Wassermolekül-Kationen-Brücken führt. Ein Einfluss der Vernetzung auf die Bleidesorption war nicht messbar, was erste Hinweise darauf liefert, dass die ausgebildete Vernetzung durch Zugabe von Wasser in Zusammenhang mit zusätzlicher physikalischer Beanspruchung durch Schütteln und einer Abnahme des pH-Wertes schnell reversibel war.

1 General Introduction

1.1 T_g and T^* in Soil Organic Matter (SOM) a short review

SOM has a high influence on all soil functions since it is responsible for soil characteristics like pH-value, oxidation processes and nutrient release. The knowledge about the molecular structure of SOM or Humic substances (HS) is of great interest in science for the last 30 years. The molecular structure gives information about central processes occur in soil environment e. g. nutrient storage and release, water interaction, carbon storage and degradation (physical, chemical and biological), cation exchange, and sorption and desorption of contaminants.

For describing the molecular structure of humic substances two models were discussed in literature:

- 1) HS are seen as macromolecular substances with polymer characteristics formed by secondary abiotic or biotic synthesis reactions. (LeBoeuf and Weber 1997, Xing and Pignatello 1997); (Swift 1999, Essington 2003)
- 2) HS are seen as supramolecular associations, aggregates, or micelles (formed in water solutions) of low-molecular-mass organic molecules forming clusters by weak van-der-Waals forces or hydrogen bonding (Von Wandruszka 1998, Piccolo 2001, Simpson, Kingery et al. 2002, Sutton and Sposito 2005)

Schaumann, 2006 suggested that both views cannot be excluded for solid and dissolved SOM (and NOM) and overall SOM (and NOM) “have to be treated as amorphous materials with a certain degree of microcrystallinity” (Schaumann 2006).

Amorphous materials are non-structured materials in contrast to crystallized structured ones with a pronounced overall symmetry. One important characteristic of an amorphous material is the so-called glass transition temperature T_g which is the specified temperature point where the substance changes from a glassy (rigid) to a rubbery state. This thermodynamical process could be regarded as second order transition and is explained by the uptake of energy as heat by mobile side chains of macromolecules (e. g. polymers). The observed increase of heat capacity at T_g is linked to the degree of increasing mobility of the molecules in the network. The glass transition temperature T_g correlates with the degree of rigidity in normal state that means a matrix with a very high rigidity at room temperature would also has a higher T_g than a matrix with a lower rigidity at room temperature. For example it is known that the uptake of water has a plasticizing effect on organic polymers and therefore causes a higher mobility of the side chains which is determined in DSC with a decreasing T_g for water wet samples.

In the following work the main characteristic of the samples to determine the rigidity of the organic molecule network in SOM is the step transition-like glass transition temperature named T^* . Therefore we would like to describe and define it in this chapter by give a short

history of glass transition and step transition-like glass transition measurements in soil organic matter and in natural organic matter (NOM).

LeBoeuf & Weber (1997) observed a T_g for the first time for water-wet and dry isolated humic acids (HA) in open aluminium pans (LeBoeuf and Weber 1997). By this thermo-dynamical behaviour the idea of regarding SOM as high molecular organic polymers was underlined. The results of the measurements were related to the so called distribution reactivity model (LeBoeuf and Weber 1997) or dual reactive domain (dual mode) model (Xing and Pignatello 1997) which accounts for isotherm non-linearity and competitive sorption (Huang and Weber Jr 1997). They differentiate SOM in two main regions described as a rubbery region responsible for linear sorption and desorption processes and a glassy region responsible for slow sorption and sequestration of organic chemicals. The relation of T_g and sorption hysteresis was shown for phenanthren and some NOM where sorbents near or at their rubbery state tends to show little to no desorption hysteresis (LeBoeuf and Weber Jr 2000). Glass transitions were also reported for fulvic acids (FA) derived from a stream (Young and LeBoeuf 2000) whereas the measured T_g of FA was lower than for HA in TM DSC (temperature modulated DSC). This observation was explained by a less complex, less aromaticity, lower molecular weight and thus, less likelihood to coil than HA which induces a higher mobility of the side chains. The plasticizing role of water was demonstrated by LeBoeuf & Weber Jr, 2000, in synthetic organic sorbents and in natural organic matter like Aldrich Humic Acid whereas the effect of decreasing T_g due to water uptake of the samples was best pronounced. The authors explained that phenomenon with the possibility of disruption of hydrogen bonds in the matrix as it was observed for pyridine swelling of coal (Mackinnon, 1994). In several studies is shown that glassy polymers and diagenetically altered kerogen and coal exhibit greater isotherm nonlinearity than rubbery polymers and young SOM (Johnson, Huang et al. 2001). Further investigation demonstrate that an important factor influencing the height of T_g are also the structural modifications by diagenetic processes, Zhang et al. (2007) observed an increasing T_g in the order of coals > charcoals, Type I and II kerogen > humic acid. Therefore T_g values were not merely a function of aromaticity (Zhang, LeBoeuf et al. 2007).

De Lapp et al. (2004) summarized the following evidences for the theory of macromolecular mobility in NOM (DeLapp, LeBoeuf et al. 2004):

1. Increased attractive forces between molecules require more thermal energy to produce molecular motion, where increases in T_g correspond directly with increases in a larger cohesive energy density σ_p (Barton 1983)
2. The internal mobility of a macromolecule chain is primarily affected by the size of the side chain...Generally, larger side-chain groups require greater activation energies to move or rotate the chain (Eisenberg 1993)
3. Macromolecules possessing aromatic or parallel bonds in their backbone have extremely stiff bonds resulting in reduction of molecular mobility (Rosen 1993)

4. Increases in the free volume of macromolecule allows more room for the macromolecule rotate, resulting in a reduction in the T_g . Thus, swelling of a macromolecule by a thermodynamically compatible solvent will tend to increase the free volume and lower the T_g . (Haward 1973, Barton 1983)

Although difficulties were seen for the observation of glass transitions in whole soil samples because of the high heterogeneity of SOM possessing multiple transitions (LeBoeuf and Weber Jr 1998) , in 2000, Schaumann & Antelmann reported signs for potential T_g also for solid and unchanged SOM of an A_h horizon of a spruce forest. Although the plasticizing effect of water was not found for the determined sample a slightly higher T_g was observed for the wet sample (Schaumann and Antelmann 2000). Further glass transitions in whole soil samples were then reported by DeLapp et al. (2004).

In 2005 Schaumann & Leboeuf describe a non reversible glass transition in air dried peat samples without a thermal pretreatment (no further removal of water) in a closed system, after some days of storage the glass transition reappears (Schaumann and LeBoeuf 2005). By conducting a thermal pretreatment for the same sample a typical glass transition with very low intensities was reported. So two transition types were present in the same sample depending on the thermal pretreatment (inducing water evaporation) and on the manner of measurement (sealed or open system). Thermomechanical Analyses (TMA) of the sample revealed a matrix softening in the same temperature range as the observed water-dependent step transition in DSC.

The observed phenomenon was explained with the hydrogen bond-based cross-linking model (HBCL-Model), which relates to the formation of water molecule bridges (also known as WaMB in recent literature) between the polymer side chains which reducing the side chain mobility. Schaumann et al. assume that the time of reformation of the cross-links depends on the diffusion time of the water molecules to the specific bridging sites in SOM which takes longer than the cooling time in a DSC run of a subsequent heating cycle. Therefore the reappearance of T_g takes a SOM specific time period. By these experiments the special role of water in SOM was demonstrated: Depending on the water content in the sample plasticizing and anti-plasticizing ($WC < 12\%$) processes were observed. Anti-plasticizing effects of water arises when water clusters in SOM expand the free volume and enhance the mobility of the molecule chains.

| | Glass transition in NOM | Glass transition-like step transition in NOM |
|---------------------------------|--|--|
| occurrence | In water-wet and water free samples (pre-heated) measured in a open system (evaporation possible), reappearance in subsequent heating cycles | Only in water containing samples measured in hermetically closed systems, reappearance after a specific time period of storage at ambient temperatures |
| Transition temperature | $T_g = 17^\circ\text{C} - 70^\circ\text{C}$ (humic and fulvic acids) (LeBoeuf & Weber, 2000; Xing, 2007) | $T^* = 48^\circ\text{C} - 68^\circ\text{C}$ (depending strongly on thermal history) |
| Intensities (in average) | $\Delta c_p = 0,0XX$ (e. g. Aldrich HA 0,03 J g ⁻¹ °C ⁻¹) | $\Delta c_p = 0,XXX$ |
| Mainly reported for | Extracted HA (Aldrich, Leonardite), FA, lignine, and biopolymers | Whole soil and peat samples with high organic carbon contents (> 5%, sample specific) |
| Possible explanations | Comparable NOM structure to high molecular organic polymers, side chain mobility of the macromolecule (due to e. g., aromaticity, diagenetic processes) | Formation of water-bridges as cross-links between the organic side chains |

Table 1: Comparison of the characteristics of the two determined step transitions in NOM and SOM, the reported values are only given in average.

To distinguish both thermal processes from each other the non-reversible glass transition was called as glass transition - like step transition (Hurrass and Schaumann 2005). Hurraß et al. (2006) reported about glass transition-like step transitions in 52 out of 102 soil samples of different soil types and horizons sampled from locations with different land-uses. For all these samples no quantitative evaluation of the classical glass transition was possible because of very low intensities. Furthermore for anthropogenic influenced soils only for a minority of the samples a step transition was detectable. The authors concluded that not enough binding sites for water molecule bridges were available in such heterogeneous samples. For the analyzable samples a positive correlation was found between Δc_p and OM content ($p < 0,0001$). In 2007, Hurrass & Schaumann, demonstrated in several samples physical aging processes due to the strengthening of cross-linking by water bridges in samples with a water-content below 10%. An increase of T_g^* of 5°C was observed during a time period of 7 months (Hurrass and Schaumann 2007). Physical aging was formerly defined as structural relaxation process of amorphous polymers below their glass transition temperature which causes reductions in segment mobility, enthalpy and free volume (Struik 1978).. The described changes induce an increase of the glassy character of the amorphous structure. Physical aging is also hypothe-

sized to be responsible for the aging of contaminants in SOM and NOM (LeBoeuf and Weber 1997). Schaumann, 2006, concluded from the observations of aging in SOM and the found transition temperatures T^* and T_g as described above that there should be also at least two mechanisms of physical aging in SOM whereas one of them is linked to water molecule bridges in SOM (Schaumann 2006) and can be demonstrated by an increasing T^* for samples stored under constant humidity conditions (Hurrass and Schaumann 2007). At the time no physical aging experiments were reported for NOM shown a classical glass transition.

1.2 The role of multi-valent cations as cross-linking agents in SOM and NOM

1.2.1 Characteristics of cations

Cations can be described by parameters like charge and ion radius. The quotient of those two characteristics gives information about the binding affinity to exchange surfaces and correlates with the hydration energy of the cation.

| Cation | r_i / pm | z^2/r_i / pm ⁻¹ | ΔH_h / kJ mol ⁻¹ | r_h / pm |
|------------------|------------|------------------------------|-------------------------------------|------------|
| Na ⁺ | 116 | 0,0086 | - 405 | 358 |
| Mg ²⁺ | 86 | 0,0465 | - 1922 | 428 |
| Ca ²⁺ | 114 | 0,0351 | - 1592 | 412 |
| Al ³⁺ | 67 | 0,1343 | - 4600 | 480 |
| Pb ²⁺ | 133 | 0,030 | - 1480 | |

Table 2: Ion radius, Hydrationenergy (ΔH_h) and hydration radius of the cations considered in this thesis. (Scheffer/Schachtschabel; and Blume 2010; Essington 2003)

Smaller cations have a higher hydration energy and therefore a thicker hydration shell than bigger cations of the same charge. Therefore bigger cations come closer to a surface than smaller cations of the same charge. (Scheffer/Schachtschabel; and Blume 2010) .

Cations can be divided in ions which exist principally as hydrated cation, ions which exist in a hydrated form and also as sparingly soluble hydroxide, and ions which only form stable oxyanions. The form depends on the ionic potential (IP) of a cation defined as quotient of ion charge (Z) and radius (r):

- Ca²⁺, Mg²⁺, Pb²⁺ and Na⁺ have a small IP (< 0,03) and tend to remain hydrated
- Al³⁺ and Fe³⁺ have a moderate to high IP (0,03 < IP < 0,1) and tend to strongly polarize water and promote hydrolysis

The presence of exchangeable Al³⁺ is therefore depending strongly on soil pH. In alkaline soil with pH > 7 the so called base cations (readily exchangeable cations) are Ca²⁺, Mg²⁺, K⁺ and

Na^+ (dominated by Ca^{2+}) whereas in acidic soils with $\text{pH} < 6$ Al^{3+} and the associated hydrolysis products AlOH^{2+} and $\text{Al}(\text{OH})_2^+$ dominate the exchange phase charge, also Mn^{2+} could be present in an exchangeable form in acidic soils. (Essington 2003)

In case of the surface complexation of cations it is to differentiate in outersphere and inner-sphere complexes. An innersphere complex is formed when no water molecules were between the ion and the surface ligand. An outersphere complex is formed when the ion keeps its hydration shell and is only adsorbed by electrostatic interactions, the interceding water molecules prevent electron sharing (Essington 2003). In contrast innersphere complexes form coordinative bindings. Co-ordinative bindings (electron sharing) are known to be much stronger than electrostatic interactions therefore cations bind by outersphere complexes can easily displaced with cations in the solution. (Scheffer/Schachtschabel; and Blume 2010)

1.2.2 Bonding characteristics to humic substances

Also for bindings with NOM the ability of cations to form inner- or outersphere complexes is an important characteristic which gives information on the stability of such a complex. Kalinichev & Kirkpatrick, 2008, presented molecular dynamics computation which demonstrates a strong innersphere complexation of Ca^{2+} with NOM supporting the idea of supramolecular, Ca-mediated NOM aggregation (Kalinichev and Kirkpatrick 2007). For fulvates both inner-sphere and outersphere complexes with metal cations are known from spectroscopic determinations e. g., NMR, fluorescence, and x-ray absorption near edge (Essington 2003)¹. Inner-sphere complexation is linked to high energy binding sites. Although in a fulvate molecule high energy binding sites are in the minority it appears to be the preferred binding mechanism if the metal ion concentration is far below the fulvate concentration. Outersphere complexations are described as weak bonding between water and O-bearing ligands after saturation of the high energy bonding sites also these low energy bonding sites were occupied by metal cations if there are enough available. Complexes can be divided in monodentate, bidentate, tridentate and polydentate complexes depending on the number of occupied positions of the coordination sphere of the metal ion by the organic ligand. Outersphere complexes are monodentate whereas innersphere complexes are often demonstrated bi- to polydentate bindings. Polydentate complexes can also be formed by hydrophilic functional groups of more than one organic molecule. (Essington 2003)

It was shown that the CEC is directly related to the organic matter content of soil samples (Batjes 1996). The exchange processes were influenced by the dissociation of the carboxylic and phenolic functional groups in SOM. Especially in acidic soils with high organic carbon content the cation exchange capacity is related so the functional groups of SOM (Kalisz and Stone 1980). This fact includes high OM-surface horizons like O_e , O_a and O_f and peat soils (Ross, Matschonat et al. 2008).

¹ Page 213

The molecular configuration of a humic acid molecule is flexible and a function of the salt concentration and pH of the aqueous environment. Due to a higher salt concentration and a low pH a condensed form of the HA with a strong coiling resulting in globular aggregates and ring like structures is expected (Essington 2003).

Due to the heterogenous distribution of different organic molecules in SOM depending on the different pathways of formation it seems unlikely to consider all characteristics in one universal cation-SOM-binding model. A realistic approach is the observation of interactions between selected cations with isolated and purified humic substances for deriving binding models under changing conditions (pH, temperature, ionic strength). In literature several models are available. In Scheffer / Schachtschabel, 2010, the Nica - Donnan model and Model VI by Tipping, 2002 (Tipping, Rey-Castro et al. 2002), were described as the two main models:

The Nica-Donnan Model based on the NICA equation (Non-ideal-competitive adsorption model) for binding of protons and metal cations derived by

- Competitive Langmuir equation
- Continuous affinity distribution
- Low and high pK_a for two different types of functional groups (carboxylic and phenolic groups)
- Description of electrostatic strength as a function of ionic strength

Humic substances were described as a Donnan-gel with a negative charge and volume depending on the ionic strength. Reliable results were observed for the Nica-Donnan-model for the descriptions of an extensive data set for the binding of metal cations (Ca^{2+} , Cd^{2+} , Cu^{2+} , Pb^{2+} , and Al^{3+}) to a purified peat humic acid (PPHA) at various pH values (Kinniburgh, Van Riemsdijk et al. 1999, Koopal, van Riemsdijk et al. 2001, Scheffer/Schachtschabel; and Blume 2010).

Model IV consists of discrete affinity distributions. Proton and metal bindings were divided in two groups because of their $\log K$ values which were homogeneously ranged around a mean value. Electrostatic effects were considered by a Boltzmann factor which depends on charge and ion strength.

Cation exchange processes are especially related to cations only forming outersphere complexes.

1.3 Effects of cations on soil and SOM properties

Regarding the last chapters it is suggested that there should be a relation between the structure of SOM with its various types of charged molecules and cations in the soil solution. Cations can act with charged functional groups of several molecules and consequently the whole molecular structure of the matrix is influenced. It can be assumed that both models of molecular structure of humic substances, macro-molecular and supra-molecular, allow the interaction of

cations in its matrix and it is hypothesized that bridges were formed between molecules and consequently the rigidity of the matrix is influenced. In such a network the availability of contaminants but also of nutrients is less pronounced and SOM acts as accumulator for various substances. But how stable is this network? Is molecular networking physically measurable?

The main objective of this thesis was to investigate the interactions between SOM and multivalent cations due to structural confirmations and to the effects of such a changed matrix e. g. on the release of lead in the environment. Cross-linking effects of multi-valent cations were discussed in connection to mineral organic associations (Kahle, Kleber et al. 2002, Kögel-Knabner 2002, Ellerbrock and Kaiser 2005, Weng, Koopal et al. 2005), aggregate stability and supramolecular nature of SOM. Simpson et al. purified a set of HA by removal of associated metals by liquid chromatography in combination with H-NMR by this aggregate disruption was demonstrated (Simpson, Kingery et al. 2002). Soil aggregation is enhanced by multivalent cations between humic acids and several clay particles of an Entisol (Piccolo and Mbagwu 1994).

In presence of multivalent cations like Ca^{2+} DOM release of soils was obviously decreased as reported by several authors (Römken and Dolfing 1998, Shen 1999, Schaumann 2000, Oste, Temminghoff et al. 2002). Such observations can be linked to coagulation and precipitation effects of multivalent cations by bridging several organic molecules with each other. Temminghoff et al. (1998) induced coagulation with Ca^{2+} and Al^{3+} in purified forest soil solutions (Temminghoff, Zee et al. 1998). Lang et al., 2005, suggested by small-angle x-ray scattering analyses cross-linking of Pb^{2+} in Pb-DOM colloids (Lang, Egger et al. 2005). Schaumann, 2006 suggested that “multivalent cations may increase the apparent molecular weight by the formation of coordinative cross-links in dissolved and undissolved matter” (Schaumann 2006). In conclusion it can be hypothesized that cross-linking by multivalent cations is one possible mechanism of supramolecular networking in SOM. Although cross-linking by multivalent cations were often discussed in literature to be responsible for observed effects on the organic molecular matrix, the effects of cations were not shown in detail until now.

1.4 Objectives

The objective of this study was to understand the mechanism and effects of cations on soil organic matter with special respect to the cross-linking hypothesis

High cross-linking in the interior of SOM should enhance a higher networking and therefore i) a reduced mobility of the side-chains of macromolecules (macromolecular view), ii) a decreasing effect on the overall mobility of a smaller molecule embedded in the network (supramolecular view), or iii) a reduced mobility of smaller molecules by precipitation instead of dissolution. In reference to these three mechanisms of postulated increasing rigidity by cross-linking of cations the influence of different contents and charge of cations should be obtained in whole organic soil samples and in precipitates. Rigidity can be measured by the glass transition temperature T_g or the glass transition-like step transition temperature T^* (WaMB Tran-

sition) depending on the cross-linking mechanism with differential scanning calorimetric (DSC). It was hypothesized that

- I) the overall rigidity of the organic matrix increases with increasing cation content in the SOM due to decreasing side chain mobility and decreasing small molecule mobility, especially for higher charged cations the increasing effects should be more pronounced than for lower charged cations
- II) the role of water in cross-linking in SOM and also in precipitates developed as negligible for high cation contents and rigidity is analysable by T_g due to the strong coordinative cross-links of multivalent cations in comparison to the weaker bondings of water molecule bridges
- III) the effect of precipitation is more pronounced for higher charged cations and the rigidity of such a matrix is also stronger
- IV) the desorption of metal cations like lead is kinetically restrained and therefore slower under cation depletion conditions with a higher degree of cross-linking in the matrix

1.5 Experimental Programme

Experiments with Ca^{2+} and Al^{3+} as networking cations were conducted. Both cations were known for their cross-linking characteristics and typically present in soils with high SOM. A soil sample with a very high degree of SOM was chosen, which is described in detail in chapter 2. This sample was mainly used for all experiments to find mechanistically differences depending on the manner of cross-link inductions. To have a closer look on the effects of structural changes in SOM by different concentrations of multivalent cations the cross-linking behaviour of Al^{3+} and Ca^{2+} was described as affecting the rigidity of solid SOM and of precipitates. Three elemental parts with specific determinations of rigidity in SOM (whole soil – SOM sample and precipitates of a DOC-solution originated from the same sample) and their environmental effects like OC losses by dissolution and lead desorption were discussed.

In the first part of this thesis hypotheses I and II were verified by determination of the rigidity of whole samples in its natural composition with varying cation contents (Al^{3+} , Ca^{2+} and Na^+). Different methods of cation addition were used to check if there is a difference in the created molecular network depending on the method of cation addition. Furthermore the effect of cation depletion was investigated on samples with different naturally occurring cation compositions in SOM. In conclusion it was possible to derive a statement about the influence of the cation content on the rigidity of the organic matrix.

In the second part hypothesis II) and III) were verified by forming precipitates with different cations with changing $\text{Me}^{n+} / \text{C}$ ratios and by observations of the precipitation process and rigidity of the precipitates. Precipitation is an important process in soils which keeps organic substances and cations in the upper soil horizons. Stability of precipitates is one special focus in soil sciences e. g. the bioavailability of precipitates. It can be assumed that also in the first part of the experiments precipitation occurs during the tests but the process cannot be avoided

from other cross-linking processes taking place in the whole sample. A very different study design is needed for analysing cross-linking effects in precipitates therefore these experiments are described in an own chapter (Chapter 3).

In the third part hypothesis IV) is verified by conducting time dependend lead desorption experiments with cation-pretreated samples. So this part is focussed on the effects of the stronger networking in the interior of SOM in contrast to the former chapters where the focus was on the description of the cross-linking in the organic matrix. But the results of the former chapters especially of chapter 2 where directly used for the experiments in the chapter 4.

As it is described each part of the thesis based on different experiments with its own hypotheses and discussion, therefore we decided to describe each part in an own chapter with introduction, materials & methods and results & discussion. So there is also the possibility for the reader to concentrate on one chapter, if you are only interested in the molecular structure of precipitates or in lead desorption choose the respective chapter.

2 Influence of multivalent cations on Soil Organic Matter: DSC experiments with solid samples (cation addition and depletion in samples)

2.1 Summary

The intention of the study was to demonstrate the correlation between the networking of organic molecules in Soil Organic Matter (SOM) determined by its rigidity with the content of cross-linking cations like Ca^{2+} and Al^{3+} . The cation content of SOM was changed by addition of cations and cation depletion as it is also take place under natural conditions. For the absorption experiments a batch and a percolation test system was used, but cation distribution was better in the batch system (results of the parallels were more consistent) and therefore matched better the requirements of that study. Ca^{2+} absorption in batch experiments was possible until a point near CEC_{eff} , in contrast Al^{3+} absorption exceeds this point clearly. Rigidity was determined with Differential Scanning Calorimetry (DSC). For a Ca^{2+} treated sample of an organic layer of a spruce forest the maximum rigidity was determined at a point of about 65% saturation of the CEC_{eff} . Rigidity of all Ca^{2+} treated samples increases with time stored under constant temperature and humidity conditions (aging). In case of addition of Al^{3+} to the same sample rigidity increases also to a maximum point but then no further changes in rigidity can be observed. In relation to the cation concentration normalized to the specific charge of the cations Al^{3+} absorption induces a stronger rigidity than Ca^{2+} absorption, this difference vanished with conditioning time. The determination of hydrophobicity by contact angle measurements demonstrates a clear correlation between hydrophobicity and increasing rigidity of the samples which anticipated conformational changes of the molecular structure of the SOM.

In contrast the effects of cation depletion on rigidity were less pronounced than expected. Depletion of cross-linking cations was managed by the addition of Na^+ and otherwise by the treatment with an acid exchange resin (demineralization experiments). Demineralisation experiments were conducted to various SOM samples from different sample sites and the results anticipate that the influence of the cations strongly depends on the sterical possibilities in the molecular structure of the SOM. Based on the results a model on Ca^{2+} and Al^{3+} was deduced to explain the correlation between matrix rigidity and cation status in SOM. In this model a further uptake of Ca^{2+} in the network results in a higher mobility of the side chains of the organic molecules at the point of saturation in contrast for a further Al^{3+} uptake no changes in the developed network can be observed and the formation of precipitates in the organic matrix is postulated.

Measurable aging effects especially for Ca^{2+} treated samples demonstrate the important role of water molecules bridges and water molecule ion bridges in the molecular network of SOM.

2.2 Introduction

Multivalent cations are known to alter the structure, solubility and degradability of Soil Organic Matter (SOM) (Tipping, Woof et al. 1991, Skjellberg 1995, Christl and Kretzschmar 2007, Scheel, Dorfler et al. 2007). The dominant metal binding groups are thought to be carboxylic and phenolic groups of the organic molecules (Essington 2003). The following study targets the behaviour of calcium and aluminium as cross-linking agents for SOM and its effect on rigidity of the organic matrix.

Calcium and aluminium are both known for their ability to complex dissolved organic (DOC) matter and to take part in cation exchange with soil organic matter (SOM). Interactions of Ca^{2+} and Al^{3+} with DOM are well known. In general a decrease in DOM is observed in attendance of Ca^{2+} or Al^{3+} (Shen 1999, Schaumann 2000, Oste, Temminghoff et al. 2002, Gustafsson, Pechova et al. 2003). Opposite effects were observed in competition with other cations: The binding of copper decreases in a Ca^{2+} - DOC solution (Iglesias, Lopez et al. 2003) but Zn sorption increases in attendance of Ca^{2+} and Al^{3+} in a soil solution (Gustafsson and van Schaik 2003).

There also can be found an effect on mineralisation due to these cations. Large contents of Al are thought to inhibit mineralization of C_{org} by flocculation, precipitation or toxic effects (Grodzinska-Jurczak and Mulder 1997). A considerable decrease of DOC mineralisation was found for solutions containing Al^{3+} with increasing initial $\text{Me}^{\text{n+}}/\text{C}$ ratio up to 0.1 (Schwesig, Kalbitz et al. 2003). In a field manipulation experiment in mature Norway spruce forest increased Al caused a pronounced decrease of DOC and a decrease of decomposition rate of SOM of 30% – 40% (Mulder, De Wit et al. 2001).

The described effects could be explained by the binding particularities of Ca and Al. Fest et al. describes the existence of metal-organic bonding with different strength and even different types of bonding were discussed (Fest, Temminghoff et al. 2005). Calcium is known for forming innersphere complexes with NOM carboxylate groups in contrast to magnesia or sodium (Kalinichev and Kirkpatrick 2007). Calcium prefers high molecular weight (HMW) organic acids for binding (Römken and Dolfing 1998). Al also forms innersphere complexes with NOM. At $\text{pH} < 4.2$ most Al is complexed by OM in form of Al^{3+} . Al^{3+} behaves as an exchanging trivalent “base forming” cation at a pH approximately 4.5 and below in organic horizons (Skjellberg 1995, Johnson 2002). Ross et al. (2008) hypothesised also separate types of bonding for exchangeable Al^{3+} and strong organically complexed Al^{3+} resulting in a not exchangeable form. The transfer between these two forms is assumed to be kinetically restrained (Bloom, Skjellberg et al. 2005). Small angle X-ray scattering (SAXS) suggested cross-linking by Pb^{2+} in Pb-DOM colloids (Lang, Egger et al. 2005). Pointing out these abilities of Ca^{2+} , Al^{3+} and other multivalent cations obviously we expect bridging behaviour of these cations between organic molecules in soil.

SOM can be regarded as a macromolecular matrix or from a supramolecular point of view (LeBoeuf and Weber Jr 1998, Lu and Pignatello 2002, Schaumann 2006). Hysteresis and non-

ideal sorption are tried to explain with this macromolecular models, which assume glassy and rubbery domains (Huang and Weber Jr 1997, LeBoeuf and Weber 1997, Xing and Pignatello 1997). Due to this point of view SOM can be compared with a synthetic polymer. These models indicate that large parts of SOM are amorphous and their structure is not in equilibrium, but changeable and dynamic. Multivalent cations are proposed to bridge free mobile side chains of these macromolecules as described for polymer networks (Huber, Praznik et al. 1993, Belfiore, McCurdie et al. 2001) and reduce their mobility (Schaumann 2006). Referring to the SOM model of a supramolecular structure (Piccolo 2002, Sutton and Sposito 2005) cations are thought to be one possibility of bridging small molecules with each other and forming an organic network where the mobility of the molecules is reduced (Simpson, Kingery et al. 2002, Schaumann 2006, Mouvenchery, Kučerík et al. 2012). Independently whether the mobility of molecular segments of macromolecules or of whole small molecules in a network is reduced in both models a higher rigidity of the matrix can be postulated. The degree of rigidity is measured with the differential scanning calorimetry (DSC) by the detection of a glass transition for amorphous substances. Glass transition temperatures were reported for isolated humic and fulvic acids (Leboeuf and Weber Jr 2000, Young and Leboeuf 2000) but also for whole soil samples (Schaumann and Antelmann 2000, Hurrass and Schaumann 2005).

The detection of glass transitions in SOM supports the described model (Hurrass and Schaumann 2005, Schaumann and LeBoeuf 2005). Up to now it is known that there exist two types of glass transitions in SOM. One named the classical one which also occurs in synthetic polymer systems and which is reversible in subsequent heating runs. The other one is only observed in water containing samples measured in a closed systems, this type of transition slowly reverse after days or weeks of storage depending on the sample (Hurrass and Schaumann 2005, Schaumann and LeBoeuf 2005, Hurrass and Schaumann 2007). The described thermal behaviour of SOM can be characterized by the glass transition-like step transition temperature named in this work step transition temperature T^* . The step transition behaviour can be explained by the hydrogen bond-based cross-linking (HBCL) model, which proposed cross-linking by individual water molecules (Hurrass and Schaumann 2005, Schaumann 2005, Schaumann and LeBoeuf 2005, Schaumann and Bertmer 2008). In addition to the bridging by water molecules an influence of multivalent cations by cross-linking organic molecules on step transition characteristics consequently on matrix rigidity is assumed (Schaumann 2006). Such assumptions are supported by experiments with fulvic acids complexed by Ca^{2+} , Tb^{2+} and Al^{3+} . Strong changes in intensity and absorption wavelength in fluorescence measurements for the Al^{3+} - fulvic acid complexes were found and the authors assume a more rigid matrix due to the results (Elkins and Nelson 2001).

Hurrass & Schaumann (2007) investigate the changes in moisture status on the thermal behaviour of SOM. The results of the study support the HBCL-Model and demonstrate a slowly reversing T after a first heating cycle. More than 7 month were required for a complete reversibility of T^* . The required reversing time was supposed to be equal with the time of form-

ing water molecule bridges in the organic matrix. From these observations we generally assume that the development of an increasing rigidity or higher networking including conformational changes in a solid matrix are related to slow processes. Therefore we also take for the formation of cation bridges slow processes in account. What means that not only the absolute cation content influences the organic matrix but also the absorption mechanism plays an important role.

Due to the description on interactions of cations and SOM and formation of cross-links in SOM the following hypotheses can be derived:

- I. Multivalent cations like Ca^{2+} and Al^{3+} induce coordinative cross-links in SOM which results in a more rigid matrix
- II. An increasing content of cations effects an increasing rigidity, a decreasing content of cations effects a decreasing rigidity
- III. Al^{3+} is more effective for rigidity than Ca^{2+}
- IV. Structural conformations due to the formation of co-ordinative cross-links with multivalent cations are based on slow processes and therefore soft and slow absorption mechanism influences matrix rigidity stronger (increasing effects) than abrupt changes in cation status
- V. The aging effect due to water bridges for the cation treated samples is less pronounced than for no-treated samples because of the higher saturation of cross-linking sites in SOM
- VI. Conformational changes and aggregation often lead to a higher hydrophobicity of samples, therefore samples with coordinative cross-links and a higher rigidity are more hydrophobic than samples with lower rigidity

The investigation of the hypotheses is conducted with a solid soil sample and different cations in varying concentrations and with different methods of cation addition. All samples were analyzed with DSC for their matrix rigidity. In the following study are three central parts to check the hypotheses: influence of cation de- and absorption on rigidity, influence of time on rigidity and influence of the found rigidity on the hydrophobicity of the samples.

2.3 Material and Methods

2.3.1 General strategy

Checking hypotheses I – IV)

To investigate the influence of multivalent cations on matrix rigidity the cation status of the sample is to change and effects are to determine by DSC. The water content remains constant for all samples at the timepoint of analyzing the rigidity in the matrix.

There are two possibilities to change the cation status in a sample: to add or to reduce the cations. More precisely it is always an exchange of cations whereby an addition means an exchange of the desired cation like Ca^{2+} or Al^{3+} with other mono-, di- and perhaps tri-valent cations but also with H^+ . A reduction means an exchange of metal cations in general with H^+ (in the chosen procedure). Hence practical methods are recommended to do this in a way nearest natural conditions with the objective to conduct homogenous results in cation content and matrix rigidity. In the following a percolation (“soft” absorption of cations) and a batch method (abrupt changes in cation status) for the absorption of cations were introduced and discussed on the results. Also a method of demineralisation is conducted inducing cation depletion by acidic conditions observed during podsolation processes (Klitzke, Lang et al. 2008). According to the chemical differences of Al^{3+} and Ca^{2+} and also according to their different acting in SOM or soil solutions mentioned before also varying effects were assumed on matrix rigidity of those multivalent cations.

Cation depletion was only conducted in a more radical way with an acidic exchange resin, because we were focussed on condition where all exchangeable cations were removed from the samples and not on a stepwise decrease of cations in the sample.

Checking Hypothesis IV)

To control the influence of water bridging between organic molecules, samples were stored for a longer time under constant humidity and temperature conditions. The question is if there is an aging effect detectable although a part of the cross-linking sites are occupied by multivalent cations. No difference in T^* measured at different time points is obtained if the cross-linking sites of water molecules and of cations are identical in SOM.

Checking Hypothesis V)

In literature hydrophobic effects are observed for air dried samples with a high amount of SOM. Is there a correlation between a formation of a network in the interior of the SOM and hydrophobic effects at the surface? For answering this question a selection of the treated samples were also investigated for their hydrophobicity.

2.3.2 Soil Samples: Preparation, characteristics and storage

Spruce Forest Soil

The soil sample used for the following experiments (addition of cations and demineralization) was an organic layer from an 80 year old spruce forest in South Germany. Immediately after sampling and homogenizing the sample was shock frozen and then stored in a freezer at minus 18°C. For the experiments the sample was unfrozen in a fridge and air dried. The water content of the samples differs between 7 and 8% percent after drying. Then the sample was sieved at 1 mm, some needles have to be collected manually from the samples and common soil characteristics were determined (Table 3): Cation exchange capacity CEC was analysed using barium chloride solution as it is described in DIN ISO 11260 (effective $\text{CEC} = \text{CEC}_{\text{eff}}$)

and DIN ISO 13536 (potential CEC = CEC_{pot}). Gustafsson and Pechova (2003) confirm extraction with barium chloride is a good indicator for active Mg²⁺ and Ca²⁺ (Gustafsson Jon, Pechova et al. 2003). Obviously there is a large difference between CEC_{eff} and CEC_{pot} for the sample this is due to the high amount of C_{org} and the low pH and also reported for other high organic and acidic forest soils (Ross, Matschonat et al. 2008). PH was measured in 0,1 M calcium chloride solution after 30 min. For further treatment the sample was stored in PE bottles at room temperature.

| pH | C _{org} /% | CEC _{pot} /mmol _c kg ⁻¹ | CEC _{eff} /mmol _c kg ⁻¹ | WC /% | Ca ²⁺ /mmol _c kg ⁻¹ | Mg ²⁺ /mmol _c kg ⁻¹ | Al ³⁺ /mmol _c kg ⁻¹ |
|-----------|------------------------|--|---|----------|--|---|---|
| 3,7 ± 0,1 | 43 ± 4 | 671 ± 50 | 303 ± 20 | 8 ± 1 | 165 ± 10 | 43 ± 5 | 60 ± 3 |

Table 3: Common soil characteristics of the used organic layer from a spruce forest

After the described treatments (cation addition by percolation / batch experiments and demineralization experiments) the samples were dried in a drying chamber at 25°C for 4 days and then stored in acryl glass desiccators at 20°C and 76% relative humidity, adjusted by saturated NaCl - solution. The conditioning time depended on the objection of each experiment and is found in each treatment description section of this work. During conditioning the samples were stored evenly distributed in open petri dishes to assure the same conditions for all particles.

Peat samples

For the demineralising experiments two peat samples were used. One peat was collected from Fuhrberg near Hannover in Middle Germany the other from the Heudorfer Ried in South - West Germany, Hegau. The common soil characteristics are presented in Table 4.

| | pH | C _{org} /% | CEC _{eff} / mmol _c ·kg ⁻¹ |
|---------------------|-----|---------------------|--|
| Peat Fuhrberg | 2.7 | 52 % | 123 |
| Peat Heudorfer Ried | 5.8 | 25 % | 680 |

Table 4: Common characteristics of the two peats

A special characteristic of the peat Fuhrberg is the fact that no microbial activity was measured, so no changes by microbial interaction can be anticipated. Furthermore much more information on this peat is found in (Jaeger, Shchegolikhina et al. 2010).

2.3.3 Preparative methodical study: developement of an optimized method to load SOM samples with cations

The objective of these treatments was to add more specific cations (Ca²⁺ or Al³⁺) to the sample in a stepwise procedure to achieve several homogeneous samples with six different cation

amounts. We want to prevent a cation uptake which exceeds the number of available exchange sites in the samples therefore the cation concentration in the solution was adjusted on the maximum amount which can be absorbed by the samples. The final concentrations in the sample should vary between the original concentration of the respective cation and the effective CEC. No formation of salt crystals in the samples was desired, because these cations have no influence on the structure of SOM. We want to find out a method which results in a high degree of cross-linking as described in chapter 2.2. On the one hand we want to achieve a slow sorption of cations in percolation experiments with a slow flow-through, several percolation cycles with drying periods during the whole procedure and a slightly increasing cation concentration in the solution at each percolation cycle. In our point of view such a method would be near environmentally conditions. In contrast to the very slow percolation method we decided to use a more abrupt method of cation addition which assures a more homogenous distribution of the cations in the samples. Therefore the samples were shaken in a batch with the cation solutions.

In the treated samples the effects of the cation content and of the method of addition on cross-linking in SOM should be determined. The experiments were in the same order conducted as described below. At the end the batch experiments turned out to be most stable for further measurements. Nevertheless it seems to be important to present also the non-succeeding methods to analyse the problems and to prevent failures for future research. However some of the percolation results are quite interesting and should be discussed further on.

Percolation with small sample amounts

The background for using percolation for the addition of cations was to use a soft method which did not alter the sample in a radical way (see hypothesis III). So observable effects can be related to cation content not to mechanical influences as happened during shaking for example. We wanted to offer conditions for supporting the “growing” of cross-links in SOM like it was reported for water molecule bridges in SOM depending on the pretreatment (Hurrass and Schaumann 2005).

Therefore we decided to use a stepwise percolation procedure interrupted by drying phases initiating further actions in SOM (e. g. effects of swelling and drying processes) and homogenous distribution of the cations in SOM.

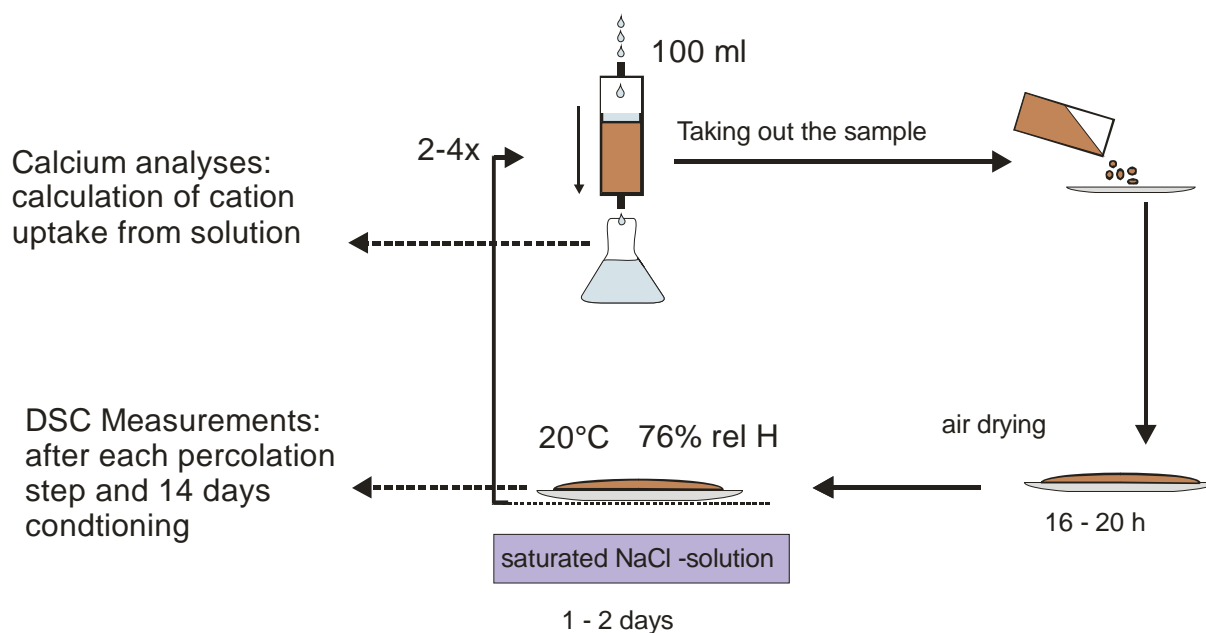


Figure 1: Procedure of percolation with Ca^{2+} solution for creating sample with different cation contents and various degrees of cross-linking in SOM

For each percolation 3.5 g of the soil sample were filled in a 25 ml PE syringe used as column and 100 ml solution were used for percolation. Three Ca^{2+} solutions ($\text{Ca}(\text{NO}_3)_2 \cdot 4 \text{H}_2\text{O} \geq 99\%$ p.a., Carl Roth GmbH) differing in concentration were used: 5 mmol l^{-1} , 8 mmol l^{-1} and 10 mmol l^{-1} . The percolations were conducted for at least two times and at most four times, each of them took 1.5 hrs until the whole solution was running through the column. The procedure is given in Figure 1. After the first percolation there was a drying phase for 3 days after that a new percolation with a solution of the same concentration took place. During each percolation cycle a short amount of the sample (few mg) was conditioned for 14 days and matrix rigidity was measured with DSC. To minimize the losses of DOC we used soil solution from the same sample as basis for the cation solutions (preparation is described in “Percolation with larger samples amounts”). The cation concentration of the solution was measured before and after passing the column to analyse the absorption of the soil sample and to calculate the soil concentration. An aliquote of the dried soil sample of each percolation step was extracted with 0,025M Ammonia – Ethylenediamine tetraacetic acid solution (EDTA \square 99%, p. a., Carl Roth GmbH) for cation analyses. The percolations were conducted in duplicate.

Percolation with larger samples amounts

After having first experiences with percolation of a very small amount of sample we now tried to percolate in larger quantities. Therefore 15 g of the organic layer was filled in a glass column (400 mm*20 mm, Lenz DIN 29/32, Duran glass) with PTFE valve. On the bottom of the column a glass wool layer with a thickness of 2 cm between two glass fiber pre-filters (GF 92, Schleicher & Schuell) were used to avoid the loss of soil particles during percolation. Solution and soil were put alternately in the column by periodically stirring. Suspension was homoge-

nized and air was removed. This procedure was stopped when the whole sample was saturated with salt solution and no dry areas in the column were observed.

The solutions for percolation were prepared from a DOC solution of the spruce forest samples. Therefore 30 g sample (sieved on 2mm) and 750 ml deionized water were horizontal shaken for 3 hrs. After shaking the suspension was filtered by pressure on 0.45 μm cellulose acetate filters (Sartorius®). The $\text{Ca}(\text{NO}_3)_2$ was first dissolved in 100 ml deionized water and then mixed with the DOC solution to prevent formation of preprecipitates.

Samples were percolated approximately for four times with a Calcium Nitrate ($\text{Ca}(\text{NO}_3)_2 \cdot 4\text{H}_2\text{O} \geq 99\%$ p.a., Carl Roth GmbH) solution. The first and second time with a concentration of 5 mmol l^{-1} , the third time with a 8 mmol l^{-1} and the fourth time with a 12 mmol l^{-1} Ca^{2+} solution. This procedure is different to the percolation experiments before but it results from the fact that after step 2 often no further increase in cation content of the samples was observed.

For each percolation 375 ml of Ca^{2+} solution was used. One percolation took 2 – 2.5 hours the flow rate was 3 ml in average regulated by a flexible tube pump. Sometimes especially for solutions with lower cation concentrations the flow stopped and the suspension in the column had to be stirred.

Then the sample was removed from the column by compressed air. Remaining solution in the sample was separated by vacuum filtration (589/2 Filter Paper Circles, ashless, Whatman®). Each sample was dried for 48 hrs at 25°C in a drying chamber and after drying it was stored at 20°C and 76 % relative humidity in a desiccator for 2 days. Before and after drying the samples were weighed to determine the remaining water after percolation. Then the percolation procedure started again. After the whole treatment the samples were stored in a desiccator at the described conditions. Finally there were four different treated samples, prepared in triplicates. One sample only was percolated with deionized water as control. The percolated solutions from each step were filtrated at 0,45 μm (Cellulose Nitrate Filter, Sartorius®) and analyzed for pH, Calcium and Dissolved Organic Carbon (DOC). An aliquote of the dried soil sample was extracted with 0,025M Ammonia – Ethylenediamine tetraacetic acid solution (EDTA 99%, p. a., Carl Roth GmbH) for cation analyses. After conditioning for 4 weeks soil samples were measured with DSC.

Batch experiments

Samples were treated at pH 4 with calcium nitrate, aluminium nitrate and sodium nitrate solutions. 10 g of the original sample were spiked with 250 ml solution in 500 ml Duran glass bottles. Altogether 8 different concentrations for Ca^{2+} (0.5, 1, 2, 4, 5, 8, 10 mmol l^{-1}) and 7 different concentrations for Al^{3+} (0.05, 0.25, 0.5, 2, 4, 6, 8 mmol l^{-1}) were chosen. Samples treated with Ca^{2+} were prepared in triplicate, samples treated with Al^{3+} were prepared in duplicate. Another set of samples was treated in the same way with different Na^+ salt solutions (10, 50, 100 mmol l^{-1}) and deionized water as control. Additionally one subsample of 10 g was moistened with 10 ml deionized water, this correlates in average with the remaining wa-

ter content of the samples after filtration. So this control does not lose any cations and organic matter. The samples were shaken for 3 hours in a horizontal shaker. PH was monitored after 0,5 and 1,5 hrs and adjusted with 1 M HNO₃ or 0.5 M NaOH to pH=4 if necessary. Then the solution was separated by vacuum filtration for 10 minutes (589/2 Filter Paper Circles, ashless, Whatman®). The soil samples were weighed to calculate the amount of remaining water and then the samples were dried and stored as described above.

The T* measurements took place after 4 weeks of conditioning for all samples. The Ca²⁺ treated samples were measured after 12 and 22 weeks, stored as described above, the Al³⁺ and Na⁺ treated samples were measured after 9 and 18 weeks.

2.3.4 Demineralisation experiments

Demineralisation experiments were conducted with an acidic cation exchange resin (ion-resin Amberlite® IR120, H⁺-Form, exchange capacity 2.3 mmol_c g⁻¹, Merck, Darmstadt) as formerly described in (Kaupenjohann and Wilcke 1995). For each experiment 2,5 g of the resin was welded in a finely meshed polypropylene net (mesh size 72 µm). Each resin bag was then washed in 10% HNO₃ – solution for 30 min and rinsed with deionized water to remove DOC and free acid. In preliminary tests measurable DOC fractions were found in blank samples.

The intention was to extract all changeable cations in SOM in exchange to H⁺ and to obtain the effect on the structure of SOM after depletion. (Hypotheses I & II)

For each sample 2 g of the peat or organic layer and 50 ml water were mixed for 15 min in a horizontal shaker in a 100 ml PE bottle. This procedure assures a complete wetting of all particles. After this “wetting procedure” the resin bags were added to the suspension and treated in a horizontal shaker for 24 hrs.

In each sample the pH were controlled after 30 min. For all samples no adjusting of pH with BaNO₃ as described in Kaupenjohann & Wilke, 1995 were necessary because all pHs are near or lower the required pH value of 3. This was also due to the fact that a highly decreasing pH can be an indication for existing salts in the sample itself. So if the pH decreases it can be assumed that not all extractable cations are absorbed to SOM but originated from soluble salts.

At the end of the extraction the pH was measured and the resin bag was rinsed again with deionized water because adhering particles had to be removed from the resin. The soil water suspension was filtered for DOC measurements (0.45 µm; Sartorius®). The resin bags were extracted in 50 ml HNO₃ solution for 2 hrs. As control deionized water was used for the extraction. The extracted solutions were then analysed for Ca²⁺ and Mg²⁺ as described in 2.3.5.

The soil samples were treated as described in 2.3.2 and T* was determined by DSC. For the samples of Fuhrberg and Heudorfer Ried only one sample was extracted, for the spruce forest layer the experiments were conducted in duplicates.

2.3.5 Chemical Analyses

The supernatant from the batch experiments were analyzed for pH, cation concentration and DOC. Immediately after the batch procedure pH and DOC were measured. For determination of DOC the solutions were filtrated with 0.45 μm cellulose nitrate filters (Sartorius®), before the filters were flushed with warm deionized water to minimize contamination. The DOC concentration was analyzed with a TOC Analyzer Multi C/N 2100 (Analytik Jena) after acidification and outgassing of inorganic carbon.

To calculate the absorption of the cations of the samples the solutions were analyzed for the added cations (Al^{3+} , Ca^{2+}). Furthermore selected sample for Mg^{2+} , Fe^{3+} and Mn^{2+} to calculate the exchange in the soil sample. Ca^{2+} and Mg^{2+} were analyzed with Flame AAS (Perkin Elmer 4100; Varian AA 240 FS for Al^{3+}) with an oxygen/acetylene flame, Al^{3+} with a nitrous oxygen / acetylene flame (Varian AA 240 FS) and Fe^{3+} and Mn^{2+} were analyzed with Graphite Tube AAS (Perkin Elmer 4100). In general a calibration curve was conducted by internal standardisation (Standardaddition) or if no differences were identified between the curves by an external standardisation in the same solution (e. g. EDTA or 10% HNO_3). The solutions of the controls were analyzed for Ca^{2+} , Mg^{2+} and Al^{3+} to calculate desorption from soil.

To quantify the cations which were linked to SOM from each soil sample two aliquots (1.5 g) were extracted with 40 ml 0,025M ammonium tetra acetate – ethylenediamine tetraacetic acid solution (EDTA \geq 99%, p. a., Carl Roth GmbH) at pH 4.6 for 3 hrs and then for 10 min with 1 M ammonium tetra acetate solution. The extracts also were further analyzed for Ca^{2+} , Al^{3+} , Mg^{2+} , Fe^{3+} and Mn^{2+} with Flame or Graphite Tube AAS as described above to verify the results from soil solution measurements and to quantify total cation contents in SOM.

So for each sample there were two values for cation content available and a validation was possible.

2.3.6 DSC measurements

Differential scanning calorimetry experiments were performed to characterize the thermal behaviour of the treated samples and to quantify the level of cross-linking of SOM. Analyses were performed with a DSC Q1000 (TA Instruments, Germany) with a refrigerated cooling system (RCS) and nitrogen as a purge gas. All samples were abruptly cooled in the DSC instrument to -50°C and then heated with 10 K min^{-1} from -50°C to 110°C , followed by a second abrupt cooling and subsequent heating cycle. Baseline was corrected with the TZero technology® by TA Instruments.

Data were analyzed using Universal Analysis version 4.1 (TA Instruments). The glass transition like step transition temperature T^* is indicated by an inflection point in the thermogram. Operationally, three tangent lines were applied for the evaluation. The change of heat capacity ($\Delta c_p = \text{J g}^{-1} \text{K}^{-1}$) was calculated from the height of the central tangent line. In the following sections only the first heating cycle will be observed because the determined T^* is a non-reversing thermal event (Schaumann and LeBoeuf 2005). The baseline correction applied by

Hurraß & Schaumann was not applicable in this study due to significant thermal events in the second heating cycle.

A total of 1-3 mg of the sample was placed into hermetically sealed Aluminum pans. 3 to 7 replicates were carried out depending on the quality of the resulting thermograms, so that for each sample at least 3 significant transition temperatures were available.

2.3.7 Contact angle measurements

The contact angle measurements were conducted with the sessile drop method as described in Diehl et al. (Diehl and Schaumann 2007). The samples are fixed by double sided adhesive tape on a glass slide (Bachmann et al., 2000b). Pictures were taken by a digital camera and then were used for geometrical analysis of drop shape and calculation of the respective contact angles. The water drop forms a shape that depends on the interfacial tensions (γ) on the three adjacent surfaces: solid (s), liquid (l) and vapour (v). the angle at the three phase contact line between the solid-liquid (sl) and the liquid-vapour (lv) interface is called the contact angle, θ .

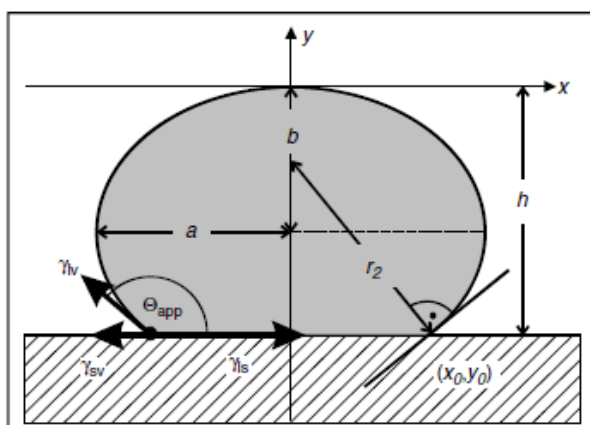


Figure 2: A sessile drop fitted as ellipsoidal cap showing the vectors of interfacial tensions, γ , at the dro-pedge, the observable contact angle θ_{app} and elliptical parameters a , b , h necessary to calculate θ_{app} and drop volume V (Diehl and Schaumann 2007).

Observing a high contact angle means a surface with a high hydrophobicity.

2.4 Results and Discussion

2.4.1 Cation addition by percolation and by batch experiments

Percolation with low sample amounts: Cation content and T^*

From the first percolation with small sample amounts results 18 samples (including the duplicates) treated with varying cation concentrations and with a varying number of percolations (2 – 4 times).

The cation content of the samples was analyzed by EDTA extraction and Flame AAS as described in chapter 2.3.5.

As seen in Figure 3 the cation uptake of the samples was higher than expected. The Ca concentration in the samples ranged between 320 and 400 mmol_c kg⁻¹. These values exceed the effective CEC of 300 mmol_c kg⁻¹. The objective of the cation addition was to achieve samples with Ca²⁺ contents ranging in uniformly distributed intervals between the original Ca content and the CEC_{eff}. This distribution was not achieved. Referring to the exceeded CEC_{eff} on the one side the formation of inorganic salts in the samples is expected on the other side due to the different experimental design in the procedure of cation exchange in CEC (over top shaking and centrifugation) and in the conducted percolation it is to consider that DOC losses are higher for the CEC method than in the percolation method and available sorption sites for cations are lost in the CEC method. We assume that both effects are responsible for the exceeding cation concentrations in the samples.

Most of the samples show an analyzable step transition in the first heating cycle. A change of heat capacity of 0.1 – 0.3 Wg⁻¹K⁻¹ in a temperature range of 58°C – 64°C can be obtained for the treated samples. This is a typical temperature range for samples with a high amount of SOM (Schaumann, 2005; Hurrass & Schaumann, 2005). The observed step transition is non reversible, what means in the second heating cycle no step transition in this temperature range can be obtained. However there is a step transition at 71°C until 74°C with a very low change of heat capacity (0.01 – 0.04 Wg⁻¹K⁻¹) in the second heating cycle. This event can be identified for all treated and also untreated samples but no changes can be obtained in dependence from the cation content or percolation cycle. In the first heating cycle the described step transition is not visible because it is overlaid by the described more intensive step transition.

Referring to the characteristics of the step transition the thermal event can be identified as glass transition-like step transition temperature T*. T* of the samples is related to the same samples analyzed for Ca²⁺ in Figure 3. It is well pronounced that all treated samples show a significant higher step transition temperature than the original sample. But there are also differences between the samples treated with different percolation solutions though the Ca²⁺ concentration in the samples are very similar.

Samples treated with a Ca²⁺ solution of 5 mmol l⁻¹ are all show higher T* on average than the samples treated with solutions of higher concentrations. Especially the 5 mmol samples with lower Ca²⁺ contents demonstrate the highest T*. The samples treated with the highest Ca²⁺ concentration in solution show the lowest increase in T*. The slope of T* increases in the following order 10mmol treatment < 8 mmol treatment < 5 mmol treatment. Hence it can be concluded that T* is not only dependent on the cation content in the sample but it also depends on the manner of addition: low concentrations in the solution promote a higher matrix rigidity of the SOM. By this result hypotheses III is supported in which the mechanism of absorption is related to structural conformations which are proposed to play an important role in the development of cross-links in the interior of the organic matrix. In hypotheses III it was postulated that abrupt changes of the cation status in the sample would have a lower effect on rigidity than slower changes.

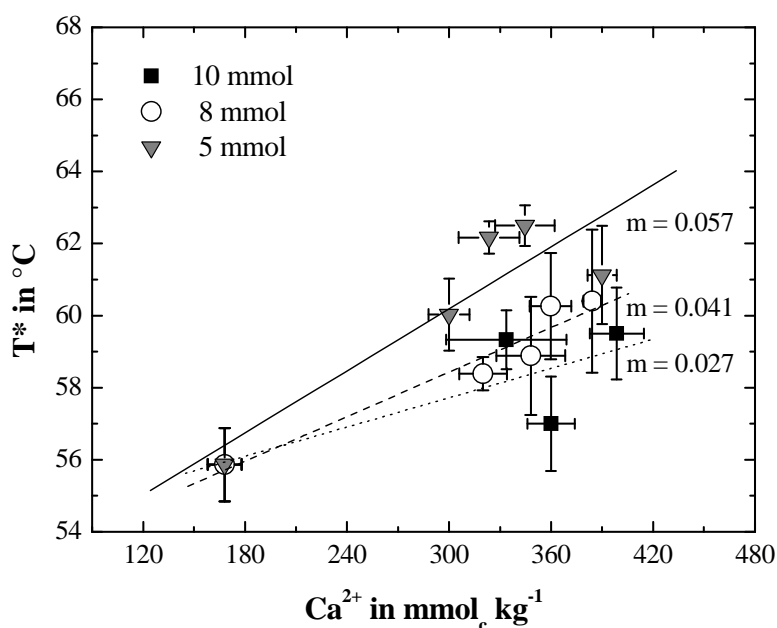


Figure 3: Step transition temperature T^* in dependence of the Ca^{2+} content of the sample and the concentration of the used percolation solution (5 mmol, 8 mmol, 10 mmol) after 4 weeks conditioning.

No influence on T^* was observable for the number of percolation cycles independently from the used percolation solution. Considering the higher number of drying and rewetting processes which is suggested to enhance conformational changes (Simpson, Kingery et al. 2002, Schaumann 2006) an effect was expected.

However with regard to the same samples aged for nine months under constant conditions in a desiccator the differences between the treated samples vanished.

As shown in Figure 4 the overall standard deviation of T^* increases for all samples from .1.0°C to 2.6 °C. Therefore the quality of linear regression of the values decreases and the increase of T^* is not as significant as it was at the 4 weeks measurements. The mean values of the treated samples are closer to each other than after 4 weeks conditioning time. Also the clear differences between the original sample and the treated samples shown in Figure 3 are not demonstrated anymore. Only the order of the increase of T^* between the different treated samples is still the same but much not significant.

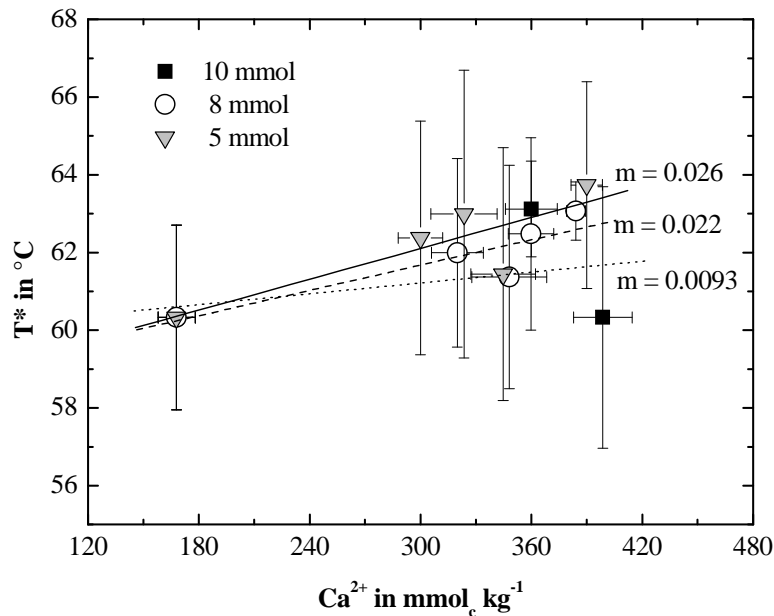


Figure 4: Step transition temperature T^* in dependence of the Ca^{2+} content of the sample and the concentration of the used percolation solution (5 mmol, 8 mmol, 10 mmol) after 9 months conditioning.

The concentration of the percolation solution have an influence on T^* by regarding a short time period, but after a longer time period this increase vanished. Hence, conformational changes induced in the samples percolated with a 5 mmol l^{-1} solution are also took place in the other samples but some more conditioning time is needed for these changes. Generally the overall increase of T^* demonstrated a high influence of water-bridges which were suggested to be responsible for matrix aging in SOM (Hurraß & Schaumann, 2005). The role of water is deeper discussed in the following chapters.

Percolation with larger sample amounts: DOC, Cations and T^*

The central variation in the experimental design of percolation with larger samples amounts in comparison to the percolation with small amounts was the change of the cation concentration in the percolation solution at percolation step 3 and 4. Nevertheless as seen in Figure 5 the use of higher concentrated solutions in the last percolation steps did not effect the cation content in the soil samples. It is demonstrated that the main uptake of Ca^{2+} took place at the first two cycles then no further significant uptake can be observed. Especially for the third cycle it cannot be excluded that there is a decrease of Ca^{2+} in the samples. Due to the results of the analyses of the percolation solution this also can be obtained for the 4. cycle. In conclusion after the second percolation cycle a constant Ca^{2+} content in the samples can be assumed for further percolations independently from the Ca^{2+} concentration in the solution. This observation is in line with the results of the percolation with smaller amounts. In the second percolation the cation uptake is much lower and did not exceed the CEC_{eff} . It can be assumed that

this is caused by the slower flow through and the higher amount of percolation solution in relation to the sample amount (3.5 g / 100 ml versus 15 g / 370 ml) at the first percolation experiment. Furthermore the samples were drained after the treatment at the second percolation so the remaining Ca^{2+} solution was lower than in the first experiments.

The differences between the results of the analyses of the percolation solution and the results of the measurements of the EDTA extracts are also shown in Figure 5. For the first three percolation cycles the values of the replicates are very similar only for the fourth percolation step the values show a significant difference. Regarding the laboratory praxis no reason for this difference can be identified. But in conclusion the values do not change the general trend of the curve. In the following figures only the results of the EDTA extraction were considered because a better comparability of the results between the different experiments in this thesis is warranted in this way.

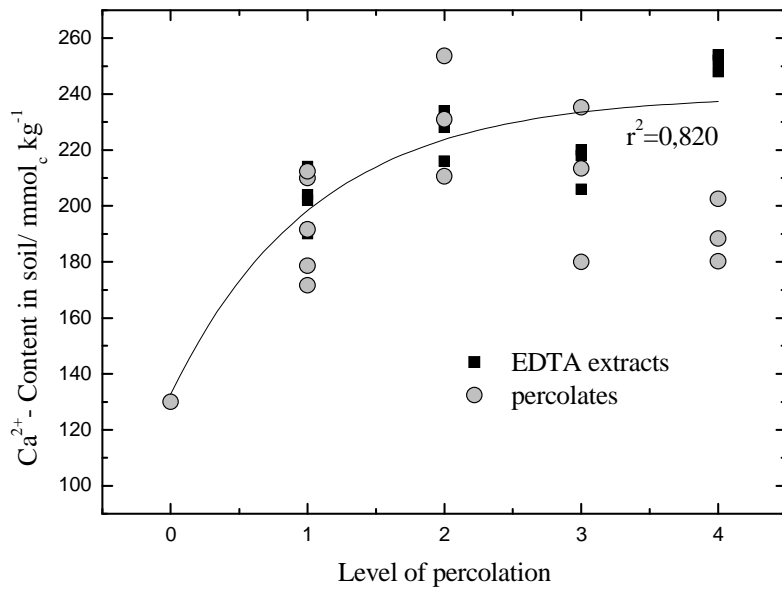


Figure 5: Ca²⁺ contents in the treated samples from the mass balance analyses in the percolation solution and from EDTA extract from the samples itself

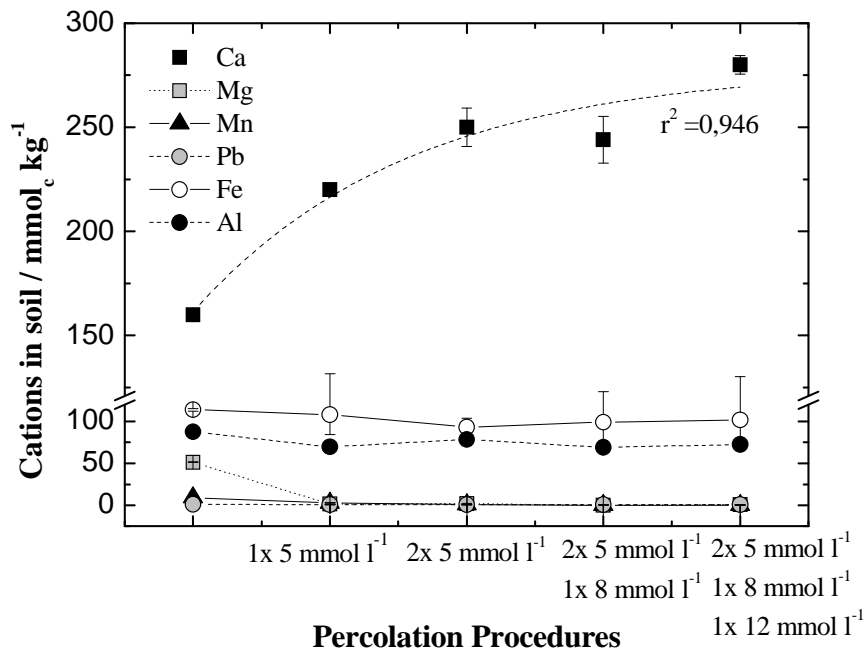


Figure 6: Cation content of the samples after each percolation cycle during the addition of Ca²⁺, the percolation cycles and its concentration are given at the x-axis. The content was measured by EDTA extraction of an aliquot of the samples.

In the EDTA Extracts additional cations were analysed to identify the main exchange partners of Ca^{2+} . This knowledge is very important for a correct interpretation of the DSC results. For example no increase on T^* can be assumed if Ca^{2+} is changed with other cross-linking cations. As it is seen in Figure 6 mainly Mg^{2+} is in exchange with Ca^{2+} also a small amount of Mn^{2+} exchanges with Ca^{2+} . The amount of H^+ ions, Na^+ , and K^+ involved in the exchange processes in acidic soils (Ross et al. 2008) is unknown but can be expected because the amount of Ca^{2+} in the samples is clearly higher than the losses of Mg^{2+} and Mn^{2+} . As what is known about the cross-linking or complexing effects of all available exchange cations (Kalinichev and Kirkpatrick 2007) there no decreasing effects on T^* by exchanging mechanism are expected.

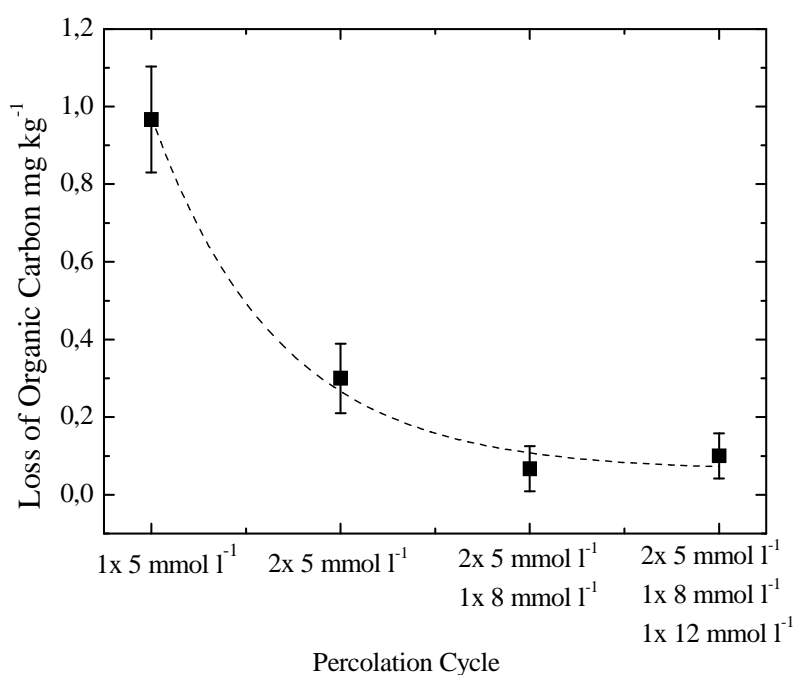


Figure 7: Losses of organic carbon during the percolation cycles, averages from all treated samples (standard deviation based on the individual values). It is stated that the values are related to the losses of DOC at the specific percolation step, what means the overall loss of DOC for the sample percolated for four times is the sum of the values in each step.

The losses of DOC decreased with an increasing number of percolations and an increasing Ca^{2+} concentration in the solution as shown in Figure 7. This result was expected because within several leaching processes the fraction of dissolved carbon should be reduced. Furthermore higher cation concentrations in the solution should prevent high losses of DOC (e. g. (Römken and Dolfing 1998, Schaumann 2000)).

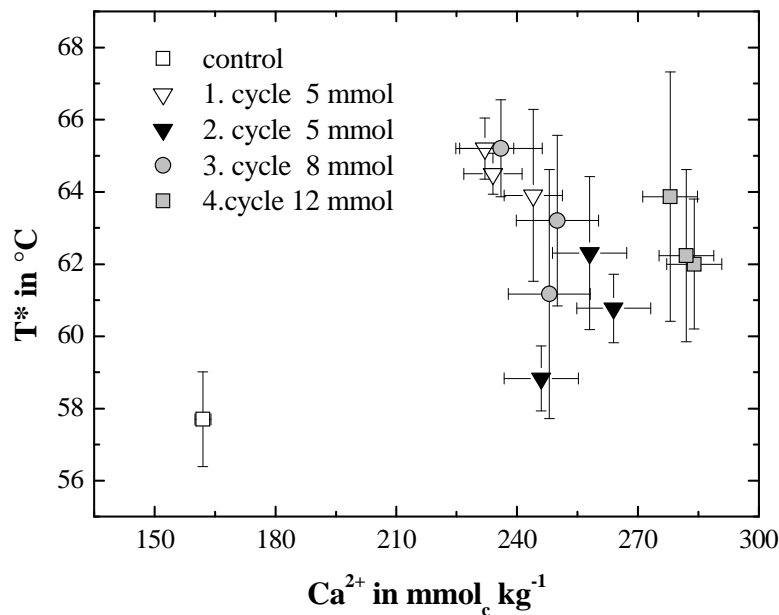


Figure 8: T* of the different treated samples of each percolation cycle and for the control

In Figure 8 the determined T* of the different percolation cycles are shown. In contrary to the first percolation no relation is recognizable between concentration of the percolation solution and step transition temperature. There is also no difference between the number of percolation cycles. The standard deviation of the temperature is very high in some cases the value is 3°C and higher therefore no significant differences are recognizable even to the control percolated with DOC solution. In general all treated samples show in average a higher T* than the control, the control and the original non treated sample show always similar values. Also in this experiment there is a lack of calcium content between 160 and 220 mmol_c / kg and therefore a Ca²⁺ content of uniformly distributed intervals was not achieved.

Looking at Figure 8 there is a downward drift recognizable for T* of higher Ca²⁺ concentrations in the sample.

This observation is underlined when the results of two percolation designs are compared with each other independently of the used solutions and the number of cycles. A decrease of T* can be observed for the treated samples. As it is shown in Figure 9 the linear fit gives a decreasing tendency with a low significance ($p = 0.2$). However it is to be mentioned that the results from the first percolation are to be analyzed carefully because the Ca²⁺ content exceeds the CEC_{eff} and the amount linked to SOM cannot be differentiated to the amount possibly available as salt crystals.

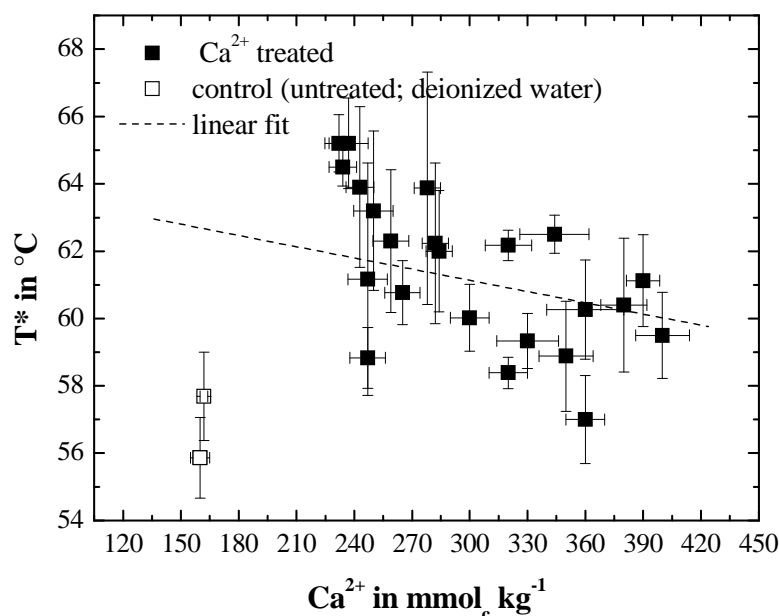


Figure 9: Decrease of T* with higher Ca²⁺ contents in the samples.

So it is to be discussed further on if the relationship of higher cation content and less matrix rigidity can be confirmed by more results on cation treated samples. In consequence to the decrease of T* there also should be an increase between Ca²⁺ contents of 160 and 220 mmol_c kg⁻¹.

For both percolation designs some problems in the performance of the experiments can be identified. No constant Ca²⁺ contents in the duplicates or triplicates were achieved (differences of ± 20 mmol_c kg⁻¹) High deviations in T* of the same treated samples referring to deviations of the original samples and to literature data (Schaumann, 2005) make general conclusions and statistical evaluations difficult. It is to point out that for the whole thesis the creation and description of cation treated samples is only the first step, more important is to know something about the effects of cations in SOM. For such experiments a large treated and homogeneous sample amount is necessary.

Batch experiments: DOC, Cations and T*

Batch experiments were performed to solve these problems of heterogeneity. This method of cation addition was not preferred at the beginning of the study because it can be stated as a relatively harsh method further from natural processes than percolation and leading to an abrupt change of the cation status and mechanical stress. But the formerly used percolations do not show a high influence of the experimental design (different percolation solutions, wetting and drying procedures between the stepwise percolation show no influence on T*). The

Batch experiments were conducted with NaNO_3 , $\text{Ca}(\text{NO}_3)_2$, and $\text{Al}(\text{NO}_3)_3$ solutions. The used solution concentrations were partly lower than for the percolation experiments to create samples especially in a concentration range where an increase of T^* is anticipated due to the results from the percolation experiments.

The cation content of samples increase with increasing concentration of the respective cation in the solution and approaches a cation-specific maximum. The maximum content of Ca^{2+} (270-300 $\text{mmol}_c \text{ kg}^{-1}$) is reached by treatment with an initial concentration of 5 mmol kg^{-1} in the solution. The CEC_{eff} is not exceeded thus no salt crystals are expected to be in the samples. It can be assumed that all accessible exchange sites in SOM are saturated with Ca^{2+} . There was no significant difference between the results of the analyses of the soil solutions or of the EDTA extractions of the soil samples. In comparison to the percolation experiments there are now also samples with 160 to 220 $\text{mmol}_c / \text{kg Ca}^{2+}$ and the standard deviation is now only $\pm 10 \text{ mmol}_c \text{ kg}^{-1}$.

The exchange partners of Ca^{2+} are the same as in the percolation experiments determined. Ca^{2+} mainly replaces Mg^{2+} from its exchange sites, which is indicated by a decrease of Mg^{2+} in the samples from 40 $\text{mmol}_c \text{ kg}^{-1}$ to almost 0 for high Ca^{2+} solutions. The amount of Manganese decreases from 10 to 4 $\text{mmol}_c \text{ kg}^{-1}$, whereas Al^{3+} and Fe^{3+} in the samples were constant even for the highest concentrated Ca^{2+} solutions.

Similar results were measured for the exchange with Na^+ (not shown): Ca^{2+} and Mg^{2+} were exchangeable with Na^+ and their content decreases with increasing Na^+ concentration in the solution. Due to analytical problems it was not possible to measure Na^+ directly in the batch solution or the EDTA extracts (EDTA was used as sodium salt). Therefore the following estimation is made based on the results of Mg^{2+} and Ca^{2+} concentrations in the batch solutions after treatment (see Table 5).

| Na^+ conc. initial solution / $\text{mmol}_c \text{ l}^{-1}$ | Ca^{2+} loss in treated samples / $\text{mmol}_c \text{ kg}^{-1}$ | Mg^{2+} loss in treated samples / $\text{mmol}_c \text{ kg}^{-1}$ | Estimated Na^+ sorption of samples / $\text{mmol}_c / \text{kg}^{-1}$ |
|---|--|--|--|
| 10 | 16 ± 1 | $8,3 \pm 0,5$ | ~ 24 |
| 50 | 40 ± 3 | $21,5 \pm 1$ | ~ 60 |
| 100 | 58 ± 4 | $27,6 \pm 1$ | ~ 90 |

Table 5: Estimated results for Na^+ sorption during batch experiments on losses of Ca^{2+} and Mg^{2+}

It can be concluded that at least 90 $\text{mmol}_c \text{ kg}^{-1}$ are presented in the samples treated with the highest Na^+ concentration. It is assumed that this value is underestimated because not all exchange partners were considered in the calculation. According to the results of Ca^{2+} - sorption of the samples it was shown that more than a double of Ca^{2+} was absorbed without analyzing an adequate exchange partner (see Figure 6). It is probable that these exchange sites were occupied with cations like potassium or H^+ which were not considered in the cation analyses.

The content of Al^{3+} and Fe^{3+} is constant for all Na^+ treatments and at the same level as in the original sample. Na^+ does not act as a cross-linking agent because the ion only forms outer-sphere complexes with NOM which were known as weak and unspecific bindings (Sutton and Sposito 2005, Kalinichev and Kirkpatrick 2007). So these treated samples are also can be defined as further controls for the experiments with Al^{3+} and Ca^{2+} .

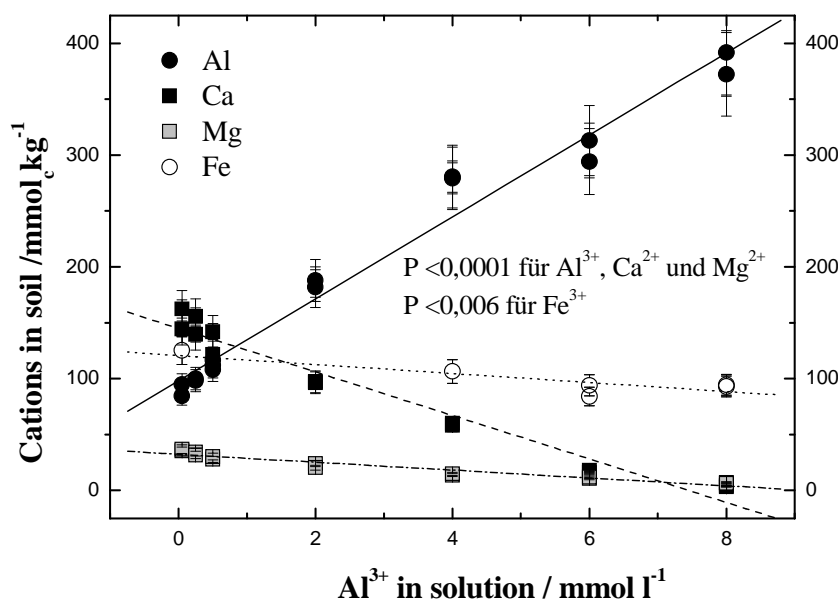


Figure 10: Cation exchange during absorption of Al^{3+} in dependence on different concentrations in the initial salt solutions; standard deviations are derived from the analytical methods in percent.

The absorption of Al^{3+} is more linear in the determined concentration ranges and no sorption limit is detectable as it was determined for the absorption of Ca^{2+} . The Al^{3+} content exceeds the measured CEC_{eff} with barium chloride. It is not possible to eliminate the formation of inorganic Al^{3+} precipitates totally so we do not know exactly, whether all Al^{3+} cations are located at the exchange sites of the samples. But inorganic precipitation at a pH of 4 is nearly negligible (Ross, Bartlett et al. 1991, Skyllberg 1994, Ross, David et al. 1996, Skyllberg 1999, Johnson 2002, Ross, Matschonat et al. 2008). It is more probable that Al^{3+} changes with cations which would not change with Barium. Direct comparisons between Al^{3+} and Ba^{2+} binding capacities to organic matter were not found in literature. But generally Ba^{2+} is known for its efficient exchange characteristics due to its high ratio of charge to hydrated radius (Ross, Matschonat et al. 2008). A weak exchange with Iron which was not obtained for the exchange with Ca^{2+} indicates that exchange with Al^{3+} cations is more radical than with a divalent cation. Besides the potential CEC averages $600 \text{ mmol}_c \text{ kg}^{-1}$ so there exist more exchange sites in the soil as the determination with the BaCl_2 method for the CEC_{eff} indicates and the amount of exchanged H^+ ions is not known.

The two control samples, one treated with deionized water in batch like the other samples and one only humidified, are not significantly different in cation content from the original sample (EDTA-Extraction). For the control treated in batch a loss of Ca^{2+} of 4,5 to 6 $\text{mmol}_c \text{kg}^{-1}$ can be calculated from the Ca^{2+} concentration in soil solution after treatment. So these values are only about 3% of total cation content and for that the difference is lower than the standard deviation of measurements of EDTA Extraction. It is also taking into account that there is a higher loss of organic carbon and probably the ratio of organic carbon to cation content does not change.

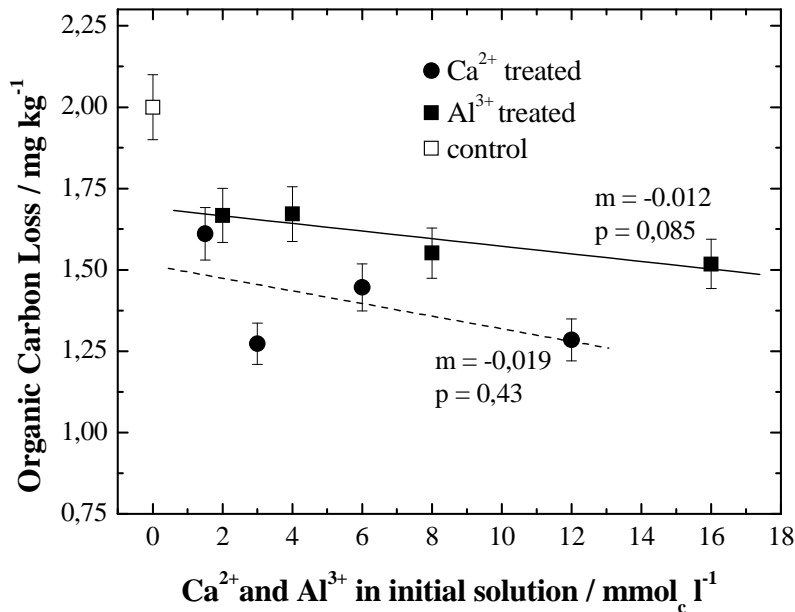


Figure 11: DOC in the soil solutions after treatment in dependence of increasing initial Ca^{2+} (●) and Al^{3+} (◻) concentrations in batch solutions and in comparison to the control sample only treated with deionized water (◻). Linear regression with $p = 0.08$ for Al^{3+} and $p = 0.1$ for Ca^{2+} .

For all treatments with cation solutions the DOC decreases with increasing initial cation concentration. As it is seen in Figure 11 there is a high decrease of DOC in solution and in consequence a lesser loss of OC from the samples by treatment even with very low concentrated salt solutions in comparison to the control solution. A significant difference between Al^{3+} and Ca^{2+} solutions was also determined. The progression of the curves is linear with a slight decreasing slope of $-0.012 \text{ mg DOC / kg / mmol}_c \text{ Ca}^{2+}$ and $-0.019 \text{ mg DOC / kg / mmol}_c \text{ Al}^{3+}$ in the experimental system. So Al^{3+} is more effective in retaining organic matter from soil than Ca^{2+} in spite of the lower concentrations normalized to cation charge. The total loss of SOM of the original sample calculated from DOC, soil amount and C_{org} is about 0.5% for the control sample and accordingly lower for the samples treated with salt solutions. In comparison to the percolation experiments the DOC loss in batch is significantly higher: using for first percolation a solution of 5 mmol l^{-1} there was an OC loss of nearly 1 mg kg^{-1} observed, using for

batch experiments a 5 mmol l^{-1} solution an OC loss of nearly $1,5 \text{ mg kg}^{-1}$ results. So this shows that percolation is softer method than batch experiments.

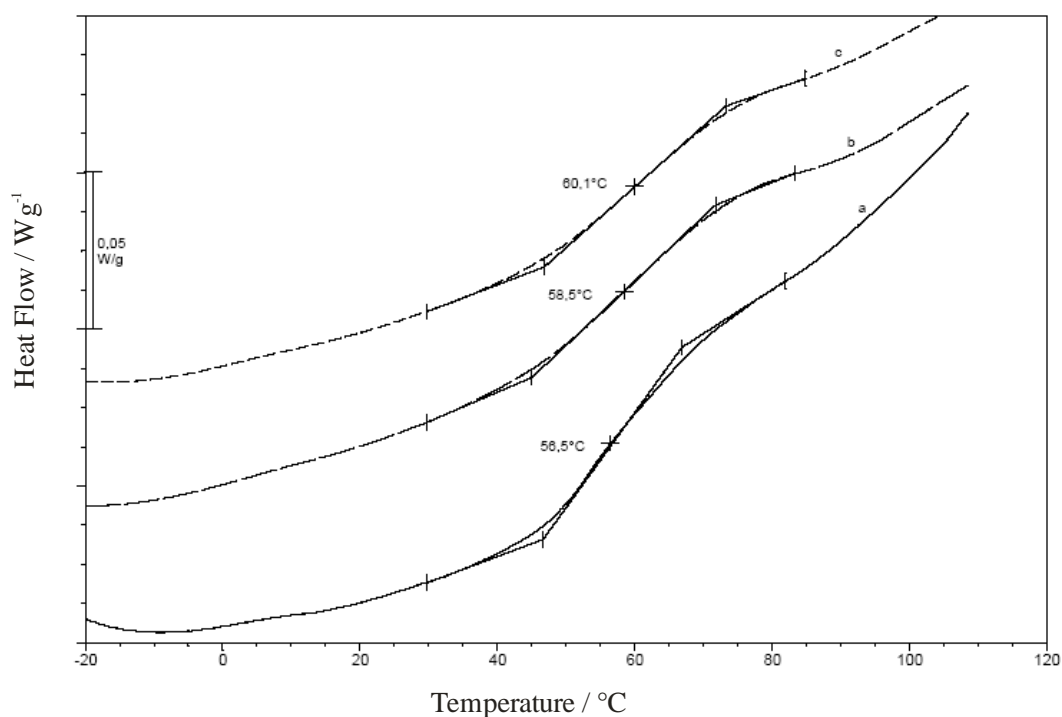


Figure 12: Representative DSC thermograms of the first heating cycle of samples treated with Ca^{2+} ; a) reference sample only humidified, Ca^{2+} content is $160 \text{ mmol}_c \text{ kg}^{-1}$, b) treated sample, Ca^{2+} content is $175 \text{ mmol}_c \text{ kg}^{-1}$, c) treated sample, Ca^{2+} content is $220 \text{ mmol}_c \text{ kg}^{-1}$

For all treated and untreated samples there is a step transition in the first heating cycle with a change of heat capacity of $0,1 - 0,3 \text{ W g}^{-1} \text{ K}^{-1}$ and in a temperature range of 56°C up to 64°C . This thermal event is non-reversing, what means in the second heating cycle there is no step transition in this temperature range. However there is a thermal event at 69°C to 72°C with very low intensities. This event is reproducible for all samples but there is no trend for increasing or decreasing values of T^* identifiable. Representative thermograms for the first heating cycle are shown in Figure 12.

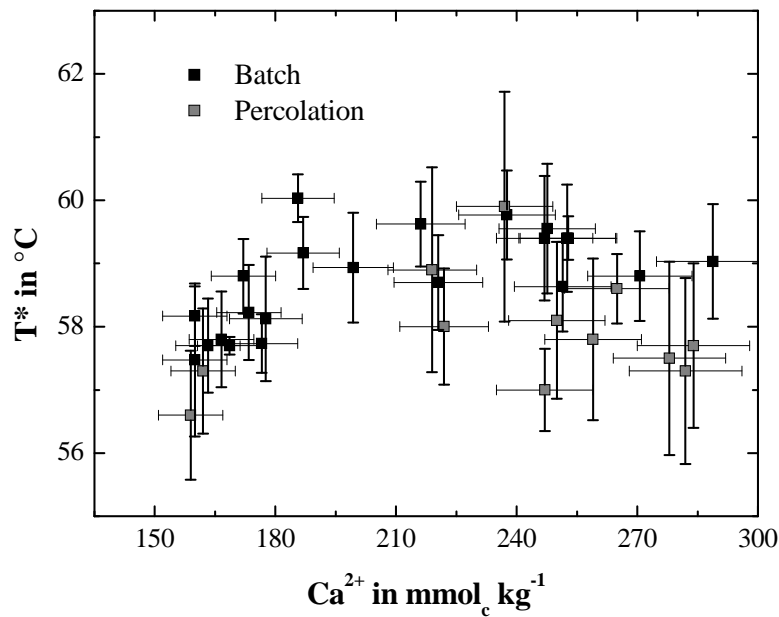


Figure 13: DSC results from Ca^{2+} treated samples in batch experiments and in percolation experiments (see chapter 0), changes of T^* with differences in Ca^{2+} content.

For Ca^{2+} treated samples there were found glass transitions like step transitions in a range of 56°C to 60°C . For the percolation results a different method of identification of T^* was used in the DSC thermograms therefore a direct comparison of the data were not possible before correction of the results. After correction it was shown that the resulting temperatures were lower than before but the relation to each other was very similar. Therefore only data for direct comparisons were evaluated with the new method not all shown data the former chapters.

As it is demonstrated in Figure 13 the percolation data and the batch data on T^* complement one another. The overall standard deviation is about $\pm 0,75^\circ\text{C}$ in average this result is in line with deviations reported in literature for DSC measurements of soil samples (Schaumann and Antelmann 2000) and much better than achieved with the percolation samples. T^* increases with increasing Ca^{2+} content in the soil until $200\text{ mmol}_c\text{ kg}^{-1}$ above $200\text{ mmol}_c\text{ kg}^{-1}$ there is no significant change of T^* to determine. The optical impression that T^* decreases with higher Ca^{2+} content which is supported by the results of the second percolation experiment. Figure 13 gives the impression that there is a specific cation content which induces a high rigidity of the SOM matrix if the Ca^{2+} content is lower or higher the matrix is softer and therefore T^* is lower.

The increase between the reference samples and the higher concentrated samples averages $1,5^\circ\text{C}$. There is no effect on T^* for the two controls at all, so the assumption that the determined increase is caused by the treatment with water can be excluded. But it is to be mentioned that the control of the percolation experiments show a lower T^* than the controls of the batch experiments this can also be observed for the untreated original samples used for the two experiments. It is not possible to clear up the reasons for this phenomenon completely but

it is important to mention that the two original samples were treated after sampling in the same way but defrozen on different points of time and perhaps there is an unknown influence affects these differences. However, this example demonstrates the importance of having controls for each experiment and for each charge of the sample.

The Na^+ treated samples do not show any changes with increasing Na^+ concentration in the used solutions also the standard deviation of T^* is the same as for the controls and the Ca^{2+} treated samples. There is also no further decrease of T^* obtained as it could assumed by examining the graph of T^* for Ca^{2+} in Figure 14 although a fraction of Ca^{2+} was exchanged via Na^+ .

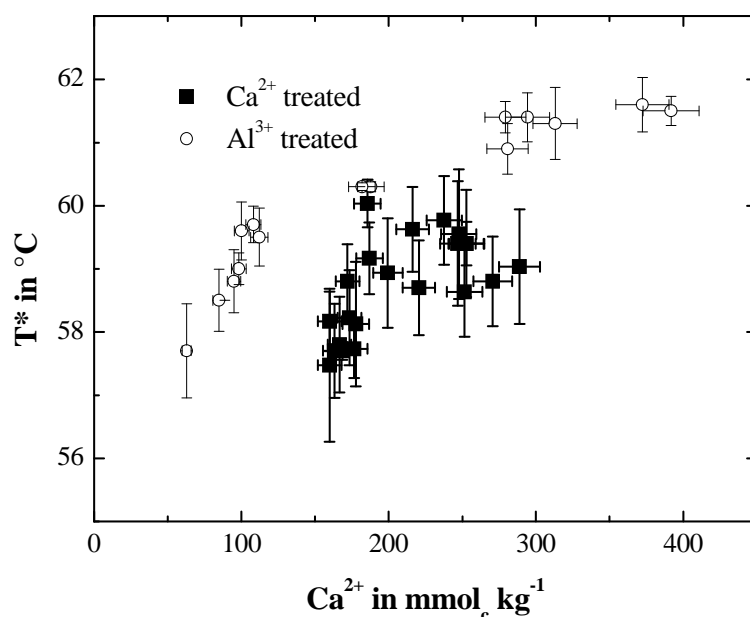


Figure 14: Glass transition like glass transition temperature in dependence on Ca^{2+} content and Al^{3+} content in soil samples after 4 weeks conditioning at 20°C and 76% humidity.

For Al^{3+} treated samples T^* ranges from 58°C to 62°C (Figure 14). The standard deviation is in average 0,3°C, this is a very low deviation for DSC measurements of original soil sample. The deviation is lower than the deviations of the controls and of the Ca^{2+} treated samples. This observation indicates that Al^{3+} has a homogenizing effect on the molecular structure of SOM. T^* increases with increasing Al^{3+} content of the samples. Furthermore the maximum T^* for Al^{3+} treated samples (62°C) is higher than maximum T^* for Ca^{2+} treated samples (60°C). The curve shape at the beginning is similar to the results of the Ca^{2+} treated samples: A high effect is noticeable for the samples with relatively low Al^{3+} concentrations and than a less distinct increase for higher concentrations can be observed. No significant difference is found for the last samples with concentrations higher than 300 $\text{mmol}_c \text{kg}^{-1}$. A possible explanation is that there are no sorption sites in SOM anymore, because the effective CEC is exhausted and Al^{3+} is bond in inorganic precipitates. Furthermore it is a similar effect as with Ca^{2+} treated samples so there is probably a saturation point for cross-linking sites in SOM.

Models

Summarizing the results described up to now and comparing to the hypotheses derived in chapter 2.2 the following conclusions are possible:

- The observed changes are all linked to the glass transition-like step transition temperature T^* which is related to the occurrence and effects of water and will be discussed after the presentation of the aging results
- Hypotheses I (induction of higher rigidity by Ca^{2+} and Al^{3+}) is supported by all experiments
- Hypotheses II (increasing cation content effects increasing rigidity) is not supported in the complete concentration range. Maximum rigidity is achieved before all sorption sites are occupied with the used multivalent cations and decreases for Ca^{2+} after achieving the maximum
- Hypotheses III (Al^{3+} is more effective than Ca^{2+}) is supported, the same mol content of Al^{3+} induces a higher rigidity, this is in line with results of Nebbioso & Piccolo (Nebbioso and Piccolo 2009), they observed a higher molecular rigidity for HA – Al bindings than for HA – Ca bindings by ^{13}C cross-polarization magic angle spinning (CP-MAS) and ^1H -diffusion order spectroscopy (DOSY) spectra
- Hypotheses IV) (abrupt changes of cation state versus slow / soft changes) is only supported by percolation 1 and is discussed below

According to the different effects of Ca^{2+} and Al^{3+} on rigidity in SOM the following molecular models were derived on the observations and the state of the art about cation bindings in organic matter to explain the differences.

In Figure 15 a simplified model is shown which considers the described observations of the cation addition experiments in three stages of networking (I – III) due to Ca^{2+} . In Figure 15 a simplified model is shown which considers the described observations of the cation addition experiments in three stages of networking (I – III) due to Ca^{2+} .

II

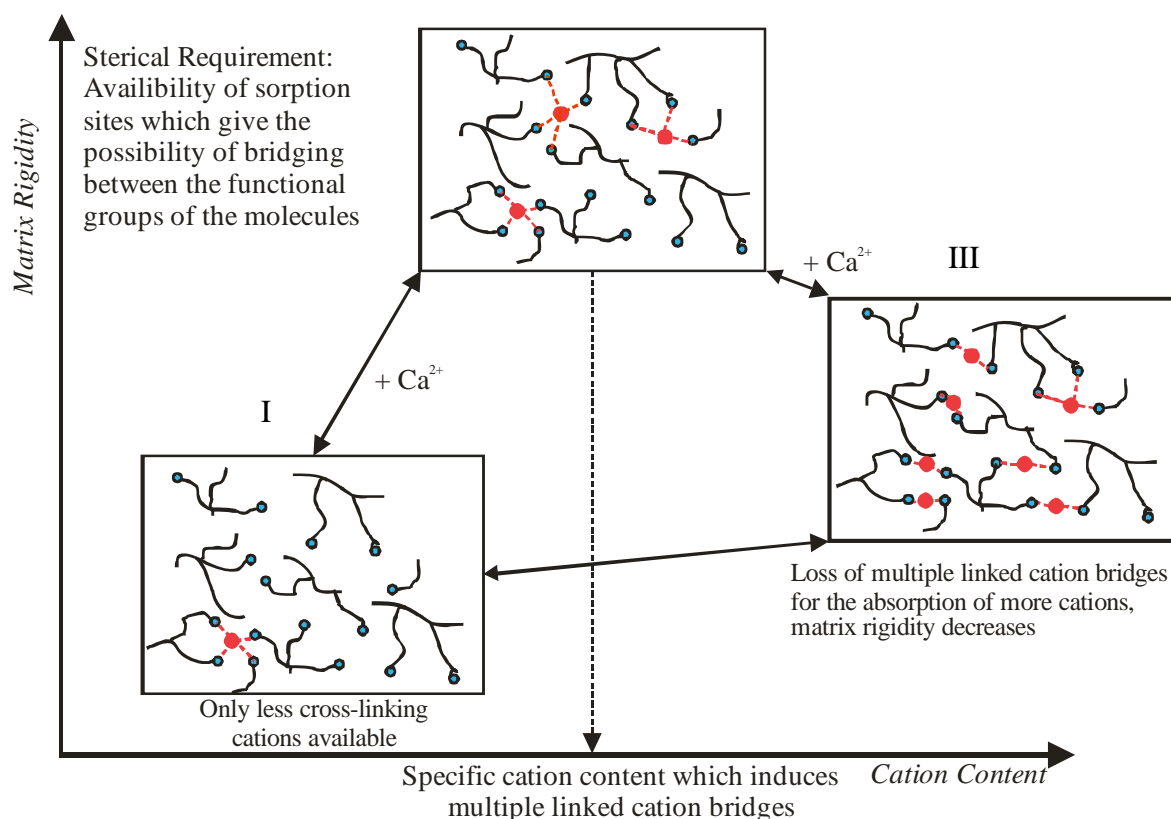


Figure 15: Simplified model for the relation of absorption of Ca²⁺ and the rigidity of SOM influenced by cross-linking between the functional groups of different molecules.

- I) Low content of crosslinking cations: Ca²⁺ is bond on sorption sites which provide inner-sphere complexes to a maximum number of co-ordination partners for a energetically stable binding between Ca²⁺ and the functional groups of the organic molecules. But not all of these preferred binding sites are occupied, because of a missing number of multivalent cations (in this case: Ca²⁺). Matrix rigidity is low.
- II) Increasing content of Ca²⁺: All of the preferred binding sites are now occupied by Ca²⁺, strong interactions provoke a rigid matrix (no side chain mobility, embedding of small molecules in the matrix)
- III) The ratio of Ca²⁺/functional groups of organic molecules increases and further uptake of Ca²⁺ effects a distribution of cations to the available binding sites in SOM. It is postulated that bidentate bindings are energetically preferred in comparison for polydentate bindings for a two-valent cation. Further co ordination of the cation with water is possible and the mobility of the side-chains increases. It is suggested by computational calculations that other sites in the co-ordination sphere of the cation are now co-ordinated by water molecules (Aquino et al., 2010). Further discussion of this point follows after the results of the aging experiments.

Referring to state II and the results in the first percolation it cannot be completely excluded that there is an influence of the mechanism of the exchange process on the resulting rigidity

(hypotheses IV: abrupt changes of cation state versus slow / soft changes). That would mean that state II is not only depending on the cation content as postulated in the model and that for higher contents also bindings as described for state II are possible. No final conclusions are possible to the reliability of percolation 1 because in percolation 2 the observed effects for samples treated with lower-concentrated solutions were not found.

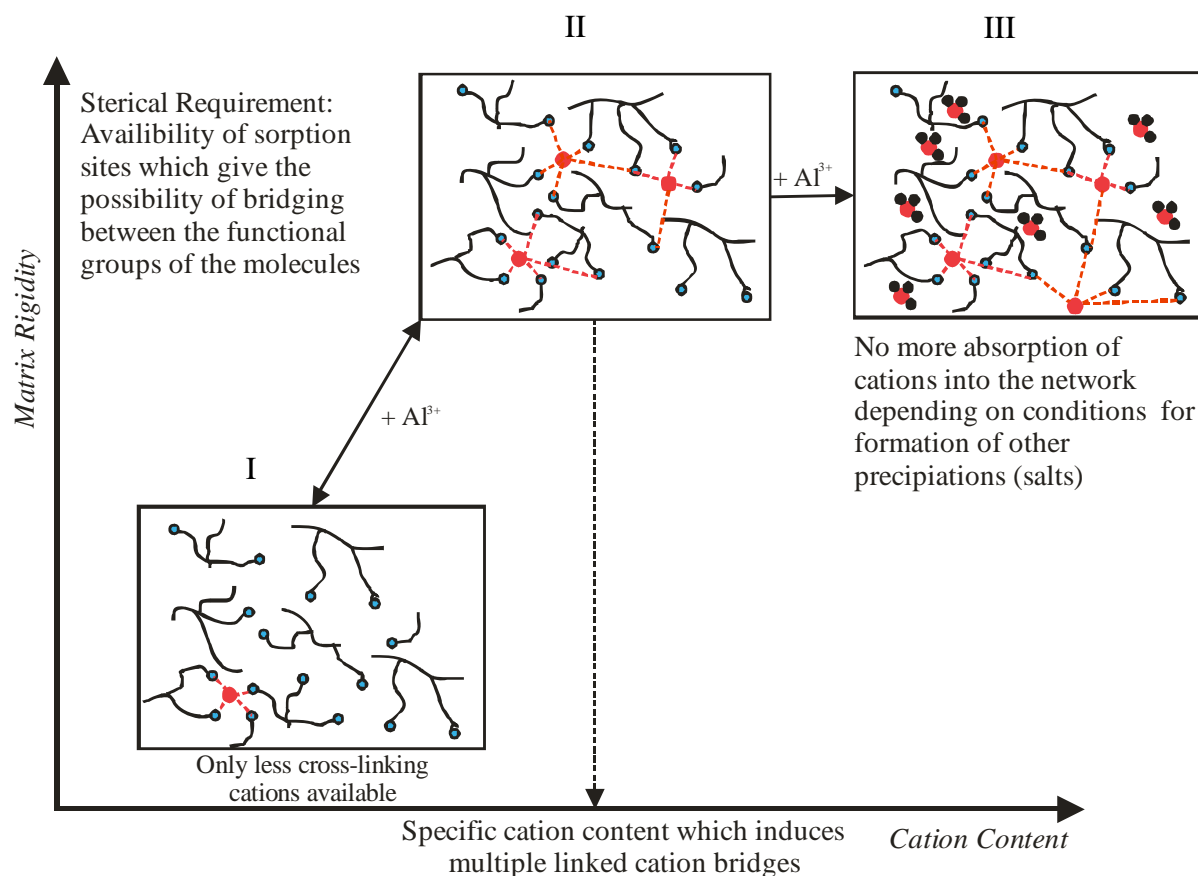


Figure 16: Simplified model for the relation of absorption of Al^{3+} and the rigidity of SOM influenced by cross-linking between the functional groups of different molecules. In contrast to Ca^{2+} further addition of cations on the matrix do not lead to a less rigidity determined with T^* .

Modelling the behaviour in rigidity for samples with Al^{3+} is more difficult because no computational calculations exist for Al binding to NOM. From literature it is known that Al form strong innersphere binding with the functional groups of NOM and induce conformational changes (Kalinichev and Kirkpatrick 2007).

- I) This state is similar to Ca^{2+} - SOM modelling the low content of multivalent cations induces polydentate complexes with the functional groups of SOM
- II) The increasing content of Al^{3+} induces an increasing rigidity by a higher number of polydentate bindings. Due to the higher charge of Al^{3+} it is assumed that Al^{3+} also can bind functional groups over a longer distance than Ca^{2+} . In literature for binding to Al^{3+} also conformational changes of NOM were observed (Elkins and Nelson 2002,

Kalinichev and Kirkpatrick 2007, Nebbioso and Piccolo 2009) and have to consider in our model. The formed bindings are supposed to be very strong.

III) Though the cation content of the soil sample increases no changes in rigidity can be observed. The constant rigidity is related to the assumption that the formed polydentate complexes are energetically preferred to bindings with a lower number of binding partners. But it is unknown in which way the other Al^{3+} cations are bind to the matrix. No hints in literature were found supporting other possibilities of binding than to the functional groups of SOM. The formation of Al-Hydroxids (inorganic precipitates) is negligible for $\text{pH} < 4,2$ (Ross, Matschonat et al. 2008). However in the model Al is shown as an inorganic precipitate with an unknown binding partner.

Increasing T^* related to cross-linking by cations was reported also by Luo et al. (Luo, Zhang et al. 2008) who observed an increasing sorption capacity and non-linearity for samples treated with Al^{3+} and Ca^{2+} solutions during sorption of phenanthren in contrast to samples treated with Na^+ solution. T^* increases in the same range as reported here. The authors concluded based on the results further evidence of the dual mode distribution model (Xing and Pignatello 1997). Same observations were also reported for interactions of heavy metals (Cu^{2+} , Ni^{2+} and Pb^{2+}) in the same soils and phenanthren sorption (Luo, Zhang et al. 2010). But it is to mention that the OC contents samples were rather low in comparison to the here determined samples. For further discussions it is also to mention that the determined changes in T^* are much lower than changes observed in T_g for organic polymers due to co-ordinative cross-links by metal ions. Here the changes average between 10 and 150°C (Belfiore, McCurdie et al. 2001).

Aging:

As it was shown for the samples of the first percolation cycle aging effects in rigidity occurs after a conditioning time of several months. also the batch samples were measured at different time points to observe aging effects as demonstrated (postulated) in literature (Schaumann, 2005, Hurraß & Schaumann, 2005). In the following the different cation treatments were shown in own figures to assure an adequate view.

The phenomenon of aging of SOM due to water molecule bridges can be determined in a significant increase of T^* (e. g. Hurraß & Schaumann, 2005). In this study for all treated and untreated samples T^* increases during the time of conditioning independently on treatment method and cation. This can also be observed for the controls without any treatment.

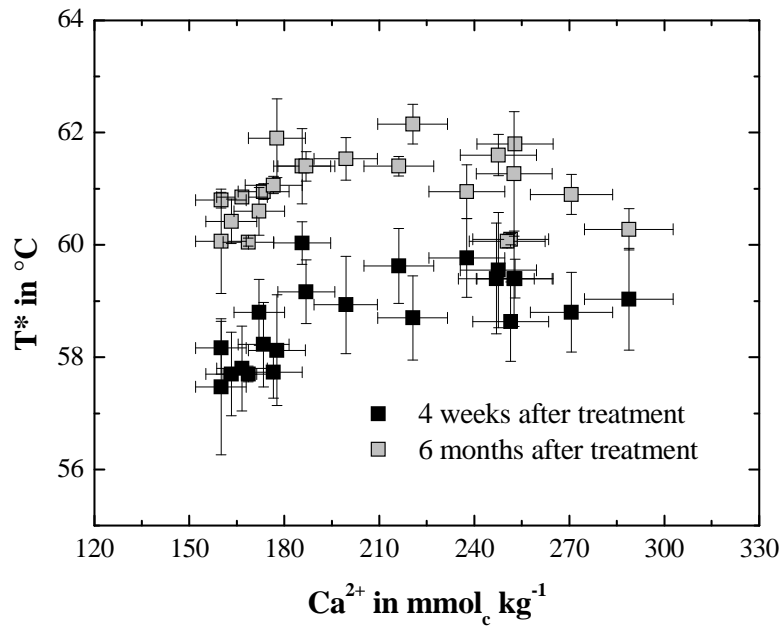


Figure 17: Step transition temperature for Ca^{2+} treated samples in batch 4 weeks and 6 months after the treatment.

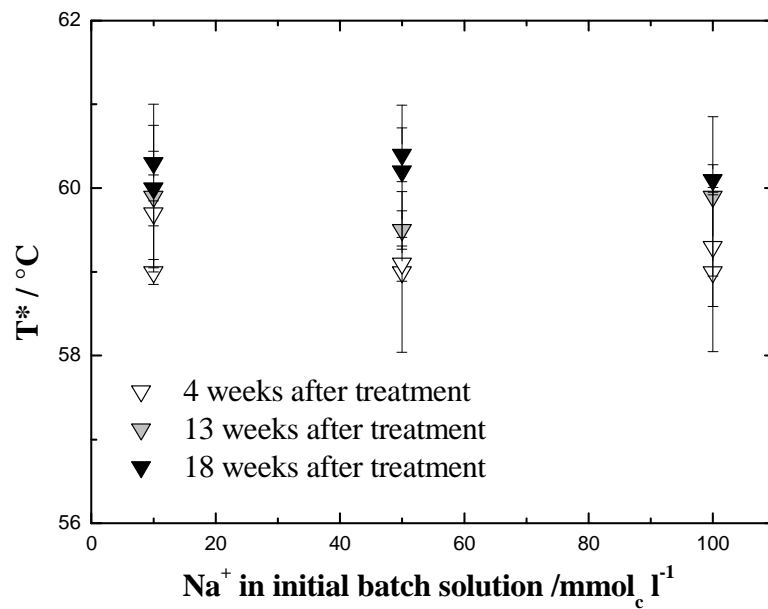


Figure 18: Step transition temperature for Na^+ treated samples in batch, 4 weeks, 13 weeks and 22 weeks after the treatment.

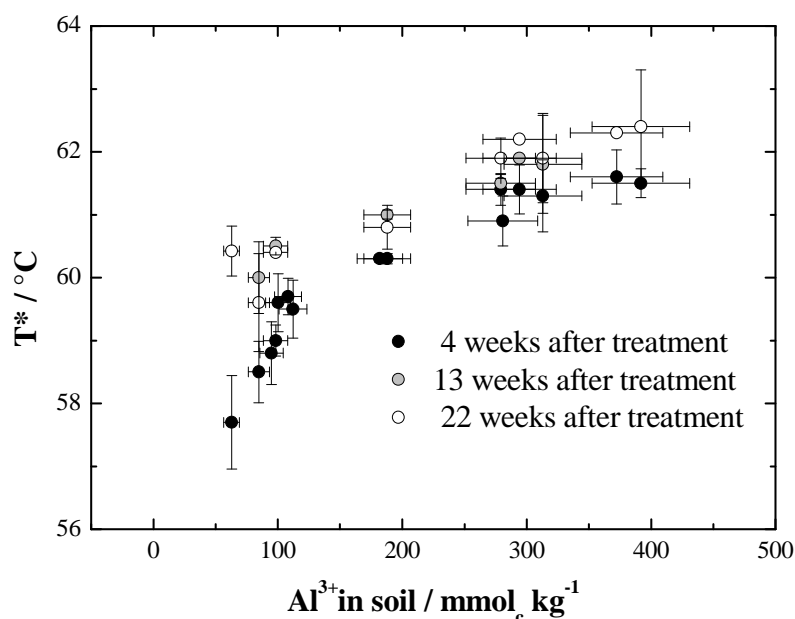


Figure 19: Step transition temperature for Al³⁺ treated samples in batch; 4 weeks, 13 weeks and 22 weeks after the treatment.

For samples treated with Ca²⁺ solution the effect of aging averages 2°C in 6 months so it is even greater than the effect of Ca²⁺ absorption (1,5°C after batch treatment with Ca²⁺ solution for the rigid samples). For the Na⁺ treated samples the aging effect ranges also between 1 and 2°C in nearly 6 months. Only for the Al³⁺ treated samples the effect of aging in nearly 6 months is with 1°C in average weaker than the increase because of the sorption of Al³⁺ from solution. For Al³⁺ treated samples there are very similar results of T* between the samples conditioned for 13 weeks and for 22 weeks. The differences of T* between the conducted cation treatments especially between Ca²⁺ and Al³⁺ vanished after a time period of 6 months, the maximum T* of the Al treated samples after 6 months is 62,4 °C the maximum T* for Ca²⁺ treated samples is 62,2 and the maximum of Na⁺ treated samples is 60,4°C. So the samples treated with cross-linking cations still show a higher rigidity than samples treated with non-cross-linking cations like Na⁺.

All curve shapes are still comparable to the shapes of the first results after 4 weeks conditioning for all samples. For Ca²⁺ the decrease for a higher content in the samples seems to be better pronounced than before. The standard deviation of the measurements after aging decreases for the Ca²⁺ treated samples; for Al³⁺ and Na⁺ treated samples they are still the same but it is to consider that for these samples the deviation is also for the first measurements relatively low.

Water molecule bridges were postulated in the HBCL-Model (see Introduction, chapter 2.2) and related to the glass-transition-like step transition temperature as also reported for the

treated samples. The occurrence of changes in T^* due to a changing cation status in the matrix demonstrates a relationship between water molecules and cations between the organic molecules. In chemistry a relationship between water and cation is described by the hydration shell of the free cation in a solution. Stabilization by water clusters in SOM and by cation bridges was shown by computational calculations (Aquino, Tunega et al. 2009, Aquino, Tunega et al. 2011, Schaumann and Thiele-Bruhn 2011) for selected functional groups. In reference to this calculations mono- and bidentate bindings of Ca^{2+} to organic functional groups are possible and depending on water content and environment (unpolar or polar). Water molecules were included in the coordination shell of the cations in these complexes. Computational calculation for Al^{3+} shows the higher bridging power of aluminum

The results show strong evidence that the observed rigidity is linked to the interaction of cations and water which complexity is unknown at this point of time. The pronounced aging for Ca^{2+} treated samples, Na^+ treated samples and the untreated samples is related to conformational changes of water molecules in a way of forming bridges between molecules as described by Schaumann & Bertmer, 2008 or calculated by Aquino, 2009. Due to the results of Al^{3+} treated samples it is assumed that Al^{3+} induces the conformational changes of the water molecules in a faster manner because of its higher binding strength. Computational calculation for Al^{3+} shows the higher bridging power of aluminum and supports the described observations (Aquino, Tunega et al. 2014) Only slight changes were possible eventually based on the lower diffusivity of the water molecules in the organic matrix.

2.4.2 Wettability / repellency of the treated and untreated samples

In order to achieve further information on differences between untreated and treated samples, contact angle measurements were conducted which is a direct measure for hydrophobicity of the samples. Hydrophobicity is linked with the surface structure of the SOM. The results of the contact angle measurements of the treated and untreated samples show a curve shape similar to the results of the step transition temperature. For Al^{3+} and for Ca^{2+} treatments the contact angle increases in comparison to the control sample and with increasing cation content in the sample. The increase is stronger pronounced at lower concentrations. At higher cation concentrations the curve flattens and decreases in average for Al^{3+} and for Ca^{2+} treated samples. Again the Al^{3+} treated samples show a more pronounced effect than the Ca^{2+} treated samples.

The outcome of a correlation for the step transition temperature T^* and the contact angle of the sample, irrespective of the mode of treatment (Ca^{2+} or Al^{3+}), is a clear linear correlation ($p < 0,001$). This result indicates that the rigidity and flexibility of the organic matrix in SOM correlates with the hydrophobic and hydrophilic behaviour of the SOM surface, respectively.

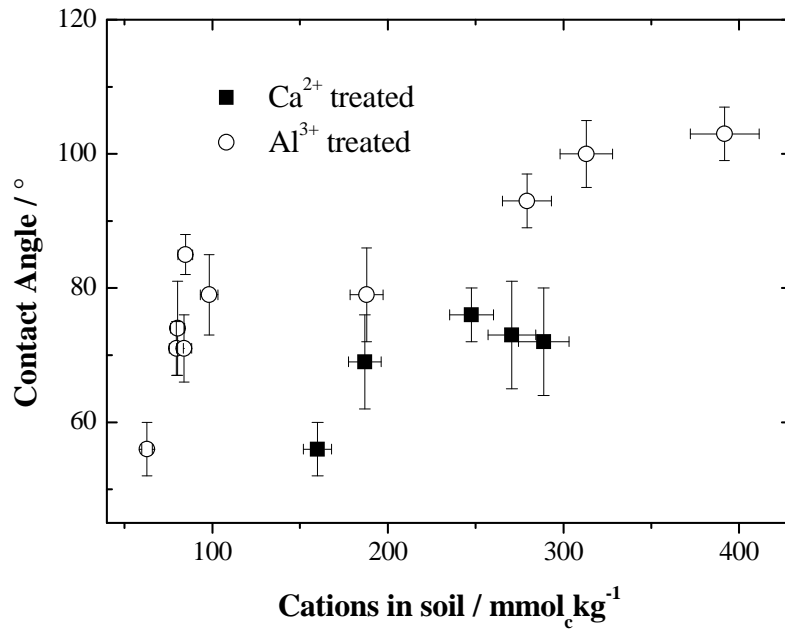


Figure 20: Contact Angle of the Ca²⁺ und Al³⁺ treated samples after 4 weeks of conditioning in relation to the cation content.

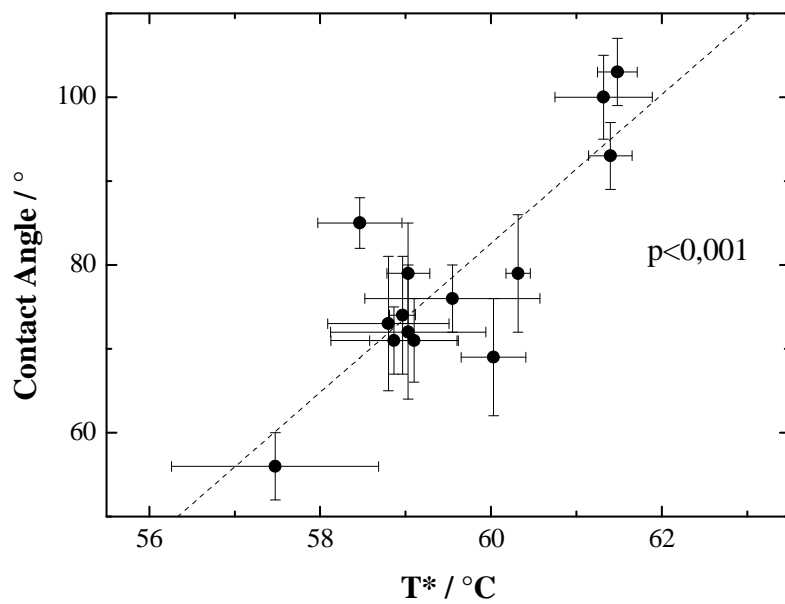


Figure 21: Correlation of T* with contact angle for all treated and untreated samples with different cation solutions in batch experiments.

Diehl & Schaumann, 2007 identified two possible processes responsible for changes in hydrophobicity of soil samples by analysing the activation energies, E_A , during the rewetting procedures. One process is mainly based on physic-chemical or pure physical changes and linked with differences in the percentage of charged functional groups of the repellent and wettable samples, whereas the other process is based on chemical reactions and linked with conformational changes of organic molecules at the surface during the drying procedure. Caused by an increase of H-bonds and ester linkages hydrophilic functional groups from the surface are orientated towards the interior of the SOM matrix leading to a lower number of hydrophilic domains at the surface. It can be assumed that referring to the second process also cations are able to induce conformational changes by linking outstanding hydrophilic groups into the interior. An increasing T^* represents a higher rigidity and thereby a more complex network in SOM as it is discussed in the former chapters. It is probable that the formed cation bridges in the interior also involves molecules of outstanding groups in this process.

For Ca^{2+} treated samples the contact angle shows also a slight decrease (not significant) as it also can be observed for T^* of samples with Ca^{2+} contents near the CEC_{eff} . Referring to the model described in Figure 15, a Ca^{2+} content near CEC_{eff} induces less cross-linking and according to the results of contact angle measurements leads to a higher degree of outward orientated hydrophilic groups caused by a reduced number of bonding partners in the interior.

For Al^{3+} treated samples the contact angle seems to be consistent for the samples with a high content (above CEC_{eff}). As discussed in the last chapter it is assumed that Al^{3+} has different (small precipitation or more exchange sites in SOM (as discussed Al^{3+} perhaps occupied more exchange sites from the potential CEC) due to its stronger binding strength therefore no conformational changes were required for absorbing more Al^{3+} cations.

Schaumann et al. (2013) found also an influence of cation bridges on the wettability of peat and soil samples which can lead to a higher water repellency. Nonetheless, in this study no difference was found between Al and Ca treated samples. (Schaumann, Diehl et al. 2013)

To achieve more information on wettability and cation content of a sample with high SOM and to validate the described model of conformational changes it is recommended to control the wettability status for the aged samples. Due to the described model an increase for Ca^{2+} treated samples and none or only a slight increase of the Al^{3+} treated samples is postulated.

It is to mark out that for a sample from a humic layer the influence of SOM is more pronounced than for more mineral samples so this result is hardly to transfer for soils with a higher amount of inorganics / minerals.

2.4.3 Influence of demineralisation on matrix rigidity

In the former chapters (batch experiments) samples were described which were treated with Na^+ this indicates a loss of multi-valent cations like Ca^{2+} and consequently a decrease of matrix rigidity. Decreasing matrix rigidity was not found for the Na^+ treated samples, the rigidity

was consistent. This should be verified for more samples and for the use of a different method which enables a stronger demineralization than exchange with monovalent cations.

Demineralization was conducted with the known spruce forest layer samples also used for the cation additions, a peat sample from Fuhrberg and a peat sample from Heudorfer Ried. The samples are described in chapter 2.3.2. Demineralization was conducted as described in 2.3.4.

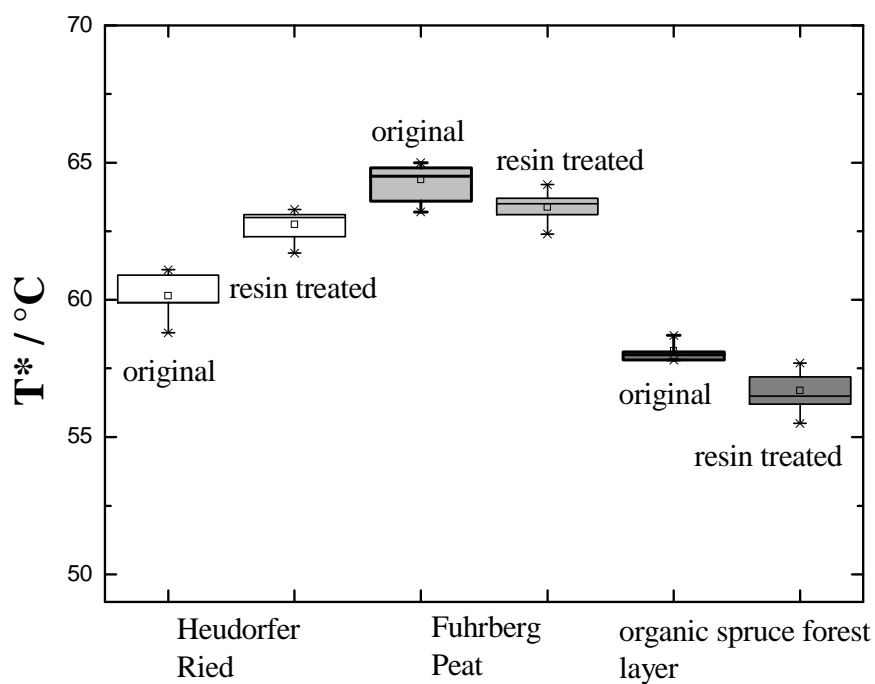


Figure 22: Step transition temperature T^* before and after demineralisation of the three samples. Box plots were created by at least 6 T^* values for each sample.

As it is seen in Figure 22 the samples from the spruce forest and from Fuhrberg act in a similar way. The exchange of cations to H^+ causes a slight decrease of T^* of about $2,5^\circ C$ for the spruce forest sample and $1,5^\circ C$ for the Fuhrberg sample. In contrast the sample from Heudorfer Ried acts different after demineralisation T^* increases for nearly $3^\circ C$. Looking for an explanation for this unexpected behaviour it is helpful to consider the characteristics of the samples before and during demineralization:

| | Loss of organic carbon during treatment / g kg ⁻¹ | Loss of Ca ²⁺ / mmol _c kg ⁻¹ | Loss of Mg ²⁺ / mmol _c kg ⁻¹ | pH at the beginning of treatment (in water) | pH at the end of treatment (in extract water) | CEC _{eff} |
|---------------|--|---|---|---|---|--------------------|
| Fuhrberg | 3,40 | 51,6 | 50,2 | 4,01 | 2,82 | 123 |
| Heudorf | 8,37 | 955 | 26 | 6,2 | 2,6 | 680 |
| Spruce Forest | 2,51 | 162 | 38 | 4,4 | 2,76 | 303 |

Table 6: Sample characteristics and behaviour during the demineralization procedure with the acid cation exchange resin.

With reference to the sample characteristics the sample from Heudorf differs evidently from the two others. The Heudorf sample features a very large content of Ca²⁺ which exceeds the effective cation exchange capacity of the sample measured with BaCl₂. The presence of Ca-salts in the sample is very probable. This fact is also complemented by the strong pH decrease during the demineralization procedure. It can be assumed that most exchange sites in SOM of Heudorf are occupied with Ca²⁺ before the demineralisation experiment.

In contrast the sample from Fuhrberg shows the lowest Ca²⁺ content and also a low CEC_{eff} for the relatively high organic carbon content of 52 %.

What we know from the cation absorption experiments is that there is a specific concentration of Ca²⁺ where T* shows a maximum then T* decreases slightly with increasing Ca²⁺ content. This maximum can be determined on a value of 220 mmol_c kg⁻¹ for Ca²⁺ which corresponds to a CEC_{eff} saturation of 72,6%. That means the spruce forest sample was demineralised in a condition where the maximum rigidity was not yet achieved because of the lower Ca²⁺ content. Transferring this to the other two samples it means that for Heudorf the point of maximum rigidity is exceeded because of the very high saturation of the CEC with Ca²⁺ the rigidity would be less pronounced; for Fuhrberg that would mean that the point of maximum rigidity is not yet achieved because of the low Ca²⁺ content (42,3 % of CEC_{eff}) similar to the spruce forest sample but eventually less rigid. So it could be concluded that before demineralization the spruce forest sample was the sample nearest its specific rigidity maximum. But this does not automatically mean that the spruce forest sample is the most rigid sample of those three. As it is seen in Figure 22 in absolute values the Fuhrberg sample is the most rigid sample due to a T* of 63 – 65°C. In our opinion this can be related to sterical reasons e. g. to sites with a higher number of cross-linking water molecule bridges. Each soil sample has its own specific point of rigidity. It is not possible to conclude nor from the cation content to the rigidity of the SOM matrix neither from the rigidity to a predicting cation content.

So after demineralization the spruce forest sample shows the highest / most pronounced decrease of T* the decrease for the Fuhrberg sample is less pronounced. Similar results for Fuhrberg were also reported by Mouvenchery et al. where also cross-linking induced by

cation bridges has a low relevance (Kunhi Mouvenchery, Jaeger et al. 2013). So this would support the prediction that the spruce forest sample is nearest at its specific rigidity maximum and therefore the decrease because of demineralisation is more pronounced than to the Fuhrberg sample. For the Heudorf sample the demineralisation leads to a higher rigidity of the sample because of the lower rigidity at the beginning due to high cation content. It can be assumed that after the demineralisation the cation content of the samples is very low why the rigidity of Heudorf is significantly increases is not fully explained by the model of the specific maximum rigidity point because there could also be the possibility that there is no change in rigidity. But it is important to point out that rigidity of SOM depends also on the formation of water-bridges. Hence it can be assumed that for each sample the number of sites where water molecule bridges can cause cross-linking effects is specific and perhaps the Heudorf sample is rich in sites like this and after the demineralisation these sites are no more occupied by cations. Due to the experiments it is not possible to exclude the effects of water-bridges on the rigidity of the matrix.

2.5 Conclusion

For all experiments where the cation status of the samples is changed by the multivalent cations Ca^{2+} and Al^{3+} (I) the induction of co-ordinative cross-links in SOM was proven by effects in matrix rigidity.

However hypotheses II was not fully supported because the absorption experiments show that an increase of Ca^{2+} and Al^{3+} do not necessarily lead to an increase of rigidity. The same behavior was observed for the decrease of cations by demineralization in different samples. Therefore it is to consider that the degree of rigidity strongly depends on the former saturation of the CEC with multivalent cations and on the conformational conditions (e. g. character of the dominating molecules). Piccolo and Nebbio, 2009, find out that saturated and unsaturated long chain alkanolic acids in HA were preferentially involved in metal complexation with Al and Ca whereas hydrophilic or mobile humic components were relatively low affected by the complexations (Nebbio and Piccolo 2009). Hence we suggest that each sample has its specific maximum point of rigidity due to the bridging of multivalent cations linked with the overall exchange capacity for cations in the SOM.

Changes in rigidity and in hydrophobicity of a spruce forest sample were more pronounced for Al than for Ca and are therefore enhancing research results concerning the binding strength and the ability of these cations to change the molecular structure (Elkins and Nelson 2001, Nebbio and Piccolo 2009) (III). The high binding strength is also demonstrated by observing the DOC losses during the experiments which were lower for treatments with Al^{3+} even for very low concentrations in the solution. The assumption of conformational changes induced by Al^{3+} absorption of the samples is further underlined by the results of the wettability measurements. An abrupt increase of hydrophobicity even for low absorption was observed for the Al^{3+} samples. For samples treated with Ca^{2+} a softening of the matrix is anticipated for concentrations near CEC_{eff} due to the results for T^* and for the decreasing contact angle in the

wettability experiment. This indicates that Ca^{2+} is not able to cause a lasting effect on conformational changes or the structure of SOM. The network of SOM reacts always flexible on the given conditions in slight in- or decreases of rigidity. For Al^{3+} at point near CEC_{eff} no further changes were observed. Nevertheless it is not possible to provide a chemically based description of the hypothesized molecular conformations which were affected by metal absorption or water molecule bridges. Therefore the described models are only based on evidence.

Overall the results suggest that conformational changes due to the enhancement of absorption mechanism like drying and rewetting only have a slight influence. Observed differences between the samples vanished after a time period of conditioning hence these processes are of a minor importance of the effects by coordinative cross-links of multivalent cations in SOM (see also Hypothesis IV).

The rigidity increases over time especially for samples treated with Ca^{2+} , Na^+ and water. These observations enhance the importance of water molecules in SOM: an interaction of water molecules and multivalent cations for bridging processes between organic molecules is a requirement for the observed effects in matrix rigidity by the glass transition-like step transition temperature T^* .

Altogether it is to mention that effects of the multi-valent cations in rigidity were observable but do not indicate revolutionary changes in the molecular conformation of the matrix. The changes do not exceed more than 3°C in average for changes in the cation status and all in all 7°C for changes in cation status + aging process in comparison to the original sample at the beginning. For changes in the water status of samples more than 10°C difference was found. But no conclusion is possible which effects in sorption or degradability are meant by the observed rigidity changes. From the wetting experiments we know that the hydrophobicity increases with increasing rigidity. Further research is necessary to describe the effects of rigidity for soil specific characteristics and functions.

3 Influence of several multivalent cations on structural characteristics of DOM based precepitates

3.1 Summary

Precipitates with Ca, Al and Pb cations were formed of a DOC solution from an acidic organic layer from a spruce forest sample. The precipitates were analysed for their thermal behaviour with a Differential Scanning Calorimetry (DSC) depending on the Me^{n+}/C ratios in the solutions. For all samples a transition step temperature (T^*) can be identified known to be caused by cation-water-molecule bridges. Highest T^* were found for Al up to 66°C as maximum. Pb and Ca generally show transitions at lower temperatures at 55°C to 60°C. Al and Pb were the two cations with the best pronounced precipitation. For Ca^{2+} neither the precipitation was well pronounced nor the step transition was easy to identify. For all samples T^* decreases at high Me^{n+}/C ratios, which indicates a less rigidity of the organic matrix if a high content of metal cations is present. The temperature range of T^* and the characteristic of the step transition is comparable to the experiments with the whole soil sample in chapter 2. No reversible step transition can be identified with the used DSC procedure, but the observed step transition has a reversing character which means that after several weeks the step transition reappears in water containing samples. In water free samples no thermal event can be detected. The resultss show the appearance of cation – water-bridges in precipitates and the influences of several cations on the occurring matrix rigidity due to the forming bridges. For further research it would be interesting to know if the measured rigidity correlates with biological and chemical stability of the precipitates.

3.2 Introduction

It is suggested that multivalent cations induce co-ordinative crosslinks in soil organic matter (SOM) (Schaumann 2006). These cross-links induce the rigidity of the matrix. Rigid or glassy areas in SOM are linked with non-linear sorption and hysteresis effects in literature (LeBoeuf and Weber 1997, Xing and Pignatello 1997). Therefore SOM is described as polymer matrix consisting of macromolecules. In contrast Picollo et al., 2002, viewed SOM as a supramolecular network consisting of small molecules forming condensed aggregations. Schaumann, 2006, suggested that independently from the point of view SOM behaves as a amorphous matrix which structure is not in equilibrium, but changeable and dynamic. The detection of a glass transition temperature in isolated humic and fulvic acids (Young and Leboeuf 2000) and in whole soil samples (Schaumann and Antelmann 2000) enhances this suggestion. In the meantime two types of glass transitions were detected for SOM (Schaumann 2006). The first one is linked to the classical type also known for polymers and in the majority found in isolated humic and fulvic acids (Zhang, Leboeuf et al. 2007) or in NOM samples (DeLapp, LeBoeuf et al. 2004, Zhang and LeBoeuf 2009). This transition is reversible in subsequent heating cycles during measurements with the differential scanning calorimetry (DSC). The

second type of transition is not reversible in a subsequent heating cycle but the disappeared step transition reappears after a specific time of conditioning. This type only appears in water containing samples and is measured in a hermetically sealed system (no water evaporation is possible) (Schaumann and LeBoeuf 2005). The transition is named glass transition-like step transition temperature T^* (Hurrass and Schaumann 2007). The observations are explained with the formation of water molecule bridges between the organic molecule segments (HBCL model = Hydrogen Bond based Cross-Linking model). Up to now the HBCL model is further enhanced by experiments with proton NMR relaxation and proton wide-line NMR (Schaumann and Bertmer 2008) and computational calculations (Aquino, Tunega et al. 2008).

The formation of water molecule bridges is supposed to be a slow process and therefore aging effects are detectable in the thermal behavior of SOM (Hurrass and Schaumann 2007). For a peat sample conditioned over a time period of several weeks T^* increases (Schaumann 2005). Also for polymers a physical aging is known dependent on the thermal history but for these materials aging is visible as an endothermal overshoot arising at the glass transition point. Hence Schaumann, 2006, suggested two types of step transitions in DSC for the two types of aging for SOM.

The effects of different cation contents on the rigidity in SOM should also be detectable in DOM precipitates formed with multivalent cations. The formation of precipitates is described as one process reduces the dissolution of SOM and consequently enhances the stability of the soil aggregates. Therefore the loss of organic carbon is reduced in soils with higher metal concentrations (Römken and Dolfing 1998, Shen 1999, Ote, Temminghoff et al. 2002, Herre, Lang et al. 2007, Martı́nez and Martı́nez-Villegas 2008). Especially for Al precipitates a higher stabilization of SOM is suggested (Grodzinska-Jurczak and Mulder 1997, Mulder, De Wit et al. 2001, Schwesig, Kalbitz et al. 2003). Stabilisation of SOM is discussed as a possibility for a sink for atmospheric CO_2 to reduce green house gas emissions (von Luetzow, Kogel-Knabner et al. 2008). Therefore the understanding of stabilisation processes of SOM is of a great importance facing increasing temperature and hence increased microbial activity in the soil.

In this study it is suggested that DOM precipitates also i) show a detectable and analyzable glass transition like step transition temperature comparable to the findings in the whole soil sample from where the DOC solution originated from. It is further hypothesized ii) that the content and the manner of multivalent cations have an influence on the rigidity and furthermore iii) the rigidity is stronger for trivalent cations like Al^{3+} . Besides we suggested that iv) the precipitates are comparable with cross-linked polymers and hence show a reversible transition type one in water-free samples. We hypothesized also v) aging effects for the created samples.

To verify the hypotheses we create solutions with different metal / OC ratios with the multivalent cations Ca^{2+} , Pb^{2+} and Al^{3+} and conduct DSC measurements with the developed precipitates of the solutions.

3.3 Material and Methods

3.3.1 Sample properties and preparation

The required DOC solution was derived from an organic layer from an 80 year old spruce forest in South Germany. Immediately after sampling and homogenizing the sample was shock freezing and then stored in a freezer at -18°C . For the experiments the sample was unfrozen in a fridge and air dried. The water content of the samples differs between 7 and 8% percent after drying. Then the sample was sieved at 1 mm, some needles have to be collected manually from the samples and common soil characteristics were determined. The common characteristics are shown in table 7.

| pH | C_{org} /% | CEC_{pot} /mmol _c kg ⁻¹ | CEC_{eff} /mmol _c kg ⁻¹ | WC /% | Ca^{2+} /mmol _c kg ⁻¹ | Mg^{2+} /mmol _c kg ⁻¹ | Al^{3+} /mmol _c kg ⁻¹ |
|---------------|------------------------|---|--|-----------|--|---|---|
| $3,7 \pm 0,1$ | 43 ± 4 | 671 ± 50 | 303 ± 20 | 8 ± 1 | 165 ± 10 | 43 ± 5 | 60 ± 3 |

Table 7: Common characteristics of the organic layer from a spruce forest used as base sample for DOC desorption in the experiments

3.3.2 Preparation of the DOC solution

For the precipitation in the fraction of SOM which is bound by interactions with cations in the organic matrix is most important. Therefore we developed a new method for the retrieval of DOC in solution. In experiments with an acid exchange resin to demineralize the soil samples (chapter 2.3.4 and 2.4.3) high losses of DOC can be determined due to the depletion of cations. Now this in the former experiments unwished side effect we use to produce our DOC solution for the precipitation experiments. By this method we postulate that especially the dissolvable organics bound to multivalent cations would be set free because the resin exchanges these cations with H^+ .

100 g of the spruce forest soil sample, 50 g exchange resin (Amberlite ®, IR-120, H^+ Form) and 700 ml deionized water were filled in a 1 l glass bottle (Duran®) and mixed overnight in an overtop shaker. After shaking the resin-soil solution was filtered by pressure over cellulose nitrate filter (Sartorius®, pore size 0,45 μm). The filters were rinsed before with moderately warm water to reduce DOC losses of the filter material. The filtration took three hours with a pressure of about 2 bar. The derived DOC solution was measured for the exact concentration and then diluted with deionized water to in average 133,3 mg l⁻¹ (11 mmol l⁻¹). This concentration was chosen to achieve a concentration of 10 mmol l⁻¹ in the final DOC – metal solution. The generated solution was used immediately after extraction for the experiments because we want to prevent changes due to microbial activity without using methods of conservation which possibly have an influence on the sample characteristics.

3.3.3 Formation of the precipitates in metal solutions

The investigated cations Ca, Pb and Al were prepared in solution from the respective nitrate. Nitrates were used because the chloride salts form strong inorganic precipitates with Pb ($L = 2 \cdot 10^{-5} \text{ mol l}^{-1}$; schwarzer Riedel). For further investigations with DSC an amount of several milligram precipitate was required which assures a complete covering of the bottom of the Aluminum sample pans for at least 3 replicates. Therefore useful Me^{n+}/C ratios for the experiments were tested in preliminary experiments. Al-DOM-precipitation depends on Al^{3+}/C ratio and on pH in the solution (Scheel, Dorfler et al. 2007). It is known that at $\text{pH} \geq 4,2$ the formation of $\text{Al}(\text{OH})_3$ dominates the Al speciation (Gustafsson 2001). Nierop et al. (2002) observed visible flocculation above an Al/C ratio of 0,1 (Nierop, Jansen et al. 2002). Hence, we started at this ratio. Also for Pb visible flocculation was observed at a Me^{n+}/C ratio of 0,1 only for Ca the beginning ratio has to be higher. In conclusion the ratios shown in Table 8 were used in the experiments.

| Al^{3+}/C | Pb^{2+}/C | Ca^{2+}/C |
|---------------------------|---------------------------|---------------------------|
| mmol mmol ⁻¹ | mmol mmol ⁻¹ | mmol mmol ⁻¹ |
| 0,1 | 0,1 | 0,5 |
| 0,5 | 0,5 | 1 |
| 1 | 1 | 2 |
| 2 | 3 | 3 |
| 5 | 5 | 5 |
| 10 | 10 | 10 |

Table 8: Me^{n+}/C ratios obtained in the different cation solutions for precipitation

For precipitation exactly 10 ml of the metal solution and 90 ml of the DOC solution were mixed in 100 ml glass bottles (Duran®) and sealed with PTFE coated PBT screw caps. As control 10 ml deionized water instead of metal solution was added. After a first shaking the pH was measured and if necessary adjusted to a value of 3,5 with 0,5 M, 1 M or 2 M NaOH or with 0,3% HNO_3 , respectively. The original pH of the solution before the adjustment ranges from 2,9 to 3,6. Then the solutions were shake over night in an over top shaker for a complete homogenisation. After shaking the samples were stored in a refrigerated incubator at 5° C for another night. The temperature was chosen to prevent changes by microbial activity in the solutions. At this time the solutions had a rest and the flocculation is not disturbed by shaking. For filtration of the solutions at a pore size of 0,45 μm a Sartorius® Vaccum Filtration construction were used with a cellulose nitrate filter at the top and among a glass fibre filter (Whatman®, GF 6, Ø 47 mm) to improve the filtration flux. The filters were rinsed before filtration with moderately warm deionized water to prevent contaminations.

3.3.4 Chemical analyses of the filtrate solution

The filtrates were measured for pH, DOC and cations in the solution. PH and DOC measurements took place immediately after ending the filtration. DOC concentration was analyzed with a TOC Analyzer Multi C/N 2100 (Analytik Jena) after acidification and out gassing of inorganic carbon.

An aliquot of each solution was diluted in a ratio of 1:1 with 10% HNO₃ for conservation and later analyses of the cations.

To calculate the loss of cations in the solution (and to calculate the cation content in the precipitates) the cation concentration in the solution was analyzed. Calcium was analyzed with Flame AAS (Perkin Elmer 4100) with an oxygen/acetylene flame and a wavelength of 422,7 nm, Al³⁺ with a nitrous oxygen / acetylene flame (Varian AA 240 FS) and with a wavelength of 308,2 nm, and lead was analyzed with Graphite Tube AAS (Perkin Elmer 4100) with the following furnace program and a wavelength of 283,3 nm:

| Temperature | Time |
|-------------|--------|
| 20° C | |
| 90° C | 30 sec |
| 110° C | 30 sec |
| 400° C | 20 sec |
| 1800° C | 5 sec |
| 2600° C | 3 sec |

Table 9: Graphite tube heating program for lead analysis in AAS

In general a calibration curve was conducted by internal standardisation (addition of an aliquote of the standards to each sample). For the described analyses no differences were identified between the curves by an external standardisation in the same solution (10% HNO₃) and an internal standardisation therefore for further analyses only external standardisation were conducted. The solutions of the controls were analyzed for Ca²⁺, Pb²⁺ and Al³⁺.

3.3.5 Preparation, storage and DSC measurements of the precipitates

After filtration the precipitates were adhered to the surface of the cellulose nitrate filters. With a spatula the precipitates were carefully scraped off and filled directly into the DSC pans. It is to mention that in preliminary experiments we dried first the precipitates on a glass surface and then transferred into the DSC pans, but this procedure turned out to be inefficient due to the difficult handling of the very small amounts of dried precipitates. Therefore we filled it directly into the pans and prevent losses by that. The samples in the open DSC pans were

dried for 4 – 5 days at 25°C in the drying oven. By weighing the pans before and after the drying procedure the water content of the wet samples can be calculated. After weighing the open pans were stored in a dessicator over silica gel. After drying the precipitates formed dry highly agglomerated clusters and the bottom of the pans were not homogenous covered with sample this causes trouble during DSC measurements because no consistent heat transfer to the sample is assured. Therefore the dried precipitates were carefully pestled with a spatula before measurements.

The samples were conditioned for 14 days and then the aluminium pans were hermetically sealed. The analyses were conducted with DSC Q1000 (TA-Instruments, Germany) with a refrigerated cooling system (RCS) and nitrogen as a purge gas. The measurements took place in several procedures to receive results on the characteristic of the step transition and the aging behaviour of the samples. It is not possible to measure the classical glass-transition and the step transition due to water molecule bridges with one DSC procedure. So, after a first characterization of all samples in “measurement 1” one part of the samples was measured by “measurement 2” and one part by “measurement 3”. For these “follow – up” measurements always three replicates with the best pronounced transitions were chosen. Unfortunately there were not enough replicates to use every ratio for each kind of measurement. The used samples are given the

| Procedure | Rationale |
|--|---|
| <p>Procedure 1 (all samples):</p> <p>→ All samples were abruptly cooled in the DSC instrument to -50°C and then heated with 10 K min⁻¹ from -50°C to 110°C, followed by a second abrupt cooling and subsequent heating cycle. Baseline was corrected with the TZero technology® by TA Instruments.</p> | <p>First characterization of all samples, the method is fitted to observe glass-transition like step transition temperature, which means the effects of water molecule bridges on rigidity can be observed</p> |
| <p>Procedure 2 (samples with an ME / C ratio of 0,1, 1, 5 and 10(only Ca)):</p> <p>14 days after the first measurements one fraction of the samples were measure again by the following procedure:</p> <p>→ Punching of three small holes (Ø 1 mm) in the lids of the sample pans</p> <p>→ Drying in the oven overnight at 105°C to remove all water, weighing</p> | <p>This procedure is appropriate to detect reversible glass transitions, therefore all water is removed from the sample. After the described drying procedure the samples were not able anymore to show a WaMB transition and it was not possible to use them in procedure 3. The precipitates of the Me/C ratios of 2 and 3 for all cations and 10 for Pb and Al were formed when the results of measurement 2 for most ratios were available and it</p> |

| | |
|---|---|
| <p>before and after the drying procedure</p> <p>→ DSC measurement with a changed heating and cooling programme starting with a heating step of 105°C for 30 min (to make sure that all water is removed from the samples), then beginning with the programme as described above for the first procedure</p> | <p>was obvious that no differences between the different ratios were found. Consequently, measurement 2 was not conducted anymore for the ratios 2, 3 and 10.</p> |
| <p>Procedure 3 (samples with a Me / C ratio of 2, 3 and 10(only Pb and Al)</p> <p>→ After the first measurements in hermetically sealed pans as described in procedure 1 further measurements were conducted with selected pans after 6 weeks and 8 weeks (in general we selected pans where a pronounced step transition is visible and mathematically analyzable)</p> | <p>If water-molecule bridges are responsible for the measurable matrix rigidity the measured glass-transition like step transition vanished in a subsequent heating cycle, but after a longer time period the glass-transition like step transition reappears, which is explained with the reconfiguration of the water molecules. This process should also be shown for the precipitates. So it seems not necessary for the interpretation of the results to conduct this measurement for the whole concentration range.</p> |

Table 10: Explanation of the used procedures for characterising the precipitates by DSC.

All data were analyzed using Universal Analysis version 4.1 (TA Instruments). The glass transition temperature T_g and the glass transition like step transition temperature T^* is indicated by an inflection point in the thermogram. Operationally, three tangent lines were applied for the evaluation. The change of heat capacity ($\Delta c_p = \text{J g}^{-1} \text{K}^{-1}$) was calculated from the inflection point between the tangent lines.

In the following sections for most samples only the first heating cycle will be observed because the determined T^* is a non-reversible thermal event (Schaumann & LeBoef).

Some thermograms of the calcium treated samples could not be analysed without further corrections of the received heat flow curve of the samples. In Figure 23 the heat flow curve for the Ca-precipitates is shown, although the derivation of the heat flow looks normal the curve shows a strong decrease until 40°C and then at about 80°C a strong increase, between 40 and 80°C a thermal event is observable. For analyzing this thermal event by applying the required tangent lines and receiving the inflection point of the step transition a rotation of the curve is required. By this correction method the heat capacity of the sample changed but the transition temperature is still the same.

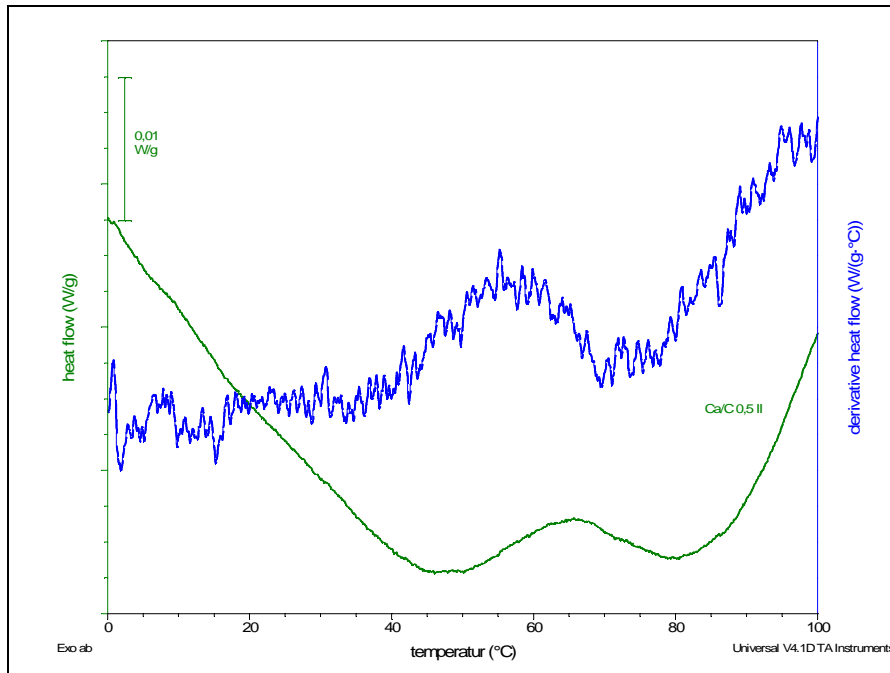


Figure 23: Heat flow curve of a DSC measurement of a Ca-precipitate, no tangent lines can be applied and no inflection point is received.

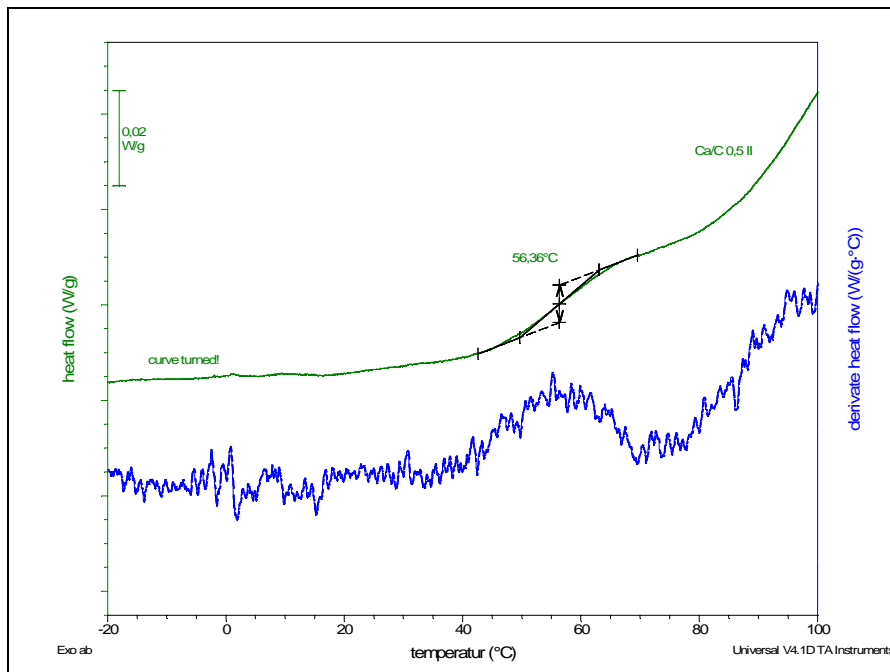


Figure 24: Corrected heat flow curve of the same sample by turning the curve in the plane with the TA instruments program, the inflection point is now analysable

All Ca samples were corrected by the shown method.

3.4 Results and Discussion

3.4.1 Qualitative observations, analyses of the filtrate and water content of the samples

In Table 11 the observation during and after the precipitation experiments were presented as evidence on the quality of precipitations.




| Ca precipitation | Al precipitation | Pb precipitation |
|--|---|--|
| First visible precipitation at a Me^{n+}/C ratio of 0,5 | First visible precipitation at a Me^{n+}/C ratio of 0,1 | First visible precipitation at a Me^{n+}/C ratio of 0,1 |
| Only slight sedimentation of the flocculation after the rest period in a defrigrator, solution is cloudy and brown | Pronounced sedimentation; solution is light brown until clear | Pronounced sedimentation; solution is light brown until clear |
|  |  |  |
| Colour of precipitate after filtration: Greyish - brown | Colour of precipitate after filtration: Brown With increasing Me^{n+}/C ratio the samples get lighter | Colour of precipitate after filtration: Dark brown With increasing Me^{n+}/C ratio the samples get lighter |
| Water content of the wet samples about 93 – 94 %, slight decrease for $Ca^{2+}/C = 10$ to about 91 % | Water content of the wet samples about 95 %, slight decrease for $Al^{3+}/C = 5$ to about 91 % | Water content of the wet samples about 95 %, no trend in different ratios observable |
| pH after treatment about 3,7 – 3,8 | pH after treatment about 3,7 – 3,8 | pH after treatment about 3,7 – 3,8 |

Table 11: Optical and analytical observations of parameters during and after the precipitation process for the three cation – DOC solutions Ca^{2+} - DOC, Al^{3+} - DOC and Pb^{2+} - DOC

As Al^{3+} and Pb^{2+} were acting very similar in precipitation observations for Ca^{2+} are often conspicuously different. Precipitation with Ca^{2+} is not as visible as for the other two cations demonstrated by weaker sedimentation of Ca precipitates and a cloudier solution after the rest

period. No differences were found in pH of the solution which was adjusted at the beginning of the precipitation process to 3,5 between the different Me^{n+}/C ratios or the used cations.

For Ca^{2+} and Al^{3+} the water content in the wet precipitates decreases for higher Me^{n+}/C ratios_{solution}, for Pb^{2+} the water content remains the same for all ratios. For the later air – dried samples (25°C in a drying chamber) which were further dried for 105°C the water content of the dry precipitates was calculated. Also here differences between the cation treatments were observed. For Pb the water content ranges until a ratio of 1 at about 7%, for a ratio of 5 the water content ranges about 3-4%. No changes for Ca precipitates were observed between the different ratios the water content ranges about 6 %. The water content of the Al precipitates is significantly higher, the content ranges about 10 % until a ratio of 1 and ranges about 16 % for a ratio of 5.

The shown masses in Figure 25 are only a rough estimation because the masses were calculated from the initial weights in the DSC pans and losses during handling with the precipitates cannot be excluded.

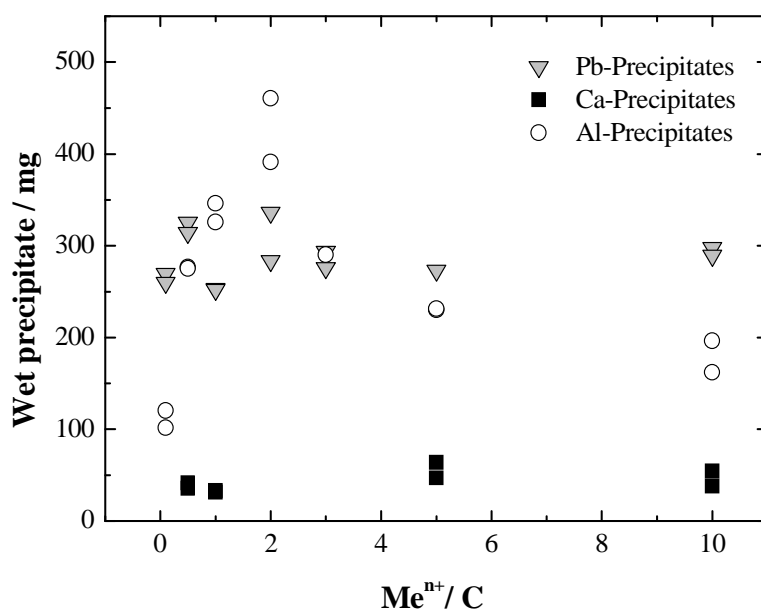


Figure 25: Amounts of wet precipitates originated during flocculation process in solutions of different Me^{n+}/C ratios with Ca^{2+} , Pb^{2+} and Al^{3+}

Nevertheless first trends were observable. So the weaker precipitation process with Ca^{2+} is underlined by the observation of the less precipitated mass for each ratio, which is about only 20 % of the mass precipitated by the two other cations. The masses for Ca precipitate range about 40 to 55 mg as for Al and Pb precipitates the masses range about 150 to 420 mg. a weak increasing trend for Ca precipitate mass is observed for the Ca^{2+}/C ratios_{solution} of 5 and 10.

Though Pb^{2+} is lower charged than Al^{3+} all in all Pb^{2+} is as same effective as Al^{3+} . But for Pb precipitation no observable increasing or decreasing trend dependent on the chosen Pb^{2+}/C

ratio_{solution} is demonstrated. In contrast Al precipitate masses increase abruptly for the Al³⁺/C ratio_{solution} of 0,1 to 2 and then there decrease for higher ratios.

A better specified parameter for effectiveness in precipitation is the measurement of the DOC losses (Figure 26).

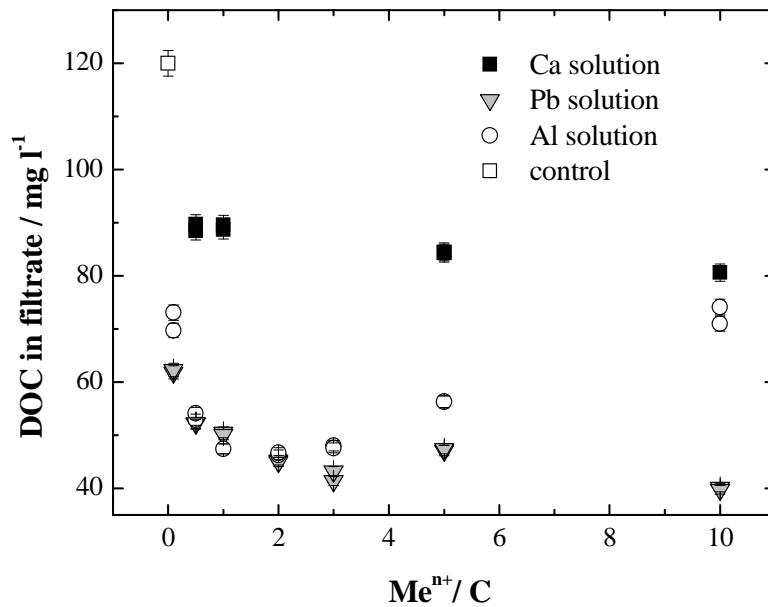


Figure 26: DOC losses of the solution after the precipitation in duplicates with Ca²⁺, Pb²⁺ and Al³⁺ in different Meⁿ⁺/C ratios.

Interestingly no pronounced differences were found for the effects of Al³⁺ and Pb²⁺ until a Meⁿ⁺/C ratio_{solution} of 3. Then for an increasing concentration of Al³⁺ in solution the losses of DOC decrease what means a fewer amount of precipitate arises. In contrast for Pb²⁺ the solution remains at the low DOC level also for higher Pb²⁺ concentrations. Therefore it can be assumed that for high Meⁿ⁺/C levels Pb is more effective in precipitation than Al. Comparing our results for Al precipitation at the ratios 0,1 and 0,5 with the results of Scheel et al. (2007) it is seen that at a ratio of 0,1 41% of the DOC was precipitated whereas in Scheel et al. (2007) 36,4% (Oa horizon of a spruce forest, pH 3,8) was precipitated, at a ratio of 0,5 55,8% was precipitated, in Scheel et al 43,1% at a ratio of 0,3 was precipitated. The higher precipitation in our experiments could be related to different sample characteristics but also to the different mechanism of DOC release in attendance of the acid cation exchange resin. The lowest effect on precipitation was observed for Ca²⁺ based on the losses of DOC in the solution which is conform to the shown precipitation masses.

For an estimation of the Meⁿ⁺/C ratio in the precipitates also the loss of cations in the solution after the precipitation procedure is to be known. Unfortunately a correlation of the loss of cations in the solutions with the loss of DOC can only be conducted for the very low Meⁿ⁺/C ratios (until a ratio of 1). For the higher tiered solutions the standard deviations of the analyses are in the same range as the cation losses therefore the values are not reliable and will not

comprise in further discussion. Hence it is not possible to calculate a Me^{n+}/C ratio in the precipitates itself for higher concentrations.

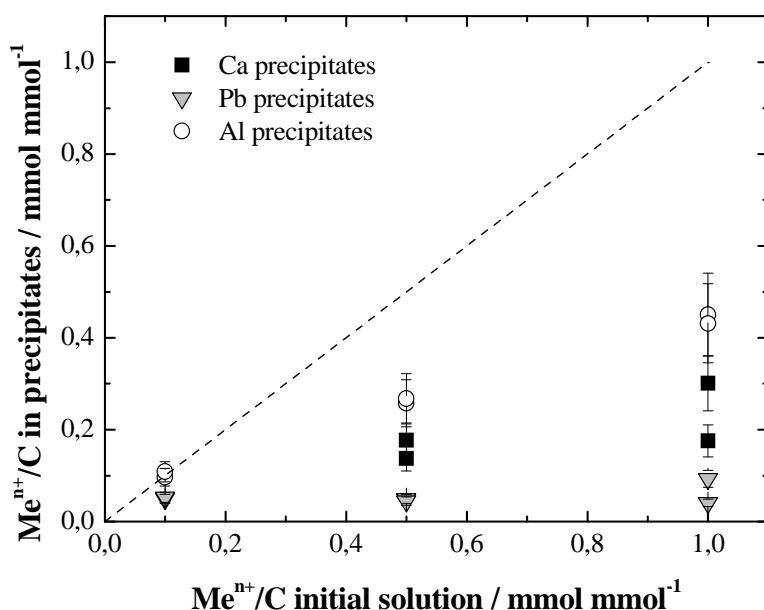


Figure 27: Cation – Organic carbon ratio for the three lowest Me^{n+}/C ratios in precipitation experiments, due to high analytical standard deviations and in relation to the absolute concentration low losses of cations for the higher tiered Me^{n+}/C ratios no Me^{n+}/C ratios in precipitates were calculated for these.

As it is shown in Figure 27 the highest Me^{n+}/C ratio in the precipitate for the three lowest cation concentrations can be observed for Al^{3+} . Although we observed in general a similar behaviour of Al and Pb in precipitation at low Me^{n+}/C ratios_{solution}, it is now contrary: no change in Pb^{2+}/C ratio in the precipitates can be observed. For the precipitates induced by Ca^{2+} no significant trend is observed according to high deviations between the duplicates. But nevertheless there is the optical impression that the Ca^{2+}/C ratio in the precipitate is higher for a ratio_{solution} of 1 than of 0,5. The Ca^{2+}/C ratio in the precipitates ranges between Pb and Al – ratios. No differentiation between inorganic and organic precipitations is possible based on the conducted measurements therefore the high precipitation of Al^{3+} could be also caused by inorganic precipitations. But due to the low pH value to prevent those kind of precipitation and the fact that also in the control no inorganic precipitations were found this possibility is unlikely realistic. Hence we have to assume that all disappeared Al^{3+} in solution is bound in OM in the precipitates. At the time we have no explanation for the low losses of Pb and the comparative high losses of Al^{3+} . It seems that much more Al can be bind to OC than Pb. It can be also assumed that Pb is not only precipitated with DOM but also bind as readily soluble complexes in a greater extent than Al^{3+} .

Our Al/C ratios in precipitates exceed the ratios reported by Scheel et al. (2007). Scheel et al. reported a maximum ratio of 0,1 at pH 3,8. We explain the higher Al/C ratios by the process

of DOC release because especially DOC with binding sites for cations was dissolved with our method and therefore more cations can be bound by precipitation.

Referring to the low reliability of the cation analyses and therefore the missing data on $\text{Me}^{\text{n+}}/\text{C}$ ratios in the precipitates for the higher ratios in following discussion we will only refer to the initial $\text{Me}^{\text{n+}}/\text{C}$ ratios in the solution and to the measured DOC values after precipitation.

3.4.2 DSC results

Results in hermetically sealed pans:

As described in procedure I all samples were measured after 14 days in hermetically sealed pans with DSC and two cooling and heating cycles were conducted for each measurement. The resulting heat flow curves of the two heating cycles differ significantly from each other. In the first heating cycle for each precipitate a thermal event is identified as step transition described for soil samples especially for samples with a high content of SOM as described in chapter 2. Also the measured step transition temperature of the precipitates is in the same range as measured for soil samples of $53^\circ\text{C} - 65^\circ\text{C}$.

In the second heating cycle the thermal event observed in the first cycle disappeared and no abruptly changes in heat flow can be identified (Figure 28 and Figure 29).

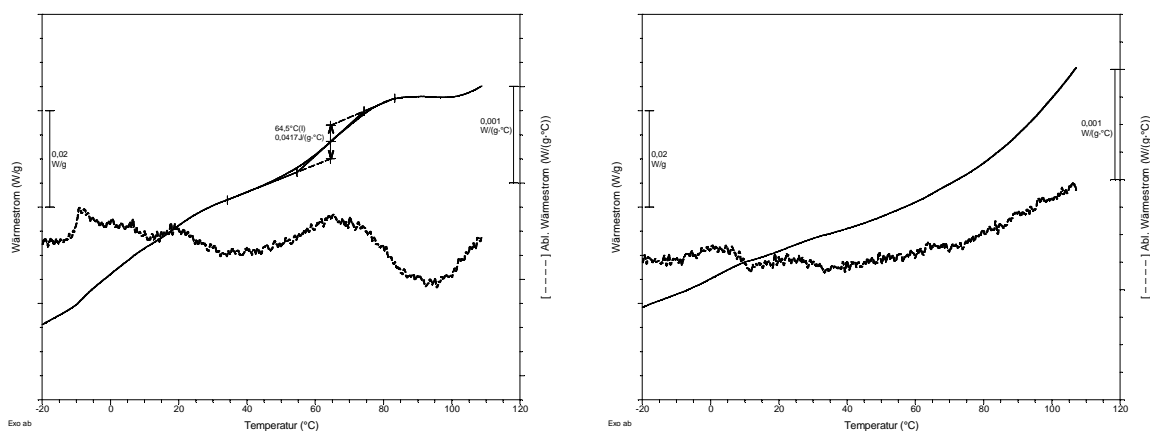


Figure 28: First (left) and second (right) heating curve of Al-precipitates ($\text{Me}^{\text{n+}}/\text{C}$ ratio = 2) in hermetically sealed pans. No analyzable thermal event in the second heating cycle (continuous line: Heating flow; dashed line: derivation of heat flow).

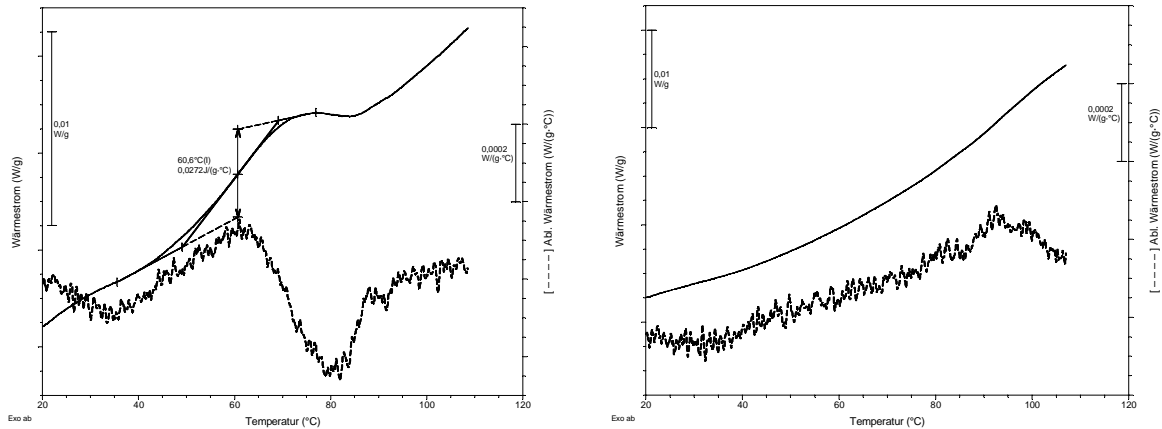


Figure 29: First (left) and second (right) heating curve of Pb-precipitates (Me^{n+}/C ratio = 2) in hermetically sealed pans. No analyzable thermal event in the second heating cycle (continuous line: Heating flow; dashed line: derivation of heat flow).

According to the non-reversing character of the step transition we assumed that the observed thermal event in the first heating cycle is similar to the so named step transition like glass transition temperature T^* . Therefore in the following sections we will discuss the results of T^* for the created precipitates.

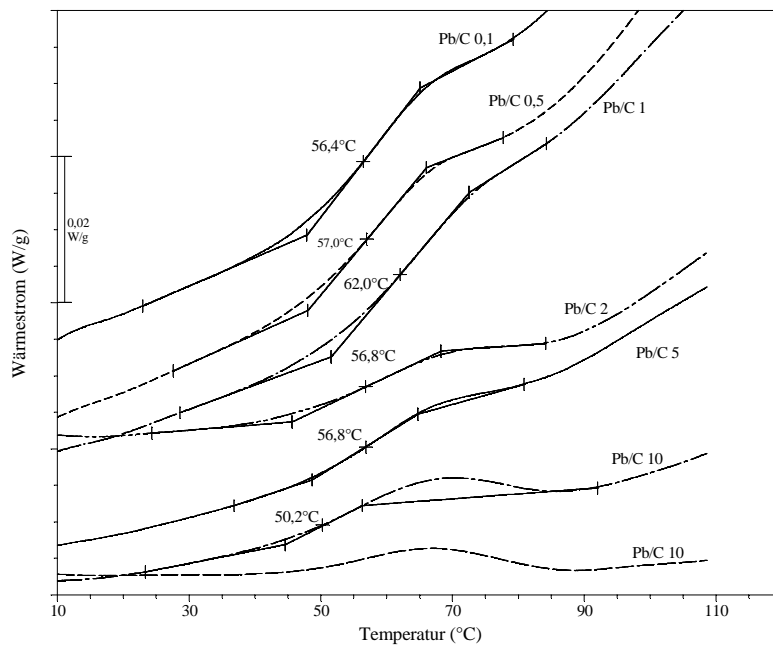


Figure 30: DSC curves and glass transition – like step transition temperature T^* of Pb-DOM precipitates produced in solutions with different Me^{n+}/C ratios. With increasing ratio the samples develop an enthalpic overshoot since for some curves (Pb/C 10) no step transition temperature can be analyzed because the step has become a peak.

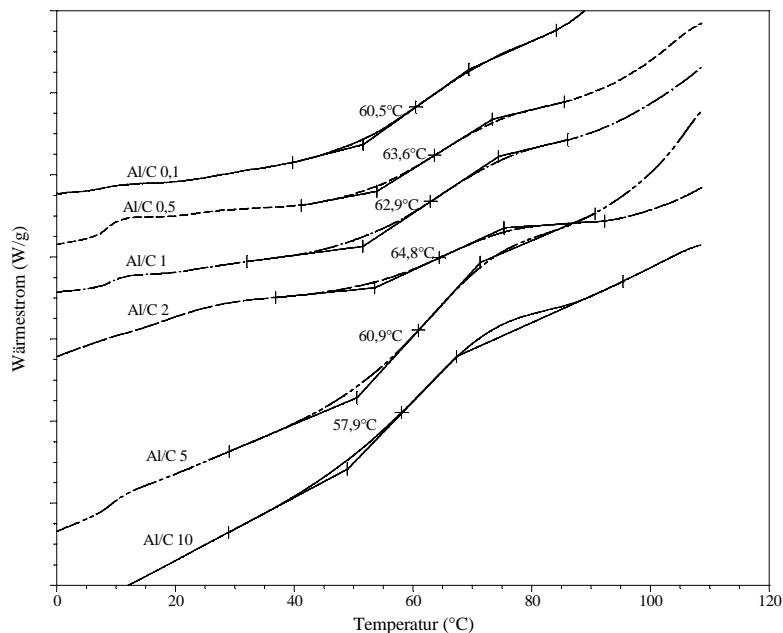


Figure 31: DSC curves of Al DOM precipitates produced in solutions with different Me^{n+}/C ratios.

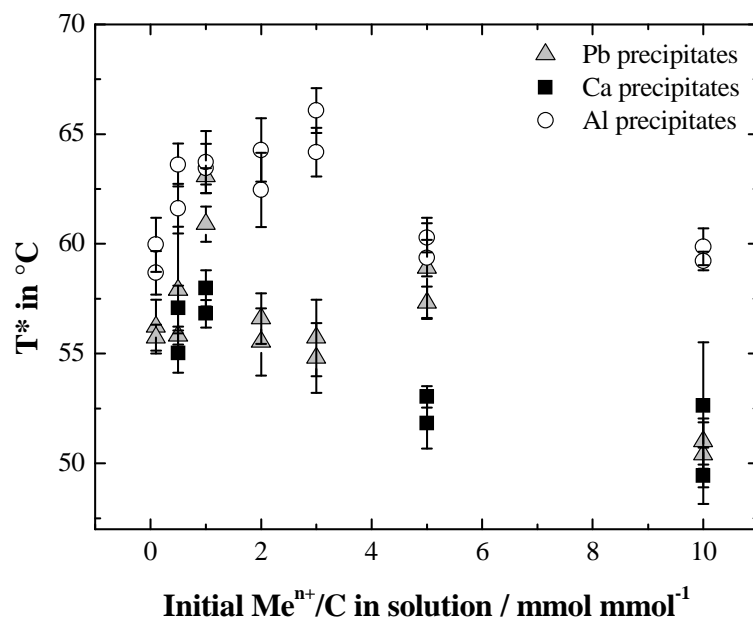


Figure 32: Step transition like glass transition temperature T^* in dependence of the initial Me^{n+}/C ratio in solution for the cation-DOM precipitates, standard deviations for T^* based on the results for the number of pans for each sample (4 -8).

The Al-precipitates show the highest T^* for all prepared precipitates. For the first three solutions with the lower $Al^{3+}/C_{\text{solution}}$ T^* of the Al precipitates increases up to about $66^\circ C$, between a $Al^{3+}/C_{\text{solution}}$ of 1 and 4 there seems to be maximum for T^* , for the $Al^{3+}/C_{\text{solution}}$ of 5 and 10 T^* decreases slightly to $62^\circ C$ in average.

Generally, T^* of the Pb precipitates ranges between the temperatures of Ca and Al precipitates. Nearly for all Pb^{2+}/C ratios_{solution} T^* averages about 60°C, only for a Pb^{2+}/C ratio_{solution} of 1 T^* increases significantly to about 65°C. It is to mention that this result appeared for the duplicates which were measured 3 and 4 times (number of the analyzable heat curves) with DSC, respectively. We cannot exclude the possibility that these values are outliers but according to the other measured characteristics in the solution of these samples like pH or DOC no hints were given that something was going wrong during the precipitation procedure. At the time we have no explanation for this behaviour in DSC. Again the Pb^{2+}/C ratios_{solution} of 2, 3 and 4 show a T^* of about 60°C, for the Pb^{2+}/C ratio_{solution} of 10 a significant decrease of T^* is observed to about 54°C.

The highest differences in T^* for increasing Me^{n+}/C ratios are observed for the Ca-precipitates. For the lower Ca^{2+}/C ratios_{solution} of 0,5 and 1 T^* ranges in most cases between 55 – 58°C whereas a weak trend of an increase can be assumed between a Ca^{2+}/C ratio_{solution} of 0,5 and 1 than for a Ca^{2+}/C ratio_{solution} of 5 and 10 T^* ranges between 49 and 53°C which is significantly lower. Furthermore it is to be mentioned that the thermal events for the precipitates of the lower Ca^{2+}/C ratios_{solution} were only weak pronounced and for a Ca^{2+}/C ratio_{solution} of 0,5 all four curves have to be turned for defining a T^* . We assume that the difficulties in analyzing the heating curves for the Ca precipitates are also linked with the low masses of precipitate available for the measurements. This caused only a heterogenous coverage of the bottoms in the DSC pans and hence an unbalanced heat transmission during the measurements. Nevertheless the values can be classified to be reliable because of a sufficient amount of replicates for each duplicate.

It is to discuss why we found only a step transition like glass transition in the precipitates and no real glass transition as for examples Leboeuf & Weber (1997) find it in humic and fulvic acids (LeBoeuf and Weber 1997). T^* is connected with cross-linking by water-bridging in SOM. As mentioned in chapter 3.4.1 all precipitates contain measureable water contents therefore water molecule bridges in the OM cannot be excluded for the precipitates. Especially for the Al precipitates the water content was significantly higher than for the Ca- and the Pb precipitates which correlates with the high T^* for Al precipitates. But for higher Al^{3+}/C also the water content increases and T^* decreases. Furthermore the water content of the Ca precipitates is higher than for the Pb precipitates but although T^* of the Pb precipitates is higher. Therefore a direct correlation between water content in the precipitates and matrix rigidity cannot be achieved by this data. We want to point out that the interaction with water molecules is diverse and there should be an influence of the cations on the formation of water molecule bridges inside the precipitated OM which cannot be demonstrated by two dimensional correlations.

Creating a ranking of rigidity according to the measured T^* of the precipitates the Al precipitates are the most rigid for nearly all Me^{n+}/C ratios followed by the Pb precipitates and at the end the Ca-precipitates. It can be assumed that Al is the best cross-linking agent of those three

because of the higher charge, also Pb is a good cross-linking agent because of its charge and high molecular mass.

Regarding the Me^{n+}/C ratios in the precipitates for Al both T^* and the Al^{3+}/C ratio_{precipitate} increases. That means a high content of Al in an organic precipitate induces also a high degree of cross-linking in the organic matrix. For the Pb precipitations T^* only increases for a Pb^{2+}/C ratio_{solution} of 1 but for this ratio no changes in Pb content related to C content can be observed. Trusting the value of T^* that would mean that in spite of the Pb content in the precipitates are still the same the manner of binding is different in such a way that cross-linking is higher than in all the other precipitates. This sounds really unlikely. Because of the difficulties in the Pb cation measurements for this inconsistency no conclusive explanation is possible. For the Ca precipitates a slight increase can be observed for the Ca^{2+}/C ratio in the precipitates and also for the rigidity of the samples. Therefore it can be assumed that an increasing Ca content in the precipitate induces also a higher cross-linking in the interior. For all cations a decreasing DOC loss was observed for the higher Me^{n+}/C ratios_{solution}. We concluded that a high cation amount also can cause a dissolution of precipitates by the formation of organo-metal complexes. That means the precipitate itself is less stable and not as good cross-linked as at a lower concentration of cations. The results for T^* underline the hypotheses for all cations. T^* decreases for the highest Me^{n+}/C ratio_{solution} of 10 which is correlated with a lower rigidity in these samples.

Results in open pans

As described in procedure II of the DSC methods chapter, the thermal behavior of an amount of the precipitates should be determined for completely water free samples therefore the precipitates were dried at 105°C.

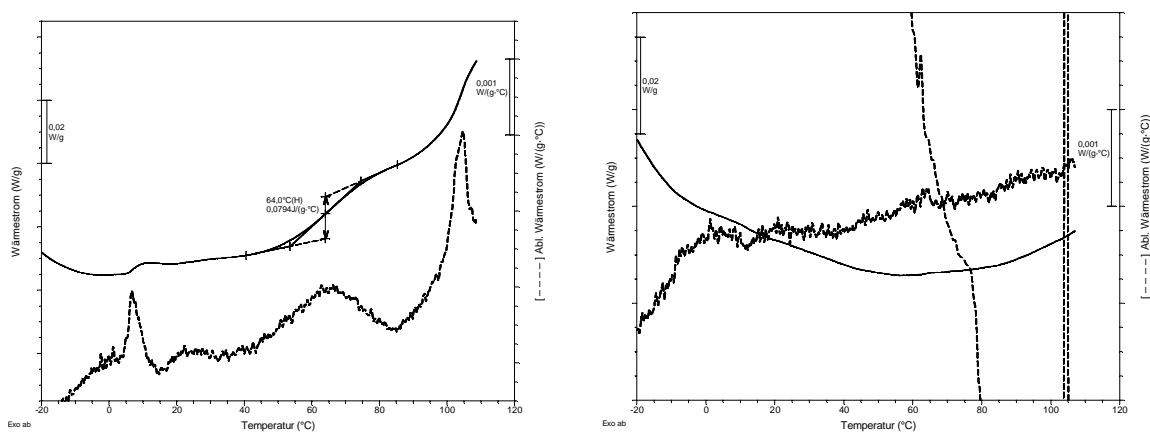


Figure 33: DSC heating curves of an Al precipitate (Me^{n+}/C ratio_{solution} = 1) before (left) and after (right) complete removal of water by drying at 105°C: no analysable thermal events can be detected anymore. The vertical curves in the left picture originated from the cooling cycle before and cannot be excluded technically. The heating curve received before cooling shows a pronounced melting peak around 0° C which is also a hint for the higher water content of the samples.

In Figure 33 the thermal behaviour of a sample is shown before and after the complete remove of water. As seen in the left picture the water causes a pronounced melting peak around 0°C and also a pronounced step transition is measured for the Al precipitate. No analyzable thermal events were measured for the water-free Al precipitate, neither observed for the heat flow curve itself nor for the derivation of the heat flow. This observation was made for all precipitates independently which cation was used for precipitation and which Me^{n+}/C ratio was adjusted in solution.

We want to point out that this result underlines the observations on the thermal behaviour of the samples in the second heating cycle during the first measurements described above. Schaumann et al. (2006) hypothesized the breaking of the water molecule bridges due to the high temperatures in the first heating cycle and therefore the vanishing of the step transition in the second heating cycle. These results demonstrate that there should be an interaction between water bridging and cations and it can be concluded that cation bridging itself induces no signals in DSC in the measured temperature range.

Multiple measurements

Schaumann et al. (2005) describes that the glass transition like step transition temperature T^* has a reversing character. It means the step transition disappears in a directly following second heating cycle, but reappears after some days of storage. This effect is related to the kinetically retained reorganization of the water molecules in the organic matrix. We also observed the disappearance of the step transition in the second heating cycle as mentioned above. Hence we controlled the presence of a reappearance by measuring specific samples after a time period of 6 weeks after the first measurement and after 2 weeks of the second measurement. The measurements were only conducted for Al and Pb precipitates with Me^{n+}/C ratios_{solution} of 2 to 10 because for Ca precipitates the samples amounts were highly limited and therefore not available for this experiment.

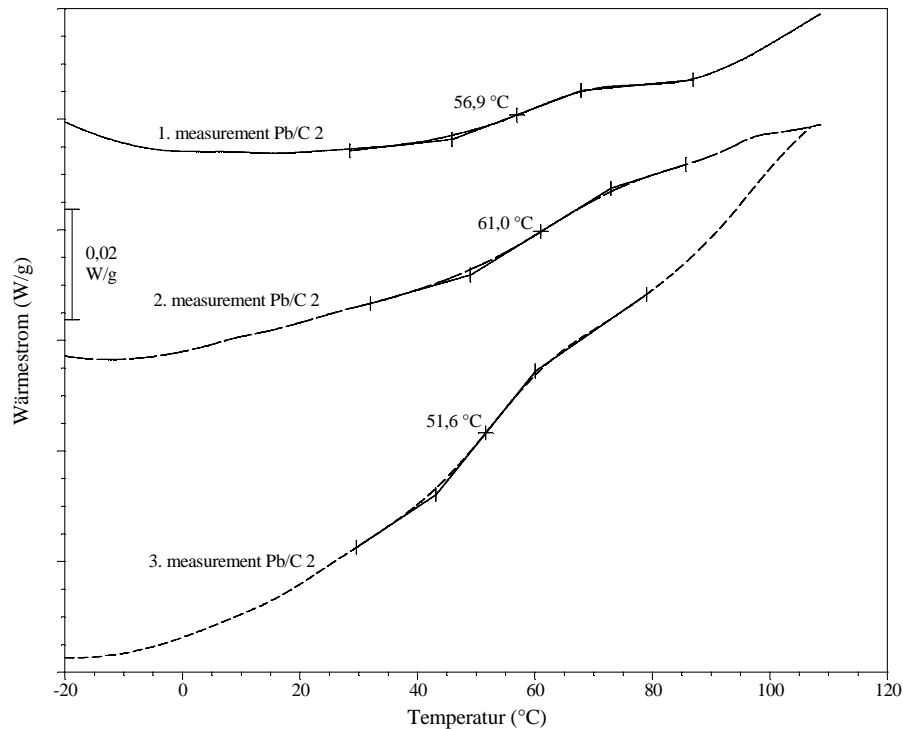


Figure 34: Heating curves of Pb precipitates (Pb^{2+}/ C ratio_{solution} = 2) measured after 2 weeks conditioning (solid line), after 6 weeks after the 1 measurement (long dash) and after 2 weeks after the 2. measurement (short dash). T^* is given of inflection point of the step transitions.

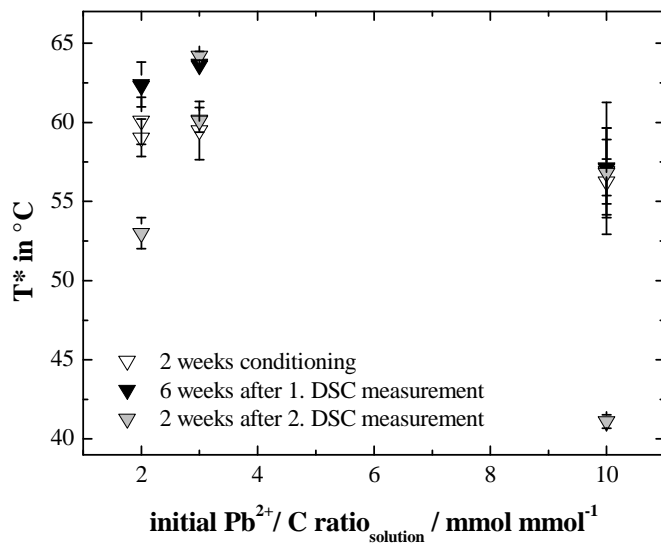


Figure 35: T^* for Pb precipitates created in different Pb^{2+}/ C ratios_{solution} in duplicates and measured after 2 weeks of conditioning, re-measured six weeks after the 1. DSC measurement and 2 weeks after the 2. DSC measurement to control the reappearance of T^* .

As it is seen in Figure 34 and Figure 36 after different time periods a step transition generally reappears this is in line with the results of Schaumann et al. for soil samples. For Pb precipitates grown in a ratio_{solution} of 2 the values are very similar for the first and second measure-

ments (Figure 34). This is comprehensible because a time period of 6 weeks should be sufficient for the matrix to achieve the same rigidity as observed at the first measurement. Two weeks after the second measurement the rigidity seems not as much pronounced as before referring to the water bridge model this means not all water molecules were reorganized in the organic matrix during this shorter time period. Also these observations are in line with Schaumann et al. But as shown in Figure 35 these observations were only made for Pb precipitates created with a Pb^{2+}/C ratio_{solution} of 2, the other Pb^{2+}/C ratios_{solution} are not in line with these observations. For a ratio of 3 no trend is observable and for a ratio of 10 one duplicate is outstanding of the others with a very low and due to the heating curves very weak pronounced step transition ($T^* = 41^\circ C$) so there is a relatively high probability that this sample is not very reliable and therefore can be marked as an outlier.

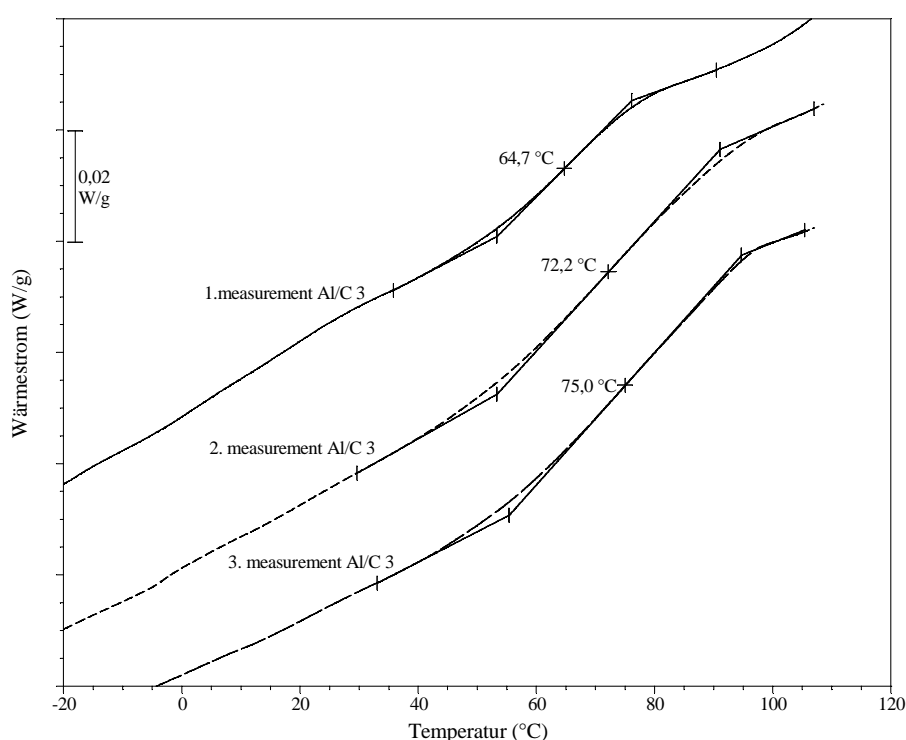


Figure 36: Heating curves of Al precipitates (Al^{3+}/C ratio_{solution} = 3) measured after 2 weeks conditioning (solid line), 6 weeks after the 1 measurement (short dash) and 2 weeks after the 2. measurement. T^* is given as inflection point of the step transitions.

In Figure 36 heating curves for Al precipitates created in a solution with a Al^{3+}/C ratio of 3 were presented. These 3 curves show nearly parallel shapes but with a shifting of the step transition temperature T^* to higher temperature. According to the water bridge model that would mean that after each DSC measurement the water molecules reorganized in a relatively short time and in a matter which induces a more rigid matrix than before. This is not in line with the until now hypothesized slow reorganisation of the water molecules and it seems probable that unknown processes (melting and solidification of the matrix? Chemical reactions? Formation of aldehyds? Oxidative Drying? Resinification?) induce these results. Furthermore it is important to mention that in the second heating cycle directly after the first no

effects were observed for the precipitates with a higher T^* as also measured for the other precipitates measured for a first time after conditioning. The described characteristic during multiple measurements for the Al precipitate basing on a $\text{ratio}_{\text{solution}}$ of 3 cannot be completely underlined by the measurements for the Al precipitates based on a $\text{ratio}_{\text{solution}}$ of 2 and 10 (Figure 37).

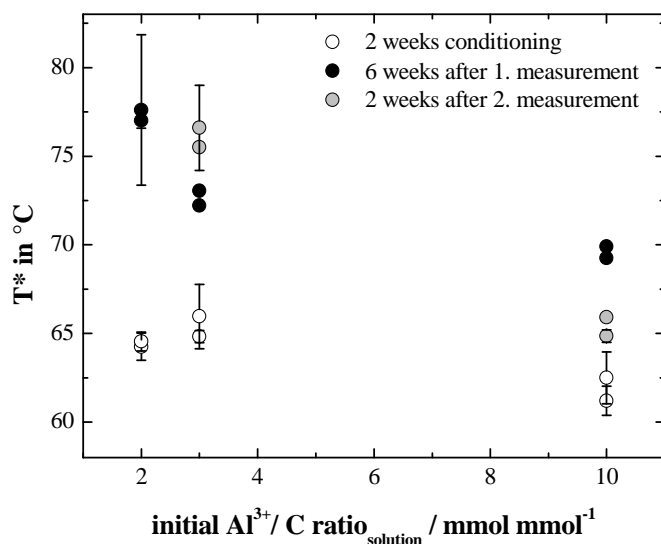


Figure 37: T^* for Al precipitates created in different Al^{3+}/C $\text{ratio}_{\text{solution}}$ and measured after 2 weeks of conditioning, re-measured six weeks after the 1. DSC measurement and 2 weeks after the 2. DSC measurement to control the reappearance of T^* .

For a $\text{ratio}_{\text{solution}}$ of 2 the thermograms were not analyzable for the measurements of 2 weeks after the 2. measurement. For a Al^{3+}/C $\text{ratio}_{\text{solution}}$ of 10 the precipitates show the highest rigidity 6 weeks after the first measurements and not as discussed for the Al precipitates with a $\text{ratio}_{\text{solution}}$ of 3 for the precipitates measured 2 weeks after the second measurement.

But it is to mention that for all multiple measurements of Al precipitates the resulting values for T^* are significantly higher in the second and the third measurement than in the first measurements. The responsible process is unknown at the moment and cannot be explained by the water bridging model.

3.5 Conclusion

The experiments demonstrate a very similar thermal behaviour of DOM precipitates and SOM in soil samples. A step transition like glass transition was obtained for the DOM precipitates in the same temperature range as it was obtained for soil samples independently of the used Me^{n+}/C ratio in the solution and the used cation. This observation is fully in line with hypothesis I. These results show that the induced cation – water molecule - DOM bindings are also present in undisturbed soil samples and the molecular structure seems to be result in the same rigidity range. It supports the assumption that also the molecular structures are very similar. Al and Pb precipitates demonstrate a high stability / rigidity of the formed DOM precipitates,

both cations can be described as good cross-linking agents due to their ability of forming precipitates. The hypothesized influence of concentration and manner of the cations on the rigidity (Hypothesis II) was supported for this thermal event.

Ca precipitates show a less rigidity and Ca^{2+} itself shows a less pronounced ability of forming precipitates than the other two cations. Therefore it can be assumed that Ca^{2+} only plays a minor role in forming precipitates in acidic soils. However it is to consider that there is more Ca^{2+} available at neutral pH values and therefore the role for Ca^{2+} of precipitation in natural soils is not negligible. Comparing the behaviour of Ca^{2+} in the whole soil samples with it in the precipitates it is to conclude that the affinity of Ca^{2+} to be sorbed to existing exchange sites seems to be higher than the tendency of forming precipitates.

It is important to consider that high cation concentrations do not automatically induce high precipitation rates. Especially for toxic cations like Pb^{2+} and Al^{3+} it is to consider that higher amounts of the cations lead to a decreasing precipitation and hence to a depletion of the cations in deeper horizons or to absorption in living organisms. Therefore the results support field observations where high cation contents induces the dissolution of metal-organic precipitates by destabilization of the organic matrix e. g. by colloidal metals (Klitzke and Lang 2009). Here shown as decreasing T^* for high cation contents in the precipitates. Otherwise in soil with very low cation concentrations a stabilization of the organic matter by increasing the cation content is conceivable. All in all it depends on the overall cation and rigidity status of SOM.

The measurements furthermore demonstrate the important role of water molecules in rigidity measurements of SOM. No signals were obtained in water-free precipitates in the observed temperature range and hypothesis III can be neglected for our measurements. It is to add that at higher temperatures deformations of the organic molecules are anticipated. Therefore to detect real glass transitions for strong bindings between the organic functional groups and the cations without the interaction of water molecules DSC is not an applicable method.

The results of the aging experiments are inconsistent for the various concentrations and it is not possible to derive a final conclusion. The results indicate that the repeated processes of heating and cooling change the structure of the organic matrix over a longer time and the influence of the cation-water-molecule-bridges cannot be divided from other chemical processes.

Further scientific discussion is necessary if the measured increasing rigidity is also in line with stability of the formed precipitates. That would mean that the samples with the highest rigidity are also the samples with the highest stability against microbial degradation or other changing environmental parameters.

4 Is there an influence on lead sorption / desorption by different cations inducing stable molecular networks in SOM? A search

4.1 Summary

The aim of the study was to demonstrate a correlation between forming of co-ordinative cross-links by multivalent cations in SOM and a kinetically retained desorption of lead (Pb). Therefore pre-treated samples with Calcium (Ca) and Aluminum (Al) cations were contaminated with Pb until reaching a concentration of about 300 mg/kg which is a naturally occurring background concentration. Before and after desorption the rigidity of samples were characterised by the step transition temperature T^* . Desorption experiments were conducted with an acidic cation exchange resin and desorbed lead was measured at different time points. An increase of rigidity was clearly demonstrated for the cation treated samples before the beginning of desorption. However, no significant effects were observed in the desorption behaviour of lead for the samples. The amounts desorbed were very similar for each sample at the specific timepoints. Results for losses of DOC and T^* of the desorbed samples also show no differences related to the pre-treatment of the samples. Surprisingly there was still a constant increase of Pb desorption after 24 hrs, which is explained with a swelling effect of the SOM during the experiment. It is concluded that the used method was possibly too harsh to find any effect or in a different way: the reversibility of the induced changes was higher than expected.

4.2 Introduction

Soil Organic Matter (SOM) is known for a high sorption capacity for lead. Especially in forest soils lead is sorbed by organic layers (Sauve, McBride et al. 1998). A close correlation is found between the C-content of a soil and the immobilizations of lead (Watmough, Hutchinson et al. 2004). But there are also transport forms of lead with dissolved organic matter (DOM) like Pb-organic complexes (Ge, Sauvé et al. 2005) and mobile Pb colloid associations (Kretzschmar, Borkovec et al. 1999, Denaix, Semlali et al. 2001).

Lang et al. found a high colloidal stability for Pb-organic agglomerates by SAXS curves formed at pH 4 (Lang, Egger et al. 2005).

During sorption Pb is in competition to other cations like Fe and Al (Pinheiro, Mota et al. 2000, Tipping, Rey-Castro et al. 2002, Titeux, Brahy et al. 2002). The known influences on Pb-sorption and desorption are pH, ion-strength (Pinheiro, Mota et al. 2000) and the concentration of competing cations in the soil solution (Koopal, Van Riemsdijk et al. 2001). Not much is known about the influence of the structure of SOM on Pb-sorption and desorption processes.

In field studies (Klitzke and Lang 2007) lead released from soils during cation depletion processes in acidic soils. Therefore the authors deduced a connection between the binding of

base cations in SOM and the depletion of lead. For multivalent cations the formation of coordinative cross-links in SOM is postulated (Lu and Pignatello 2004). It is hypothesized that these cross-links induce complex networking in SOM and therefore a higher stability and glassiness of the matrix.

In chapter 2 the changes in matrix rigidity for different cation contents were observed in an organic spruce forest layer. The rigidity was measured by the glass transition-like step transition temperature. This method originates from the polymer science in which each substance has its specific glass transition temperature demonstrating the degree of rigidity of the polymer matrix. Glass transition temperatures were also reported for isolated humic and fulvic acids (Leboeuf and Weber Jr 2000, Young and Leboeuf 2000) but furthermore for whole soil samples e. g. (Schaumann and Antelmann 2000, Hurrass and Schaumann 2007). SOM can be regarded as a macromolecular matrix or from a supramolecular point of view (LeBoeuf and Weber 1997, Lu and Pignatello 2002, Schaumann 2006) and the occurrence of a glass transition in NOM supports the suggested similarity with synthetic polymers. Up to now it is known that there exist two types of step transitions in SOM. One named the classical one which also occurs in synthetic polymer systems and which is reversible in subsequent heating runs. The other one is only be observed in water containing samples measured in a closed systems, this type of transition slowly reverse after days or weeks of storage depending on the sample (Hurrass and Schaumann 2005, Schaumann and LeBoeuf 2005, Hurrass and Schaumann 2007). The described thermal behaviour of SOM can be characterized by the glass transition-like step transition temperature named in this work step transition temperature T^* . The step transition behaviour can be explained by the hydrogen bond-based cross-linking (HBCL) model, which proposed cross-linking by individual water molecules (Hurrass and Schaumann 2005, Schaumann 2005, Schaumann and LeBoeuf 2005, Schaumann and Bertmer 2008). The results in chapter 2 and chapter 3 of this thesis indicates additionally the forming of cation-water-molecule bridges between the functional groups of the organic matter. These bridges can be postulated in whole soil samples and also in metal-organic precipitates forming in soil solutions. The models were supported by computational calculations e. g. (Aquino, Tunega et al. 2008).

Hysteresis and non-ideal sorption are tried to explain with this macromolecular models, which assume glassy and rubbery domains (Huang and Weber Jr 1997, LeBoeuf and Weber 1997, Xing and Pignatello 1997) but furthermore it can also be assumed that inorganic toxicants like lead were released in the soil solution during the dissolution of existing networks. The factors influencing the stability of those networks are widely unknown but it is to assume that I) the more rigid a network is, the stronger the lead cations are also linked in the network. That would mean that in a molecular organic matrix with a high degree of coordinative cross-links desorption of lead should be kinetically retained and therefore slower than in a less cross-linked matrix. In the following study the stability of those networks is characterized and their ability of lead binding is analyzed.

Therefore the Al and Ca treated samples were used as investigated in chapter 2. A correlation between cation composition and rigidity was demonstrated for these samples. Further treatment with lead was planned to achieve a background contamination as it is occurred in environmental samples. A cation depletion was simulated with an acid cation exchange resin. At specific time points desorption of lead was determined.

4.3 Material and Methods

4.3.1 Preparation and storage of the samples

The soil sample used for the study was an organic layer from an 80 year old spruce forest in South Germany. The main characteristics of the sample are shown in Table 3, preparation of the sample after sampling is described in chapter 2.3.2. For further treatment the sample was stored in PE bottles at room temperature.

| pH | C_{org} / % | CEC_{pot} / mmol_c kg^{-1} | CEC_{eff} / mmol_c kg^{-1} | WC / % | Ca^{2+} / mmol_c kg^{-1} | Mg^{2+} / mmol_c kg^{-1} |
|---------------|-------------------------|--|--|-----------|---|---|
| $3,7 \pm 0,1$ | 43 ± 4 | 671 ± 50 | 303 ± 20 | 8 ± 1 | 165 ± 10 | 43 ± 5 |

Table 12: Common soil characteristics of the used organic layer from a spruce forest

Samples were treated at pH 4 with calcium nitrate, aluminium nitrate and lead nitrate solutions in various concentrations (see Table 13). 20 g of the original sample were mixed with 500 ml solution in 500 ml Duran glass bottles. Altogether 4 different concentrations for Ca^{2+} (2, 4, 8, 16 $\text{mmol}_c \text{ l}^{-1}$) and 4 different concentrations for Al^{3+} (1,5, 3, 6, 12 $\text{mmol}_c \text{ l}^{-1}$) were chosen. These concentrations based on the results of chapter 2.4.1. It is assured that with this method cation concentrations were available in an equal distribution between the original cation concentration and the CEC_{eff} . One control was treated in the same way with 500 ml deionized water. At the end 9 different treated samples were available for desorption experiments. The cation loss of the control sample was lower than the standard deviation of the analyzes. Therefore the measured cation values for control and original sample were the same.

| Sample | Cation concentration in solution / $\text{mmol}_c \text{ l}^{-1}$ | Resulting cation content in soil / $\text{mmol}_c \text{ kg}^{-1}$ |
|--------|---|--|
| Ca-1 | 2 | 169 |
| Ca-2 | 4 | 203 |
| Ca-4 | 8 | 240 |
| Ca-8 | 16 | 320 |

| | | |
|---------|-----|--------------------------|
| Al-0,5 | 1,5 | 108 |
| Al-1 | 3 | 144 |
| Al-2 | 6 | 220 |
| Al-4 | 12 | 365 |
| Control | 0 | See original Table 12 |

Table 13: Concentrations of the basic samples conducted for Pb spiking. The cation contents were calculated from the analyses of the solutions after the treatment.

The samples were shaken for 3 hours in a horizontal shaker. PH was monitored after 0,5 and 1,5 hrs and adjusted with 1 M HNO₃ or 0.5 M NaOH to pH=4 if necessary. Then the solution was separated by vacuum filtration for 10 minutes (589/2 Filter Paper Circles, ashless, Whatman®). The soil samples were weighed to calculate the amount of remaining water and then the samples were dried in a drying chamber at 25°C for 4 days and stored in closed PE bottles at room temperature for further treatments.

For contamination with Pb²⁺ 16 g of the samples were spiked with 160 ml lead nitrate solution of 0,1 mmol l⁻¹ and were shaking over night in a 250 ml Duran® Bottle. In preliminary experiments with this treatment a Pb concentration of 300 mg kg⁻¹ was achieved in the samples. The amount of solution was lower than during the other cation addition procedures to reduce the DOC losses during the treatments. After shaking the samples were treated, filtrated and dried as described above. The dry samples were then stored in acryl glass desiccators at 20°C and 76% relative humidity, adjusted by saturated Na⁺ - solution. During conditioning the samples were stored evenly spread in open petri dishes to assure the same conditions for all particles.

After two weeks of conditioning desorption experiments were conducted.

4.3.2 Desorption experiments

Desorption experiments were conducted with an acidic cation exchange resin (ion-resin Amberlite® IR120, H⁺-Form, exchange capacity 2.3 mmol_c g⁻¹, Merck, Darmstadt). For each experiment about 1,5 g of the resin was welded in a finely meshed polypropylene net (mesh size 72 µm). Each resin bag was then washed in 10% HNO₃ – solution for 30 min and rinsed with deionized water to remove DOC and free acid. In preliminary tests measurable DOC fractions resulting from the resin were found.

For each sample 2 g of the organic layer and 50 ml water were treated for 15 min in a horizontal shaker in 100 ml PE bottles. This procedure assures a complete wetting of all particles which show a high hydrophobicity. After this “wetting procedure” the resin bags were added to the suspension and treated in a horizontal shaker for 1 to 24 hrs.

In each sample the pH were controlled after 30 min. As described in Kaupenjohann & Wilke (1995) it is necessary to adjust the pH at 3 with BaNO_3 (Kaupenjohann and Wilcke 1995). In this case it was possible to delete this step because all pH values were near or lower the required pH value of 3. A highly decreasing pH can be an indication for existing salt crystals in the sample. So if the pH decreases it can be assumed that not all extractable cations are linked to SOM. In the described procedure the decrease was moderate because the naturally occurring pH ranges around 3,5.

At the end of the extraction the pH were measured and the resin bag was rinsed again with deionized water because adhering particles had to be removed from the resin. The soil water suspension was filtered for DOC measurements ($0.45 \mu\text{m}$; Sartorius®). The resin bags were extracted in 50 ml HNO_3 solution for 2 hrs. As control deionized water was used for the extraction. The extraction were then analysed for Pb^{2+} as described in 2.3.5.

The extractions were conducted in duplicates for each desorption time, the chosen desorption times were 1h, 3h, 8h, 24h, 96h. Unfortunately it was not possible only to change the resin bags at the mentioned time points. The losses of SOM particles which remain in the bags were significantly too high in relation to the treated sample amount. In preliminary tests a change of the bag material did not improve the results therefore we decided to use for each time point separate samples.

4.3.3 Chemical analyses

The following chemical analyses of the solutions were conducted at the different steps of the procedure:

- 1) Samples treated with Al^{3+} solution and control: Al, DOC in the solution after shaking
Samples treated with Ca^{2+} solution: Ca, DOC in the solution after shaking
- 2) Samples treated with Pb solution: Pb for controlling absorption and DOC, Al for the Al treated samples to control eventually losses
- 3) Analyzing the extract of the exchange resin for Pb
Analyzing the soil solution of desorption for DOC

For the determination of DOC the solutions were filtrated with $0.45 \mu\text{m}$ cellulose nitrate filters (Sartorius®), before that the filtration filters were flushed with warm deionized water to minimize contamination. DOC concentration was analyzed with a TOC Analyzer Multi C/N 2100 (Analytik Jena) after acidification and outgassing of inorganic carbon.

To calculate the sorption of cations of the samples the solutions were analyzed for the added cations (Al^{3+} , Ca^{2+}). Ca^{2+} was analyzed with Flame AAS (Perkin Elmer 4100; Varian AA 240 FS for Al^{3+}) with an oxygen/acetylene flame, Al^{3+} with a nitrous oxygen / acetylene flame (Varian AA 240 FS). In general a calibration curve was conducted by internal standardisation (Standardaddition) or if no differences were identified between the curves by an external

standardisation in the same solution (e. g. EDTA or 10% HNO₃). The solutions of the controls were analyzed for Ca²⁺ and Al³⁺ to calculate desorption from soil.

4.3.4 DSC measurements

To characterize the rigidity of the treated SOM matrix Differential Scanning Calorimetric (DSC) measurements were conducted. All samples were characterized after the first absorption of the base cations, directly before the desorption experiment and after drying and conditioning for the samples after desorption experiments.

Analyses were performed with a DSC Q1000 (TA Instruments, Germany) with a refrigerated cooling system (RCS) and nitrogen as a purge gas. All samples were abruptly cooled in the DSC instrument to -50°C and then heated with 10 K min⁻¹ from -50°C to 110°C, followed by a second abrupt cooling and subsequent heating cycle. Baseline was corrected with the TZero technology® by TA Instruments.

Data were analyzed using Universal Analysis version 4.1 (TA Instruments). The glass transition like step transition temperature T* is indicated by an inflection point in the thermogram. Operationally, three tangent lines were applied for the evaluation. The change of heat capacity ($\Delta c_p = \text{J g}^{-1} \text{K}^{-1}$) was calculated from the height of the central tangent line. In the following sections only the first heating cycle will be observed because the determined T* is a non-reversing thermal event (Schaumann and LeBoeuf 2005). The baseline correction applied by Hurraß & Schaumann was not applicable in this study due to significant thermal events in the second heating cycle (Hurrass and Schaumann 2007).

A total of 1-3 mg of the sample was placed into hermetically sealed Aluminum pans. 3 to 7 replicates were carried out depending on the quality of the resulting thermograms, so that for each sample at least 3 significant transition temperatures were available.

4.4 Results and Discussion

In chapter 2 the outcome of the treatment with multivalent cations is described in detail therefore in this chapter focussed on the results of the Pb desorption and not on the cation absorptions in general.

Lead and DOC losses during desorption

No significant differences or trend can be observed for the determined samples in desorption experiments of lead. Even for the original samples no difference is found to the Pb spiked samples (Figure 38) after one hr and three hrs desorption. Primary after 8 hrs a clear difference can be observed between the treated samples and the original.

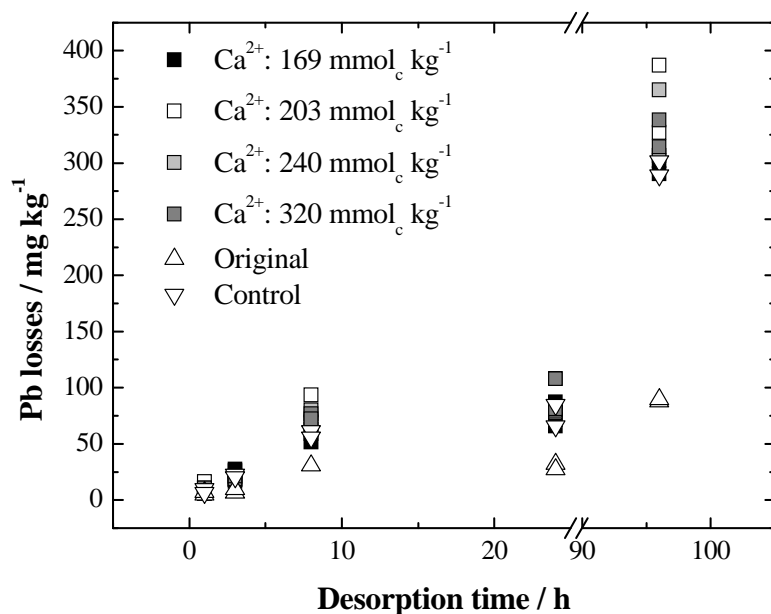


Figure 38: Desorption of lead during the extraction with an acid cation exchange resin for samples with different contents of Ca^{2+} . The original sample is a no treated sample the control is only spiked with Pb^{2+} but not with additional Ca^{2+} (Ca^{2+} content of the control: $160 \text{ mmol}_c \text{ kg}^{-1}$)

According to the hypotheses in 4.2 a lower desorption of lead was assumed for the treated samples because of their more complex network due to coordinative cross-links by multivalent cations. But especially by comparing the control sample (only spiked with Pb, no pre-treatment) with the pre-treated samples no significantly pronounced difference can be observed. But it is to mention that after desorption of 96 hrs the lowest Pb loss for the Pb spiked samples is found for the control samples where no pre-treatment took place and for the samples with the lowest Ca^{2+} spiking. For both the values range from 290 to 300 mg kg^{-1} , for the other samples all values range above 305 mg kg^{-1} . Furthermore it is to mention that the Pb loss after 96 hrs is unexpectedly higher than after 24 hrs. This observation contradicts the proposition of Lang et al. (2004), where no significant increase can be observed after 24 hrs and therefore an extraction time of 24 hrs is stated as sufficient. It is assumed that the extremely high content of organic carbon in the samples (43%) is responsible for this effect. Swelling processes for example could induce further Pb release during the long time of wetting and shaking. Results of sorption experiments with naphthalene-2-ol in hydrated soil demonstrate a higher release by a higher water content (Schneckenburger, Schaumann et al. 2012).

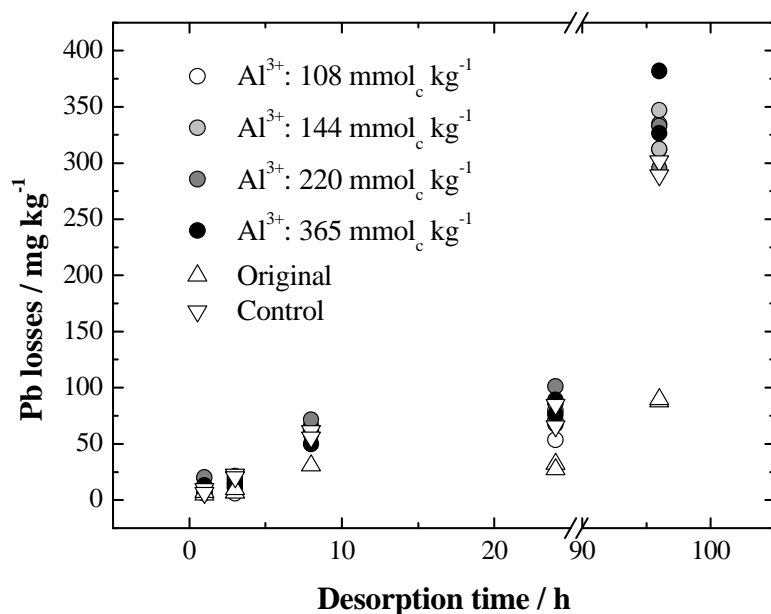


Figure 39: Desorption of lead during the extraction with an acid cation exchange resin at different time points for samples with different contents of Al^{3+} given in the legend. The original sample is a no treated sample the control is only spiked with Pb^{2+} but not with additional Al^{3+} (Al^{3+} content of the control: $80 \text{ mmol}_c \text{ kg}^{-1}$).

For the Pb desorption of the samples pre-treated with Al^{3+} similar results were observed as for the samples pre-treated with Ca^{2+} (Figure 39). Also no significant differences can be obtained for the determined desorption time points. Again for the 96 hrs samples the Pb losses are nearly complete and again the control sample show at this time point the lowest losses (except the original sample, but here the overall Pb concentration was not influenced by Pb spiking).

Another important characteristic of the desorption process due to cation depletion is the release of DOC from the samples. The DOC release is also an indication for the stability of the organic matrix. A high release can be related to a less stable and therefore a less pronounced molecular network.

In the presented experiments the losses of organic carbon in form of DOC were for the original sample significantly higher than for all the other samples at each determined time point in desorption (Figure 40 and Figure 41). Regarding that no pre-treatment was conducted and no DOC loss took place this effect is comprehensible. After a desorption time of 8 hrs no further significant changes can be observed for the DOC releases for all samples. This is in contrast to the Pb releases where after a desorption of 96 hrs a pronounced increase results. Therefore we anticipate that the proportion of lead which is released after 24hrs extraction is not involved in stabilisation effects of SOM.

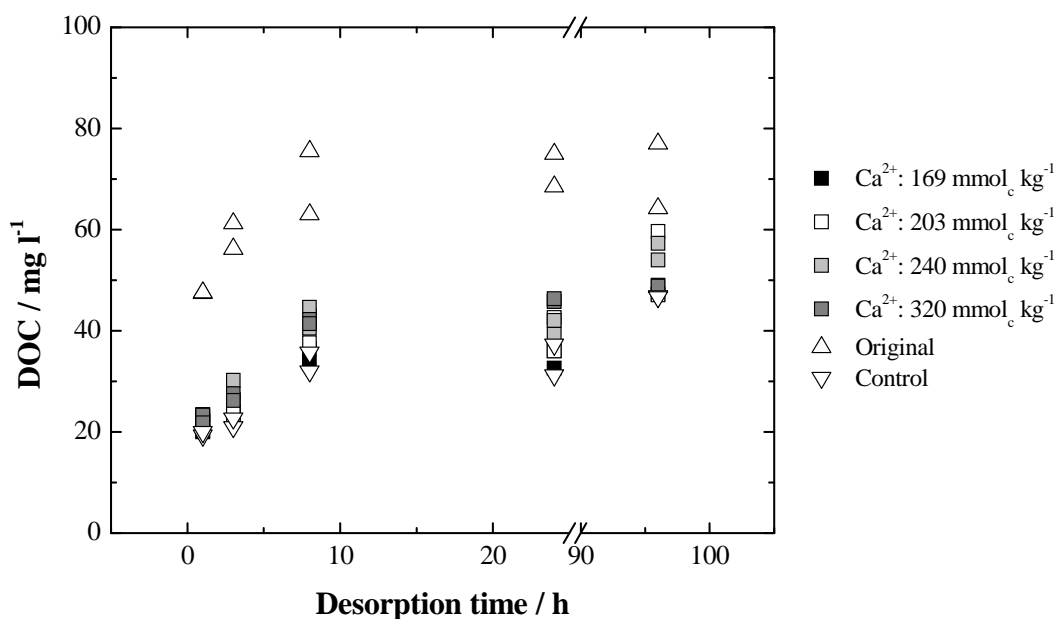


Figure 40: DOC release of the samples during the desorption experiments with an acid cation exchange resin at different time points for samples with different contents of Ca^{2+} given in the legend. The original sample is a no treated sample the control is only spiked with Pb^{2+} but not with additional Ca^{2+} (Ca^{2+} content of the control: $160 \text{ mmol}_c \text{ kg}^{-1}$). The standard deviation of the DOC measurements ranges about 5%, we do not include the standard deviation in the diagram to keep a clear view.

Between all the other samples no pronounced differences are shown in DOC release via cation depletion (see Figure 40). The control sample and the samples with the lowest Ca content always show the lowest DOC losses, but this is only be interpreted as a slight trend. However, this trend contradicts the expectation the DOC losses should be better pronounced for samples with low cation contents. Also a comparison between the samples pre-treated with Ca^{2+} and pre-treated with Al^{3+} does not demonstrate a differing behaviour in DOC release. Even the control which is only treated with Pb show the same DOC release as the pre-treated samples with Al^{3+} (see Figure 41). This is a remarkable observation by considering the fact that only $2,028 \text{ mmol}_c \text{ kg}^{-1}$ Pb were absorbed by the sample in contrast the samples absorbed during the pre-treatment procedure $28 - 293 \text{ mmol}_c \text{ kg}^{-1}$ Al^{3+} and $10 - 160 \text{ mmol}_c \text{ kg}^{-1}$ Ca^{2+} . So it is to conclude that there is no effect of the cations on the retention of DOC release at the measured time points with this experimental design. A possible explanation is that the desorption of the cations is also very fast so there was no effect measurable.

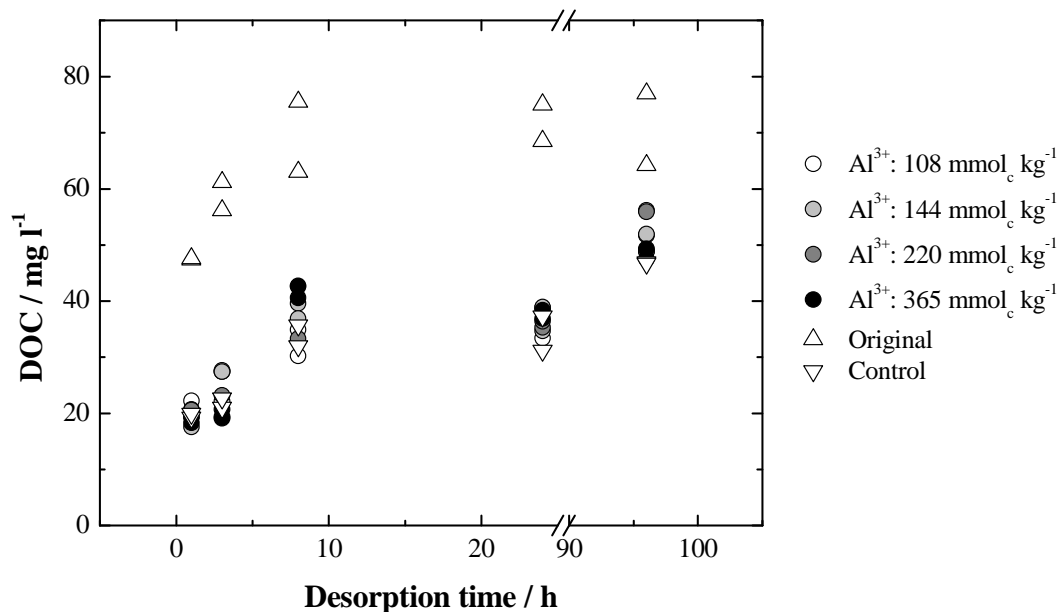


Figure 41: DOC losses of the samples during the desorption experiments with an acid cation exchange resin at different time points for samples with different contents of Al^{3+} given in the legend. The original sample is a no treated sample the control is only spiked with Pb^{2+} but not with additional Al^{3+} (Al^{3+} content of the control: $80 \text{ mmol}_c \text{ kg}^{-1}$). The standard deviation of the DOC measurements ranges about 5%, we do not include the standard deviation in the diagram to keep a clear view.

DSC results during desorption

Another characteristic for the stability of an organic matrix is the rigidity of a matrix measured with DSC. The rigidity of the matrix was measured before the desorption process and in the dried and conditioned samples formed during the desorption experiments. In reference to the hypotheses a decrease of rigidity is postulated for cation depletion and therefore a higher desorption of lead is assumed.

As also mentioned in chapter 2.4.1 for all treated and untreated samples there is a step transition in the first heating cycle with a change of heat capacity of $0,1 - 0,3 \text{ Wg}^{-1}\text{K}^{-1}$ and in a temperature range of 58°C up to 62°C . This thermal event is non-reversing, what means in the second heating cycle there is no step transition in this temperature range. However there is a thermal event at 69°C to 72°C with very low intensities. This event is reproducible for all samples but there is no trend for increasing or decreasing values of T^* identifiable.

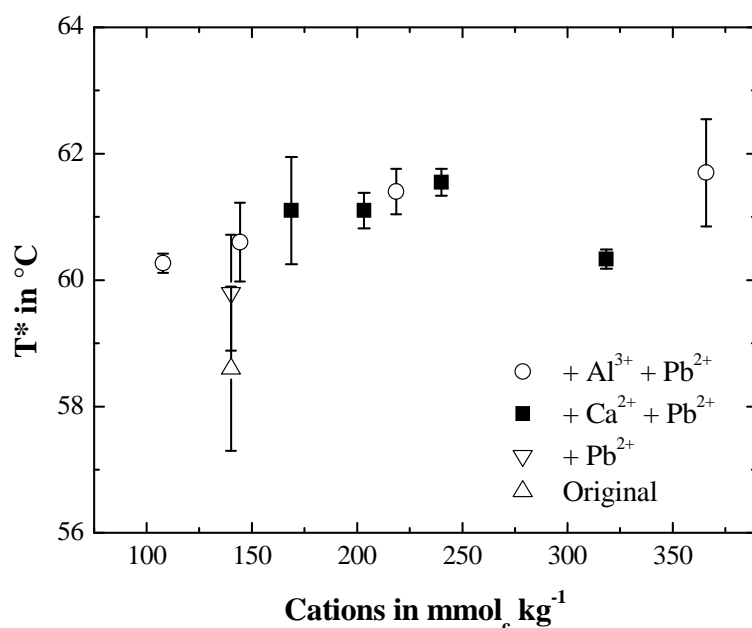


Figure 42: T^* of the created samples of different cation contents directly before the beginning of the desorption experiments. The untreated original and the control sample only spiked with Pb is linked with the original Ca^{2+} content in the sample and could also be transferred to the original Al content of $63 \text{ mmol}_c \text{ kg}^{-1}$. The standard deviations originated from 3 DSC measurements conducted for each sample.

As seen in Figure 42 the original untreated sample has got a significantly lower T^* than all the other sample independently of the type of treatment, but also the standard deviation is the highest. Only a slight increase in T^* can be observed for the control sample only spiked with lead. Samples pre - treated with Ca^{2+} or Al^{3+} solution all show higher step transition temperatures whereas only for the high absorbing samples treated with the maximum concentrations of Ca^{2+} and Al^{3+} a difference between the two cations in inducing matrix rigidity is observed. The sample pre-treated with Ca^{2+} show a decreasing T^* but for the sample pre-treated with Al^{3+} the rigidity remains on a high level. This observation is similar to the observations in chapter 2.4.1 and is explained with a matrix softening at the saturation point because of less multiple linked cation bridges in the molecular network. In contrast to the observations in 2.4.1 we do not find a higher rigidity for Al^{3+} than for Ca^{2+} treated samples. But it is to consider that also Pb^{2+} influences the rigidity and an additional effect on the Ca^{2+} samples is seen here. The rigidity of Al^{3+} treated samples is more stable and is no changes were observed by addition of for Pb^{2+} cations or more Al^{3+} cations.

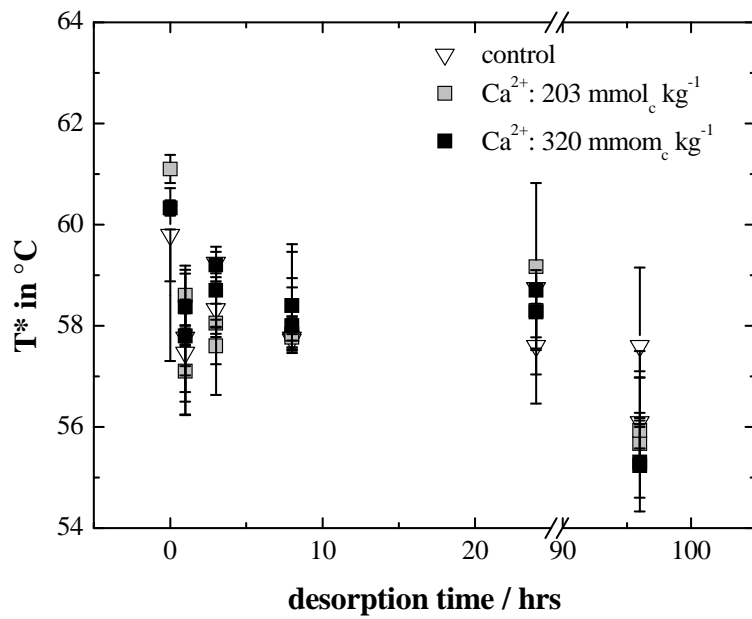


Figure 43: Step transition like glass transition temperature T^* in selected samples from the desorption experiments with an acid cation exchange resin at different time points with different contents of Ca^{2+} and the control (only spiked with Pb). Showing the other Ca^{2+} treated samples would not provide more information. The standard deviations originated from 3 DSC measurement conducted for each sample.

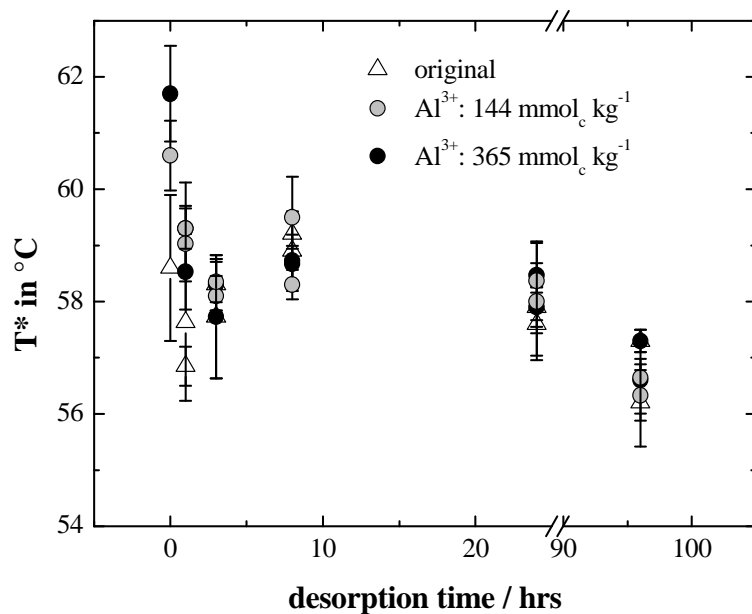


Figure 44: Step transition like glass transition temperature T^* during the desorption experiments with an acid cation exchange resin at different time points for selected samples with different contents of Al^{3+} and the original sample. Showing the other Ca^{2+} treated samples would not provide more information. The standard deviations originated from 3 DSC measurement conducted for each sample.

With the beginning of desorption all samples show a decrease in T^* and all ranges in the same temperature limits of $57^\circ\text{C} - 59^\circ\text{C}$. No pronounced differences can be observed for the desorption times of 1,3,8 and 24 hrs or for Ca^{2+} pre-treated samples neither for Al^{3+} pre-treated samples shown in Figure 43 and Figure 44, respectively. Only for desorption time of 96 hrs a stronger decrease of T^* can be observed especially for the Ca^{2+} treated samples (not significant). For the longest desorption time the samples show a T^* ranging from 55°C to 57°C .

Also the original sample (shown in Figure 44) and the control sample (shown in Figure 43) show the same behaviour than the pre-treated samples and its T^* ranges in the same temperature limits as for the pre-treated samples.

4.5 Conclusion

It was hypothesized that the Pb release of rigid organic matrices due to co-ordinative cross-linking by multivalent cations is lower than for less rigid organic matrices with a lower degree of cross – linking in the molecular network of SOM. But for all samples we find a similar behaviour during the designed desorption experiments with an acid cation exchange resin. Even the control sample acted in the same way as the samples pre- treated with Ca^{2+} or Al^{3+} solutions in different concentrations. The determined characteristics Pb desorption, DOC release and step transition like glass transition temperature T^* are in line with each other for the samples before desorption and at each determined desorption time point.

Regarding the results especially on rigidity of the samples after the first desorption times it seems that the designed experiment has a very strong influence on the sample itself what means the changes are very pronounced from the first time point on. Therefore it is to discuss if the chosen method is appropriate for answering the question behind this study. It is anticipated that the induced co-ordinative cross-links and the higher rigidity of the matrix may be highly reversible. The induced molecular changes by absorption of further base cations may be very variable and highly depends on environmental influences in such a degree as minimum changes in the environment like water content, physical forces (e. g. shear force), temperature and pH are able to alter the molecular network. In conclusion that would mean the measured increase of rigidity is a snap-shot of the structure of SOM belonging to very special environmental conditions and cannot be related to the term stability under all circumstances.

It is to discuss how appropriate the used method is, to simulate a time dependent desorption under the natural conditions of cation depletion in acidic soils. In former studies the method was mainly used to determine the potential of cation release of an acidic soil as substitution for the pH stat method (Lang and Kaupenjohann 2004). It could be possible that effects are more pronounced by using a softer desorption method e. g. a stirred-flow experiment described by Strawn & Sparks (2000) (Strawn and Sparks 2000).

Furthermore it is to discuss if a longer storage time would have a stabilizing effect on the samples. Experiments in chapter 2 and 3 demonstrate that time is one of the most influencing factor for rigidity.

5 General conclusions & perspective: Forming a network

At the beginning of this thesis four main hypotheses were developed on the current knowledge:

- I) According to the model of decreasing side chain mobility and decreasing small molecule mobility the overall rigidity of the matrix should increase with increasing cation content especially for higher charged cations the increasing effects should be pronounced
- II) Due to the strong co-ordinative cross-links of multivalent cations the role of water in cross-linking in SOM and also in precipitates developed as negligible for high cation contents and rigidity is analysable by T_g
- III) According to the effect of precipitation a higher precipitation rate and a higher degree of cross-linking and rigidity is assumed for an increasing cation content in the DOC solution
- IV) With a higher degree of cross-linking in the matrix the desorption of metal cations like lead is kinetically restrained and therefore slower under cation depletion conditions

Hypothesis I +II)

No detectable classical glass transition was found for the treated samples of the organic layer, the peats and the metal cation-DOM-precipitates in the measured temperature range. This was independent of if the samples were air-dried (about 7-8% Water content) or oven-dried (water-free). Instead for all air dried samples (storage at 76% relative humidity) a glass transition-like step transition is detectable which is linked with water molecule bridges between the organic functional groups (see chapter 1.1). This result was not expected, because the intention was to form cation bridges between the organic functional groups of the SOM which induces a higher rigidity determined via T_g . Nevertheless it was possible to determine effects of various cation compositions with the measured step transition like glass transition temperature T^* which is linked to the interaction with water molecules. T^* changes in dependence of the cation type (Na^+ , Ca^{2+} , Al^{3+} or Pb^{2+}) and of the saturation of the sample with this cation. As postulated in hypothesis I the effects are generally better pronounced for the triple charged Al than for the double charged Ca or Pb (in DOM-precipitates).

But an increasing T^* was only observed up to a special content of the used cation in the soil samples and in the precipitates, further increasing cation contents induce no changes in T^* or a decreasing T^* . T^* stay constantly high for Al treated samples but T^* decreases for Ca treated samples. This effect was also identified for the precipitates but here also for Al a slight decreasing trend is demonstrated. A loss of multivalent cations by exchange with Na^+ and cation depletion in general do not automatically induce a decreasing T^* in different soil samples. Consequently the concentration range of cations in soil in which changes of the rigidity can be observed is surprisingly small.

The mentioned results do not support hypothesis II: There is an important role of water although the observed changes can be related to differences in cation content and composition in the samples. The observations give evidence for interactions between water molecules (or clusters) and cation bridges. It is not possible to divide in water molecule bridges on the one side and cation bridges on the other side as it was postulated at the beginning of this work. We do not found a step transition which can be related to cation bridges in the matrix like T_g but we also do not found a T^* , in former studies related to water molecule bridges, which do not show any effect by changing the cation status in the matrix. So it comes finally to the conclusion that cation - watermolecule bridges were formed in the matrix. Aquino et al. (2010, 2011 & 2014) postulated such cation-watermolecule bridges via calculation of molecular modeling. In this model rigidity depends on the ratio between cation and interacting water molecules. The less water molecules are involved in such bindings the stronger is the binding and the more rigid is the matrix. In our experiments the water content was always the same and such differences were not possible to identify with the chosen study design.

The transition temperature fully disappears for water-free samples. Referring to the described model of Aquino these explanations are possible:

- The cation water molecule bridges break because of the low amount of water molecules and conformational impossibilities to form cation – bridges, consequently the cations are bound in the SOM without forming new bridges
- The cation bridges remain without the interaction of water and very strong coordinative bindings are formed, consequently the theoretically occurring T_g should be detectable at temperatures above 110°C

In both cases T^* would disappear and no thermal event is detectable with DSC in the used temperature range. It is possible that both processes appear in SOM. If the functional groups are sterically too far apart from each other and water molecules are necessary as “building block” the bridges break due to the removal of the water. If the functional groups are near enough the bridge get stronger by the binding of the cation. The described effects are independent of the cation content. The disappearance of the step transition was found for the treated “soil” samples but also for the precipitates. So the idea is waived that a high background emission of the heterogenous soil samples avoids the detection of the classical glass transition. It is assumed that the precipitates are a little less heterogenic than the solid soil samples, because only a specific part of a soil sample is observed.

Regarding this fact it is comprehensible that some results are similar between the precipitates and the soil sample but also slight differences are obtained. As it is described above in treated soil samples a maximum rigidity was determined at specific cation concentrations in SOM. After that maximum there was a decrease for Ca-treated samples and a consistent rigidity for Al treated samples. In the precipitates for all cations at very large Me^{n+} / C ratios the rigidity decreases but less pronounced for Al precipitates than for Pb and Ca precipitates. This observation enhances the model of different binding stages / status (bidentate versus polydentate

bindings) depending on the cation content in the organic matrix (see also chapter “Models”). The results indicate that if there is a high supply of cations in solution bidentate binding is energetically preferred in the precipitate independently of the cation type. In soil samples this was only demonstrated for Ca-treated samples and the decrease was less pronounced than in the precipitates. There could be several reasons for this difference. First of all during the precipitation process a completely new molecular structure influenced by the cation in the solution is formed. But in solid soil samples there is only an influence of the cations on a given structure. It is very likely that in solid samples are much more sterical borders in conformational changes. Furthermore the organic molecules acting in the precipitates are only the ones which were able to solute in water because of their size and their functional groups. Therefore effects coming from the interaction of the organic molecules and the cations are anticipated to be more pronounced in the precipitates than in the treated soil samples. So this less pronounced decreasing rigidity for Al precipitates supports the model about the dependence between the type of binding and the supply of cations in the solution. Computational calculations suggest bidentate bindings for Al between organic functional groups (Aquino, Tunega et al. 2014) But in soil samples this effect was not measurable due to the heterogeneity of the samples and the resulting derivation during the measurements.

In conclusion, hypothesis III (increasing rigidity with increasing cation content in precipitates) it was only partly supported by the results as hypothesis I.

It was hypothesized that a higher degree of cross-linking in SOM is responsible for a retained desorption of lead under cation depletion conditions. But this hypothesis was neglected. No relation was found between lead desorption and the content of multivalent cations in the treated samples. The formed network was highly reversible in relation to the used desorption method.

Many studies suggested a relation between rigidity and sorption and desorption behaviour of organic chemicals. Furthermore for some organic contaminants a better sorption by direct linkage of cations is known e. g. (Lu and Pignatello 2004). However, in the cited study they worked with Al cross-linked humic acids and not with naturally occurring SOM samples. As it is discussed above about the differences in the results of the treated soil samples and the precipitates the more homogenous the matrix is the easier is it to find pronounced effects in DSC. So, it is difficult to compare the results of Lu & Pignatello with the desorption results of this study. The extractability of nonylphenol and phenanthren from a sandy soil only showed very low changes for different cation saturations in the treated samples (Shchegolikhina, Schulz et al. 2012). However, the organic carbon content of the sandy soils was very low in comparison to this thesis. Schneckenburger et al. analyzed the sorption behaviour of naphthalene 2-ol in a peat sample in dependence on hydration effects. As there was a negative correlation between sorption constants and water content no correlation was found for the measured matrix rigidity and the sorbed amount (Schneckenburger, Schaumann et al. 2012). So all these results including these of this study demonstrate the difficulties to describe the sorption

behaviour of a complex matrix like SOM. Depending on the characteristics of the used samples opposed effects can be observed.

In general a higher rigidity which means a glassy character of the SOM is automatically related to a higher stability of SOM in literature. Higher stability means especially that the matrix is more resistant to microbial degradation or other inorganic forms of degradation. Scheel et al. conducted experiments with precipitates and their microbial degradation but no conclusions on the rigidity of the matrix were available. For further research a correlation should be targeted between biodegradation and matrix rigidity of SOM to understand the mechanism of stabilisation and preventing soil as a carbon storage medium.

Moreover it is to consider that less is known about the molecular composition of the investigated soil samples (e. g. aromaticity of the sample, aliphatic groups etc.). Scheel et al. demonstrated in their biodegradation study that the degradation of precipitates depends especially on this composition. Hence, it can be postulated that also the influence of multivalent cations highly depends on the molecular composition in SOM. A stronger molecular network in SOM is only possible if it is sterically possible. To achieve a deeper insight in molecular interactions more research is necessary by comparing effects of multivalent cation on SOM with different molecular compositions. The demineralisation experiments in this thesis indicate that the influence of cations on the degree of networking in the matrix depends on the molecular composition. It would be important to know on which SOM types characterised by its functional groups and molecular structure a greater or a lesser influence on cations is to be expected. Computational calculations suggest that the influence should be higher for SOM rich in organic molecules with functional groups. If it would be possible to predict the structure of SOM due to its composition (type of organic molecules, cation content, rigidity status etc.) than it is assessable if the addition of base cations enhance the sorption behaviour or in worst case enhances the desorption of contaminants. Furthermore more research is recommended on the role of water and water clusters in SOM. How could look an interaction between water-cations-organic functional groups and under which conditions is a formation of bridges expected.

6 Literature

Aquino, A. J. A., D. Tunega, H. Pasalic, G. Haberhauer, M. H. Gerzabek and H. Lischka (2008). "The thermodynamic stability of hydrogen bonded and cation bridged complexes of humic acid models - A theoretical study." Chemical Physics **349**(1-3): 69-76.

Aquino, A. J. A., D. Tunega, G. E. Schaumann, G. Haberhauer, M. H. Gerzabek and H. Lischka (2009). "Stabilizing capacity of water bridges in nanopore segments of humic substances: A theoretical investigation." Journal of Physical Chemistry C **113**(37): 16468-16475.

Aquino, A. J. A., D. Tunega, G. E. Schaumann, G. Haberhauer, M. H. Gerzabek and H. Lischka (2011). "The functionality of cation bridges for binding polar groups in soil aggregates." International Journal of Quantum Chemistry **111**(7-8): 1531-1542.

Aquino, A. J. A., D. Tunega, G. E. Schaumann, G. Haberhauer, M. H. Gerzabek and H. Lischka (2014). "Proton transfer processes in polar regions of humic substances initiated by aqueous aluminum cation bridges: A computational study." Geoderma **213**: 115-123.

Barton, A. F. M. (1983).

Batjes, N. H. (1996). "Total carbon and nitrogen in the soils of the world." European Journal of Soil Science **47**(2): 151-163.

Belfiore, L. A., M. P. McCurdie and P. K. Das (2001). "Macromolecule-metal complexes: Ligand field stabilization and thermophysical property modification." Polymer **42**(25): 9995-10006.

Bloom, P. R., U. Skjellberg and M. E. Sumner (2005). Soil acidity. Chemical processes in soils. M. A. Tabatbai and D. L. Sparks. Madison, WI, Soil Science society of America: 411-459.

Christl, I. and R. Kretzschmar (2007). "C-1s NEXAFS spectroscopy reveals chemical fractionation of humic acid by cation-induced coagulation." Environmental Science & Technology **41**(6): 1915-1920.

DeLapp, R. C., E. J. LeBoeuf and K. D. Bell (2004). "Thermodynamic properties of several soil- and sediment-derived natural organic materials." Chemosphere **54**(4): 527-539.

Denaix, L., R. M. Semlali and F. Douay (2001). "Dissolved and colloidal transport of Cd, Pb, and Zn in a silt loam soil affected by atmospheric industrial deposition." Environmental Pollution **114**(1): 29-38.

Diehl, D. and G. E. Schaumann (2007). "The nature of wetting on urban soil samples: Wetting kinetics and evaporation assessed from sessile drop shape." Hydrological Processes **21**(17): 2255-2265.

Eisenberg, A. (1993).

Elkins, K. M. and D. J. Nelson (2001). "Fluorescence and FT-IR spectroscopic studies of Suwannee river fulvic acid complexation with aluminum, terbium and calcium." Journal of Inorganic Biochemistry **87**(1-2): 81-96.

Elkins, K. M. and D. J. Nelson (2002). "Spectroscopic approaches to the study of the interaction of aluminum with humic substances." Coordination Chemistry Reviews **228**(2): 205-225.

- Ellerbrock, R. H. and M. Kaiser (2005). "Stability and composition of different soluble soil organic matter fractions-evidence from d13C and FTIR signatures." Geoderma **128**(1-2): 28-37.
- Essington, M. E. (2003). Soil and Water Chemistry, Crc Press Inc.
- Fest, E. P. M. J., E. J. M. Temminghoff, J. Griffioen and W. H. Van Riemsdijk (2005). "Proton buffering and metal leaching in sandy soils." Environmental Science & Technology **39**(20): 7901-7908.
- Ge, Y., S. Sauvé and W. H. Hendershot (2005). "Equilibrium speciation of cadmium, copper, and lead in soil solutions." Communications in Soil Science and Plant Analysis **36**(11-12): 1537-1556.
- Grodzinska-Jurczak, M. and J. Mulder (1997). "The rate of microbial decomposition of soil humic compounds: the effect of acid rain induced Al depletion." Polish journal of environmental studies **6**: 49-54.
- Gustafsson Jon, P., P. Pechova and D. Berggren (2003). "Modeling metal binding to soils: the role of natural organic matter." Environmental science & technology **37**(12): 2767-2774.
- Gustafsson, J. P. (2001). "Modeling the acid-base properties and metal complexation of humic substances with the Stockholm Humic Model." Journal of Colloid and Interface Science **244**(1): 102-112.
- Gustafsson, J. P., P. Pechova and D. Berggren (2003). "Modeling metal binding to soils: The role of natural organic matter." Environmental Science & Technology **37**(12): 2767-2774.
- Gustafsson, J. P. and J. W. J. van Schaik (2003). "Cation binding in a mor layer: batch experiments and modelling." European Journal of Soil Science **54**(2): 295-310.
- Haward, R. N. (1973).
- Herre, A., F. Lang, C. Siebe, R. Dohrmann and M. Kaupenjohann (2007). "Mechanisms of acid buffering and formation of secondary minerals in vitric Andosols." European Journal of Soil Science **58**(2): 431-444.
- Huang, W. and W. J. Weber Jr (1997). "Thermodynamic Considerations in the Sorption of Organic Contaminants by Soils and Sediments. 1. The Isosteric Heat Approach and its Application to Model Inorganic Sorbents." Environmental Science and Technology **31**(11): 3238-3243.
- Huber, A., W. Praznik and G. Curin (1993). Characterization of aqueous dissolved biopolymers.
- Hurrass, J. and G. E. Schaumann (2005). "Is glassiness a common characteristic of soil organic matter?" Environmental Science and Technology **39**(24): 9534-9540.
- Hurrass, J. and G. E. Schaumann (2007). "Influence of the sample history and the moisture status on the thermal behavior of soil organic matter." Geochimica Et Cosmochimica Acta **71**(3): 691-702.
- Iglesias, A., R. Lopez, S. Fiol, J. M. Antelo and F. Arce (2003). "Analysis of copper and calcium-fulvic acid complexation and competition effects." Water Research **37**(15): 3749-3755.

- Jaeger, F., A. Shchegolikhina, H. van As and G. E. Schaumann (2010). "Proton NMR relaxometry as a useful tool to evaluate swelling processes in peat soils." Open Magnetic Resonance Journal **3**(SPEC. ISS.1): 27-45.
- Johnson, C. E. (2002). "Cation exchange properties of acid forest soils of the northeastern USA." European Journal of Soil Science **53**(2): 271-282.
- Johnson, M. D., W. Huang and W. J. Weber Jr (2001). "A distributed reactivity model for sorption by soils and sediments. 13. Simulated diagenesis of natural sediment organic matter and its impact on sorption/desorption equilibria." Environmental Science and Technology **35**(8): 1680-1687.
- Kahle, M., M. Kleber and R. Jahn (2002). "Carbon storage in loess derived surface soils from Central Germany: Influence of mineral phase variables." Journal of Plant Nutrition and Soil Science **165**(2): 141-149.
- Kalinichev, A. G. and R. J. Kirkpatrick (2007). "Molecular dynamics simulation of cationic complexation with natural organic matter." European Journal of Soil Science **58**(4): 909-917.
- Kalisz, P. J. and E. L. Stone (1980). "Cation Exchange Capacity of Acid Forest Humus Layers1." Soil Sci. Soc. Am. J. **44**(2): 407-413.
- Kaupenjohann, M. and W. Wilcke (1995). "Heavy-Metal Release from a Serpentine Soil Using a Ph-Stat Technique." Soil Science Society of America Journal **59**(4): 1027-1031.
- Kinniburgh, D. G., W. H. Van Riemsdijk, L. K. Koopal, M. Borkovec, M. F. Benedetti and M. J. Avena (1999). "Ion binding to natural organic matter: Competition, heterogeneity, stoichiometry and thermodynamic consistency." Colloids and Surfaces A: Physicochemical and Engineering Aspects **151**(1-2): 147-166.
- Klitzke, S. and F. Lang (2007). "Hydrophobicity of soil colloids and heavy metal mobilization: Effects of drying." Journal of Environmental Quality **36**(4): 1187-1193.
- Klitzke, S. and F. Lang (2009). "Mobilization of soluble and dispersible lead, arsenic, and antimony in a polluted, organic-rich soil - Effects of pH increase and counterion valency." Journal of Environmental Quality **38**(3): 933-939.
- Klitzke, S., F. Lang and M. Kaupenjohann (2008). "Increasing pH releases colloidal lead in a highly contaminated forest soil." European Journal of Soil Science **59**(2): 265-273.
- Kögel-Knabner, I. (2002). "The macromolecular organic composition of plant and microbial residues as inputs to soil organic matter." Soil Biology and Biochemistry **34**(2): 139-162.
- Koopal, L. K., W. H. van Riemsdijk and D. G. Kinniburgh (2001). "Humic matter and contaminants. General aspects and modelling metal ion binding." Pure and Applied Chemistry **73**: 2005-2016.
- Koopal, L. K., W. H. Van Riemsdijk and D. G. Kinniburgh (2001). "Humic matter and contaminants. General aspects and modeling metal ion binding." Pure and Applied Chemistry **73**(12): 2005-2016.
- Kretzschmar, R., M. Borkovec, D. Grolimund and M. Elimelech (1999). Mobile Subsurface Colloids and Their Role in Contaminant Transport. **66**: 121-193.
- Kunhi Mouvenchery, Y., A. Jaeger, A. J. A. Aquino, D. Tunega, D. Diehl, M. Bertmer and G. E. Schaumann (2013). "Restructuring of a Peat in Interaction with Multivalent Cations: Effect of Cation Type and Aging Time." PLoS ONE **8**(6).

- Lang, F., H. Egger and M. Kaupenjohann (2005). "Size and shape of lead-organic associations." Colloids and Surfaces A: Physicochemical and Engineering Aspects **265**(1-3): 95-103.
- Lang, F. and M. Kaupenjohann (2004). "Trace element release from forest floor can be monitored by ion exchange resin tubes." Journal of Plant Nutrition and Soil Science **167**(2): 177-183.
- LeBoeuf, E. J. and W. J. Weber Jr (1998). "Evaluation of a Flory-huggins-based partitioning model for natural organic matter." ACS Division of Environmental Chemistry, Preprints **38**(2): 91-93.
- Leboeuf, E. J. and W. J. Weber Jr (2000). "Macromolecular characteristics of natural organic matter. 2. Sorption and desorption behavior." Environmental Science and Technology **34**(17): 3632-3640.
- LeBoeuf, E. J. and W. J. Weber (1997). "A distributed reactivity model for sorption by soils and sediments. 8. sorbent organic domains: discovery of a humic acid glass transition and an argument for a polymer-based model." Environmental Science and Technology **31**(6): 1697-1702.
- Lu, Y. and J. J. Pignatello (2002). "Demonstration of the "conditioning effect" in soil organic matter in support of a pore deformation mechanism for sorption hysteresis." Environmental Science and Technology **36**(21): 4553-4561.
- Lu, Y. and J. J. Pignatello (2004). "Sorption of apolar aromatic compounds to soil humic acid particles affected by aluminum(III) ion cross-linking." Journal of Environmental Quality **33**(4): 1314-1321.
- Luo, L., S. Zhang and P. Christie (2010). "New insights into the influence of heavy metals on phenanthrene sorption in soils." Environmental Science and Technology **44**(20): 7846-7851.
- Luo, L., S. Zhang, Y. Ma, P. Christie and H. Huang (2008). "Facilitating effects of metal cations on phenanthrene sorption in soils." Environmental Science and Technology **42**(7): 2414-2419.
- Martínez, C. E. and N. Martínez-Villegas (2008). "Copper-alumina-organic matter mixed systems: Alumina transformation and copper speciation as revealed by EPR spectroscopy." Environmental Science and Technology **42**(12): 4422-4427.
- Mouvenchery, Y. K., J. Kučerík, D. Diehl and G. E. Schaumann (2012). "Cation-mediated cross-linking in natural organic matter: A review." Reviews in Environmental Science and Biotechnology **11**(1): 41-54.
- Mulder, J., H. A. De Wit, H. W. J. Boonen and L. R. Bakken (2001). "Increased levels of aluminium in forest soils: Effects on the stores of soil organic carbon." Water Air and Soil Pollution **130**(1-4): 989-994.
- Nebbioso, A. and A. Piccolo (2009). "Molecular Rigidity and Diffusivity of Al³⁺ And Ca²⁺ Humates As Revealed by NMR Spectroscopy." Environmental Science & Technology **43**(7): 2417-2424.
- Nierop, K. G. J., B. Jansen and J. A. Verstraten (2002). "Dissolved organic matter, aluminium and iron interactions: precipitation induced by metal/carbon ratio, pH and competition." Science of the Total Environment **300**(1-3): 201-211.

- Oste, L. A., E. J. M. Temminghoff and W. H. v. Riemsdijk (2002). "Solid-solution partitioning of organic matter in soils as influenced by an increase in pH or Ca concentration." Environmental Science and Technology **36**: 208-214.
- Piccolo, A. (2001). "The supramolecular structure of humic substances." Soil Science **166**: 810-832.
- Piccolo, A. (2002). The supramolecular structure of humic substances: A novel understanding of humus chemistry and implications in soil science. **75**: 57-134.
- Piccolo, A. and J. S. C. Mbagwu (1994). "Humic substances and surfactants effects on the stability of two tropical soils." Soil Science Society of America Journal **58**(3): 950-955.
- Pinheiro, J. P., A. M. Mota and M. F. Benedetti (2000). "Effect of aluminum competition on lead and cadmium binding to humic acids at variable ionic strength." Environmental science & technology **34**: 5137-5143.
- Römken, P. and J. Dolfing (1998). "Effect of Ca on the solubility and molecular size distribution of DOC and Cu binding in soil solution samples." Environmental Science and Technology **32**: 363-369.
- Rosen, S. L. (1993).
- Ross, D. S., R. J. Bartlett and F. R. Magdoff (1991). Plant-soil Interactions at Low PH: 81-92.
- Ross, D. S., M. B. David, G. B. Lawrence and R. J. Bartlett (1996). Soil Science Society of America Journal **60**(6): 1926-1932.
- Ross, D. S., G. Matschonat and U. Skyllberg (2008). "Cation exchange in forest soils: the need for a new perspective." European Journal of Soil Science **59**(6): 1141-1159.
- Sauve, S., M. McBride and W. Hendershot (1998). "Soil solution speciation of lead (II): Effects of organic matter and pH." Soil Sci Soc Am J **62**: 618-621.
- Schaumann, G. E. (2000). "Effect of CaCl₂ on the kinetics of the release of dissolved organic matter (DOM)." Journal of Plant Nutrition and Soil Science **163**(5): 523-529.
- Schaumann, G. E. (2005). "Matrix relaxation and change of water state during hydration of peat." Colloids and Surfaces A: Physicochemical and Engineering Aspects **265**(1-3): 163-170.
- Schaumann, G. E. (2006). "Soil organic matter beyond molecular structure Part I: Macromolecular and supramolecular characteristics." Journal of Plant Nutrition and Soil Science-Zeitschrift Fur Pflanzenernahrung Und Bodenkunde **169**(2): 145-156.
- Schaumann, G. E. (2006). "Soil organic matter beyond molecular structure Part II: Amorphous nature and physical aging." Journal of Plant Nutrition and Soil Science-Zeitschrift Fur Pflanzenernahrung Und Bodenkunde **169**(2): 157-167.
- Schaumann, G. E. and O. Antemann (2000). "Thermal characteristics of soil organic matter measured by DSC: A hint on a glass transition." Journal of Plant Nutrition and Soil Science **163**(2): 179-181.
- Schaumann, G. E. and M. Bertmer (2008). "Do water molecules bridge soil organic matter molecule segments?" European Journal of Soil Science **59**(3): 423-429.
- Schaumann, G. E., D. Diehl, M. Bertmer, A. Jaeger, P. Conte, G. Alonzo and J. Bachmann (2013). "Combined proton NMR wideline and NMR relaxometry to study SOM-water interactions of cation-treated soils." Journal of Hydrology and Hydromechanics **61**(1): 50-63.

- Schaumann, G. E. and E. J. LeBoeuf (2005). "Glass transitions in peat - their relevance and the impact of water." Environmental Science and Technology **39**(3): 800-806.
- Schaumann, G. E. and S. Thiele-Bruhn (2011). "Molecular modeling of soil organic matter: Squaring the circle?" Geoderma **166**(1): 1-14.
- Scheel, T., C. Dorfler and K. Kalbitz (2007). "Precipitation of dissolved organic matter by aluminum stabilizes carbon in acidic forest soils." Soil Science Society of America Journal **71**(1): 64-74.
- Scheffer/Schachtschabel; and H.-P. B. Blume, G. W.; Horn, R.; Kandeler, E.; Kögel-Knabner, I.; Kretzschmar, R.; Stahr, K.; Wilke, B.-M.; Thiele-Brun, S.; Welp, G. (2010). Lehrbuch der Bodenkunde. Heidelberg, Spektrum Akademischer Verlag.
- Schneckenburger, T., G. E. Schaumann, S. K. Woche and S. Thiele-Bruhn (2012). "Short-term evolution of hydration effects on soil organic matter properties and resulting implications for sorption of naphthalene-2-ol." Journal of Soils and Sediments **12**(8): 1269-1279.
- Schwesig, D., K. Kalbitz and E. Matzner (2003). "Effects of aluminium on the mineralization of dissolved organic carbon derived from forest floors." European Journal of Soil Science **54**(2): 311-322.
- Shchegolikhina, A., S. Schulz and B. Marschner (2012). "Interacting effects of cation saturation and drying, freezing, or aging on the extractability of nonylphenol and phenanthrene from a sandy soil." Journal of Soils and Sediments **12**(8): 1280-1291.
- Shen, Y. H. (1999). "Sorption of humic acid to soil: The role of soil mineral composition." Chemosphere **38**(11): 2489-2499.
- Simpson, A. J., W. L. Kingery, M. H. B. Hayes, M. Spraul, E. Humpfer, P. Dvortsak, R. Kerssebaum, M. Godejohann and M. Hofmann (2002). "Molecular structures and associations of humic substances in the terrestrial environment." Naturwissenschaften **89**(2): 84-88.
- Skyllberg, U. (1994). Interciencia **19**: 356-365.
- Skyllberg, U. (1995). "Solution Soil Ratio and Release of Cations and Acidity from Spodosol Horizons." Soil Science Society of America Journal **59**(3): 786-795.
- Skyllberg, U. (1999). "pH and solubility of aluminium in acidic forest soils: A consequence of reactions between organic acidity and aluminium alkalinity." European Journal of Soil Science **50**(1): 95-106.
- Strawn, D. G. and D. L. Sparks (2000). "Effects of soil organic matter on the kinetics and mechanisms of Pb(II) sorption and desorption in soil." Soil Science Society of America Journal **64**: 144-156.
- Struik, L. G. E. (1978). Physical Aging in Amorphous Polymers and Other Materials Elsevier Sci. Publ. Comp., Amsterdam-Oxford-New York
- Sutton, R. and G. Sposito (2005). "Molecular structure in soil humic substances: The new view." Environmental Science and Technology **39**(23): 9009-9015.
- Swift, R. S. (1999). "Macromolecular properties of soil humic substances: fact, fiction, and opinion." Soil Science **164**(11): 790-802.

- Temminghoff, E. J. M., S. V. d. Zee and F. A. M. D. Haan (1998). "Effects of dissolved organic matter on the mobility of copper in a contaminated sandy soil." European Journal of Soil Science **49**: 617-628.
- Tipping, E., C. Rey-Castro, S. E. Bryan and J. Hamilton-Taylor (2002). "Al(III) and Fe(III) binding by humic substances in freshwaters, and implications for trace metal speciation." Geochimica et Cosmochimica Acta **66**(18): 3211-3224.
- Tipping, E., C. Woof and M. A. Hurley (1991). "Humic Substances in Acid Surface Waters - Modeling Aluminum Binding, Contribution to Ionic Charge-Balance, and Control of Ph." Water Research **25**(4): 425-435.
- Titeux, H., V. Brahy and B. Delvaux (2002). "Metal complexing properties of forest floor leachates might promote incipient podzolization in a Cambisol under deciduous forest." Geoderma **107**(1-2): 93-107.
- von Luetzow, M., I. Kogel-Knabner, B. Ludwig, E. Matzner, H. Flessa, K. Ekschmitt, G. Guggenberger, B. Marschner and K. Kalbitz (2008). "Stabilization mechanisms of organic matter in four temperate soils: Development and application of a conceptual model." Journal of Plant Nutrition and Soil Science-Zeitschrift Fur Pflanzenernahrung Und Bodenkunde **171**(1): 111-124.
- Von Wandruszka, R. (1998). "The micellar model of humic acid: Evidence from pyrene fluorescence measurements." Soil Science **163**(12): 921-930.
- Watmough, S. A., T. C. Hutchinson and P. J. Dillon (2004). "Lead dynamics in the forest floor and mineral soil in south-central Ontario." Biogeochemistry **71**(1): 43-68.
- Weng, L. P., L. K. Koopal, T. Hiemstra, J. C. L. Meeussen and W. H. Van Riemsdijk (2005). "Interactions of calcium and fulvic acid at the goethite-water interface." Geochimica et Cosmochimica Acta **69**(2): 325-339.
- Xing, B. and J. J. Pignatello (1997). "Dual-mode sorption of low-polarity compounds in glassy poly(vinyl chloride) and soil organic matter." Environmental Science and Technology **31**(3): 792-799.
- Young, K. D. and E. J. Leboeuf (2000). "Glass transition behavior in a peat humic acid and an aquatic fulvic acid." Environmental Science and Technology **34**(21): 4549-4553.
- Zhang, L. and E. J. LeBoeuf (2009). "A molecular dynamics study of natural organic matter: 1. Lignin, kerogen and soot." Organic Geochemistry **40**(11): 1132-1142.
- Zhang, L., E. J. Leboeuf and B. S. Xing (2007). "Thermal analytical investigation of biopolymers and humic- and carbonaceous-based soil and sediment organic matter." Environmental Science & Technology **41**(14): 4888-4894.

Figures

| | |
|---|----|
| Figure 1: Procedure of percolation with Ca^{2+} solution for creating sample with different cation contents and various degrees of cross-linking in SOM | 27 |
| Figure 2: A sessile drop fitted as ellipsoidal cap showing the vectors of interfacial tensions, γ , at the drop edge, the observable contact angle θ_{app} and elliptical parameters a, b, h necessary to calculate θ_{app} and drop volume V (Diehl and Schaumann 2007). | 31 |
| Figure 3: Step transition temperature T^* in dependence of the Ca^{2+} content of the sample and the concentration of the used percolation solution (5 mmol, 8 mmol, 10 mmol) after 4 weeks conditioning. | 33 |
| Figure 4: Step transition temperature T^* in dependence of the Ca^{2+} content of the sample and the concentration of the used percolation solution (5 mmol, 8 mmol, 10 mmol) after 9 months conditioning. | 34 |
| Figure 5: Ca^{2+} contents in the treated samples from the mass balance analyses in the percolation solution and from EDTA extract from the samples itself | 36 |
| Figure 6: Cation content of the samples after each percolation cycle during the addition of Ca^{2+} , the percolation cycles and its concentration are given at the x-axis. The content was measured by EDTA extraction of an aliquot of the samples. | 36 |
| Figure 7: Losses of organic carbon during the percolation cycles, averages from all treated samples (standard deviation based on the individual values). It is stated that the values are related to the losses of DOC at the specific percolation step, what means the overall loss of DOC for the sample percolated for four times is the sum of the values in each step. | 37 |
| Figure 8: T^* of the different treated samples of each percolation cycle and for the control | 38 |
| Figure 9: Decrease of T^* with higher Ca^{2+} contents in the samples. | 39 |
| Figure 10: Cation exchange during absorption of Al^{3+} in dependence on different concentrations in the initial salt solutions; standard deviations are derived from the analytical methods in percent. | 41 |
| Figure 11: DOC in the soil solutions after treatment in dependence of increasing initial Ca^{2+} () and Al^{3+} (○) concentrations in batch solutions and in comparison to the control sample only treated with deionized water (□). Linear regression with $p = 0.08$ for Al^{3+} and $p = 0.1$ for Ca^{2+} . | 42 |
| Figure 12: Representative DSC thermograms of the first heating cycle of samples treated with Ca^{2+} ; a) reference sample only humidified, Ca^{2+} content is $160 \text{ mmol}_c \text{ kg}^{-1}$, b) treated sample, Ca^{2+} content is $175 \text{ mmol}_c \text{ kg}^{-1}$, c) treated sample, Ca^{2+} content is $220 \text{ mmol}_c \text{ kg}^{-1}$ | 43 |
| Figure 13: DSC results from Ca^{2+} treated samples in batch experiments and in percolation experiments (see chapter 0), changes of T^* with differences in Ca^{2+} content. | 44 |
| Figure 14: Glass transition like glass transition temperature in dependence on Ca^{2+} content and Al^{3+} content in soil samples after 4 weeks conditioning at 20°C and 76% humidity. | 45 |
| Figure 15: Simplified model for the relation of absorption of Ca^{2+} and the rigidity of SOM influenced by cross-linking between the functional groups of different molecules. | 47 |

Table of Figures

| | |
|---|----|
| Figure 16: Simplified model for the relation of absorption of Al^{3+} and the rigidity of SOM influenced by cross-linking between the functional groups of different molecules. In contrast to Ca^{2+} further addition of cations on the matrix do not lead to a less rigidity determined with T^* . | 48 |
| Figure 17: Step transition temperature for Ca^{2+} treated samples in batch 4 weeks and 6 months after the treatment. | 50 |
| Figure 18: Step transition temperature for Na^+ treated samples in batch, 4 weeks, 13 weeks and 22 weeks after the treatment. | 50 |
| Figure 19: Step transition temperature for Al^{3+} treated samples in batch; 4 weeks, 13 weeks and 22 weeks after the treatment. | 51 |
| Figure 20: Contact Angle of the Ca^{2+} und Al^{3+} treated samples after 4 weeks of conditioning in relation to the cation content. | 53 |
| Figure 21: Correlation of T^* with contact angle for all treated and untreated samples with different cation solutions in batch experiments. | 53 |
| Figure 22: Step transition temperature T^* before and after demineralisation of the three samples. Box plots were created by at least 6 T^* values for each sample. | 55 |
| Figure 23: Heat flow curve of a DSC measurement of a Ca-precipitate, no tangent lines can be applied and no inflection point is received. | 66 |
| Figure 24: Corrected heat flow curve of the same sample by turning the curve in the plane with the TA instruments program, the inflection point is now analysable | 66 |
| Figure 25: Amounts of wet precipitates originated during flocculation process in solutions of different $\text{Me}^{n+} / \text{C}$ ratios with Ca^{2+} , Pb^{2+} and Al^{3+} | 68 |
| Figure 26: DOC losses of the solution after the precipitation in duplicates with Ca^{2+} , Pb^{2+} and Al^{3+} in different $\text{Me}^{n+} / \text{C}$ ratios. | 69 |
| Figure 27: Cation – Organic carbon ratio for the three lowest Me^{n+}/C ratios in precipitation experiments, due to high analytical standard deviations and in relation to the absolute concentration low losses of cations for the higher tiered Me^{n+}/C ratios no Me^{n+}/C ratios in precipitates were calculated for these. | 70 |
| Figure 28: First (left) and second (right) heating curve of Al-precipitates (Me^{n+}/C ratio = 2) in hermetically sealed pans. No analyzable thermal event in the second heating cycle (continuous line: Heating flow; dashed line: derivation of heat flow). | 71 |
| Figure 29: First (left) and second (right) heating curve of Pb-precipitates (Me^{n+}/C ratio = 2) in hermetically sealed pans. No analyzable thermal event in the second heating cycle (continuous line: Heating flow; dashed line: derivation of heat flow). | 72 |
| Figure 30: DSC curves and glass transition – like step transition temperature T^* of Pb-DOM precipitates produced in solutions with different Me^{n+}/C ratios. With increasing ratio the samples develop an enthalpic overshoot since for some curves (Pb/C 10) no step transition temperature can be analyzed because the step has become a peak. | 72 |
| Figure 31: DSC curves of Al DOM precipitates produced in solutions with different Me^{n+}/C ratios. | 73 |
| Figure 32: Step transition like glass transition temperature T^* in dependence of the initial Me^{n+}/C ratio in solution for the cation-DOM precipitates, standard deviations for T^* based on the results for the number of pans for each sample (4 -8). | 73 |

- Figure 33: DSC heating curves of an Al precipitate ($\text{Me}^{\text{nt}}/\text{C ratio}_{\text{solution}} = 1$) before (left) and after (right) complete removal of water by drying at 105°C : no analysable thermal events can be detected anymore. The vertical curves in the left picture originated from the cooling cycle before and cannot be excluded technically. The heating curve received before cooling shows a pronounced melting peak around 0°C which is also a hint for the higher water content of the samples. 75
- Figure 34: Heating curves of Pb precipitates ($\text{Pb}^{2+}/\text{C ratio}_{\text{solution}} = 2$) measured after 2 weeks conditioning (solid line), after 6 weeks after the 1 measurement (long dash) and after 2 weeks after the 2. measurement (short dash). T^* is given of inflection point of the step transitions. 77
- Figure 35: T^* for Pb precipitates created in different $\text{Pb}^{2+}/\text{C ratios}_{\text{solution}}$ in duplicates and measured after 2 weeks of conditioning, re-measured six weeks after the 1. DSC measurement and 2 weeks after the 2. DSC measurement to control the reappearance of T^* . 77
- Figure 36: Heating curves of Al precipitates ($\text{Al}^{3+}/\text{C ratio}_{\text{solution}} = 3$) measured after 2 weeks conditioning (solid line), 6 weeks after the 1 measurement (short dash) and 2 weeks after the 2. measurement. T^* is given as inflection point of the step transitions. 78
- Figure 37: T^* for Al precipitates created in different $\text{Al}^{3+}/\text{C ratios}_{\text{solution}}$ and measured after 2 weeks of conditioning, re-measured six weeks after the 1. DSC measurement and 2 weeks after the 2. DSC measurement to control the reappearance of T^* . 79
- Figure 38: Desorption of lead during the extraction with an acid cation exchange resin for samples with different contents of Ca^{2+} . The original sample is a no treated sample the control is only spiked with Pb^{2+} but not with additional Ca^{2+} (Ca^{2+} content of the control: $160 \text{ mmol}_c \text{ kg}^{-1}$) 87
- Figure 39: Desorption of lead during the extraction with an acid cation exchange resin at different time points for samples with different contents of Al^{3+} given in the legend. The original sample is a no treated sample the control is only spiked with Pb^{2+} but not with additional Al^{3+} (Al^{3+} content of the control: $80 \text{ mmol}_c \text{ kg}^{-1}$). 88
- Figure 40: DOC release of the samples during the desorption experiments with an acid cation exchange resin at different time points for samples with different contents of Ca^{2+} given in the legend. The original sample is a no treated sample the control is only spiked with Pb^{2+} but not with additional Ca^{2+} (Ca^{2+} content of the control: $160 \text{ mmol}_c \text{ kg}^{-1}$). The standard deviation of the DOC measurements ranges about 5%, we do not include the standard deviation in the diagram to keep a clear view. 89
- Figure 41: DOC losses of the samples during the desorption experiments with an acid cation exchange resin at different time points for samples with different contents of Al^{3+} given in the legend. The original sample is a no treated sample the control is only spiked with Pb^{2+} but not with additional Al^{3+} (Al^{3+} content of the control: $80 \text{ mmol}_c \text{ kg}^{-1}$). The standard deviation of the DOC measurements ranges about 5%, we do not include the standard deviation in the diagram to keep a clear view. 90
- Figure 42: T^* of the created samples of different cation contents directly before the beginning of the desorption experiments. The untreated original and the control sample only spiked with Pb is linked with the original Ca^{2+} content in the sample and could also be transferred to the original Al content of $63 \text{ mmol}_c \text{ kg}^{-1}$. The standard deviations originated from 3 DSC measurements conducted for each sample. 91

Figure 43: Step transition like glass transition temperature T^* in selected samples from the desorption experiments with an acid cation exchange resin at different time points with different contents of Ca^{2+} and the control (only spiked with Pb). Showing the other Ca^{2+} treated samples would not provide more information. The standard deviations originated from 3 DSC measurement conducted for each sample. 92

Figure 44: Step transition like glass transition temperature T^* during the desorption experiments with an acid cation exchange resin at different time points for selected samples with different contents of Al^{3+} and the original sample. Showing the other Ca^{2+} treated samples would not provide more information. The standard deviations originated from 3 DSC measurement conducted for each sample. 92

Tables

| | |
|---|----|
| Table 1: Comparison of the characteristics of the two determined step transitions in NOM and SOM, the reported values are only given in average. | 13 |
| Table 2: Ion radius, Hydrationenergy (ΔH_h) and hydration radius of the cations considered in this thesis. (Scheffer/Schachtschabel; and Blume 2010; Essington 2003) | 14 |
| Table 3: Common soil characteristics of the used organic layer from a spruce forest | 25 |
| Table 4: Common characteristics of the two peats | 25 |
| Table 5: Estimated results for Na^+ sorption during batch experiments on losses of Ca^{2+} and Mg^{2+} | 40 |
| Table 6: Sample characteristics and behaviour during the demineralization procedure with the acid cation exchange resin. | 56 |
| Table 7: Common characteristics of the organic layer from a spruce forest used as base sample for DOC desorption in the experiments | 61 |
| Table 8: Me^{n+}/C ratios obtained in the different cation solutions for precipitation | 62 |
| Table 9: Graphite tube heating program for lead analysis in AAS | 63 |
| Table 10: Explanation of the used procedures for characterising the precipitates by DSC. | 65 |
| Table 11: Optical and analytical observations of parameters during and after the precipitation process for the three cation – DOC solutions Ca^{2+} - DOC, Al^{3+} - DOC and Pb^{2+} - DOC | 67 |
| Table 12: Common soil characteristics of the used organic layer from a spruce forest | 83 |
| Table 13: Concentrations of the basic samples conducted for Pb spiking. The cation contents were calculated from the analyses of the solutions after the treatment. | 84 |

7 Curriculum Vitae

Daniela Gildemeister

Geboren in Berlin, am 08. August 1973

Deutsche Staatsangehörigkeit

Verheiratet

4 Kinder



Beruflicher Werdegang

-
- | | |
|-------------------|--|
| Seit 08 - 2009 | Wissenschaftliche Angestellte am Umweltbundesamt im Fachgebiet „Arznei-, Wasch- und Reinigungsmittel, Nanomaterialien“; zuständig für Umweltprüfung von Tier- und Humanarzneimitteln |
| 08/2006 – 07/2009 | Wissenschaftliche Mitarbeiterin an der Universität Koblenz – Landau (Campus Koblenz) im Fachgebiet „Organische Chemie und Umweltchemie“, DFG Projekt CROSSLINK, Betreuung der Studierenden in analytischer Chemie/Umweltchemie |
| 07/2004 – 06/2006 | Promotionsstipendiatin des Nachwuchsförderprogrammes an der TU – Berlin zum Thema „Perkutane Resorptionsverfügbarkeit organischer Schadstoffe aus Bodenpartikeln“ |
| 01/2004 – 06/2004 | Wissenschaftliche Mitarbeiterin an der TU-Berlin, FG Umweltchemie, Institut für Technischen Umweltschutz, Erarbeitung eines Forschungsantrages im BMBF Projekt „BIO - REFINE“ für den Expositionspfad Boden – Mensch |

Ausbildung

| | |
|-------------------|--|
| 10/1993 – 08/2001 | <p>Studium „Technischer Umweltschutz“ an der TU Berlin, Abschluss als „Diplom-Ingenieurin“ (Note: Sehr gut)</p> <p>Studienschwerpunkte:</p> <p>Bodenschutz / Bodensanierung</p> <p>Umweltchemie</p> <p>Luftreinhaltung</p> <p>Diplomarbeit: „<i>Endotoxine – Vorkommen und Bedeutung in Innenräumen</i>“</p> |
| 09/1986 – 06/1993 | <p>Goethe – Oberschule Berlin (Gymnasium), Abschluss: Abitur (Note: 1,6)</p> |
| 09/1980 – 06/1986 | <p>Kronach Grundschule, Berlin</p> |

Veröffentlichungen (Peer Review)

Mikutta, R.; G. E. Schaumann; D. Gildemeister; S. Bonneville; M. G. Kramer; J. Chorover; O. A. Chadwick und G. Guggenberger, 2009, "Biogeochemistry of mineral-organic associations across a long-term mineralogical soil gradient (0.3-4100 kyr), Hawaiian Islands." Geochimica Et Cosmochimica Acta. 73 (7), p. 2034 – 2060

Schaumann, G. E.; Gildemeister D.; Kunhi Mouvenchery, Y.; Spielvogel, S.; Diehl, D. 2013. Interactions between cations and water molecule bridges in soil organic matter.

Journal of soils and sediments.13 (9).1579-1588

Gildemeister, D.; Metreveli, G.; Spielvogel, S.; Hens, S.; Lang, F.; Schaumann; G. E. 2014. Stabilisation of precipitates of pedogenic dissolved organic matter by multivalent cations. Journal of soils and sediments. DOI 10.1007/s11368-014-0946-9

Veröffentlichungen (Non - Peer Review)

Daniela Gildemeister, Nadine Tauchnitz, Silvia Berkner (2011), „Tierarzneimittelmischungen in landwirtschaftlich genutzten Böden“, In: Böden verstehen - Böden nutzen - Böden fit machen, 3. - 9. September 2011, Berlin (Berichte der DBG)

Daniela Gildemeister, Gabriele E. Schaumann (2007), "Koordinative Quervernetzungen in der organischen Bodensubstanz: Effekte bei der Belegung mit Calcium" Mitteilungen der deutschen bodenkundlichen Gesellschaft 110 (1), 191-192

Daniela Gildemeister, Gabriele E. Schaumann, W. Rotard (2005), "Konzept zur Untersuchung der dermalen Resorptionsverfügbarkeit bodenassoziierter Schadstoffe" Mitteilungen der deutschen bodenkundlichen Gesellschaft 107 (1), 131-132